

200

b

THE STRUCTURE AND SPECTRA OF FIVE-COORDINATE COMPLEXES

A THESIS

Presented to

The Faculty of the Graduate Division

by

Donald Lee Plymale

In Partial Fulfillment

of the Requirements for the Degree

Doctor of Philosophy in the

School of Chemistry

Georgia Institute of Technology

February, 1966

THE STRUCTURE AND SPECTRA OF FIVE-COORDINATE COMPLEXES

Approved:

*on R.H.G.*  
Chairman *Chen*

*17 - 101 54-6*  
Date approved by Chairman: 16 March, 1966

## ACKNOWLEDGMENTS

The author would like to thank Dr. J. A. Bertrand for his understanding and invaluable advice during the course of this research. To the other members of the reading committee, Dr. W. H. Eberhardt and Dr. D. J. Royer, the author expresses his thanks for their help and suggestions.

The author wishes to express his gratitude to his wife and children for their patience and encouragement.

The National Science Foundation has supported this work through GP1999 and GP3826 and this support is gratefully acknowledged.

The author gratefully acknowledges the cooperation of the personnel at the Rich Electronic Computer Center, without the aid of the computing facilities the structure determination would not have been possible.

## TABLE OF CONTENTS

	Page
ACKNOWLEDGMENTS . . . . .	ii
LIST OF TABLES . . . . .	v
LIST OF ILLUSTRATIONS . . . . .	vii
SUMMARY . . . . .	ix
Chapter	
I. INTRODUCTION . . . . .	1
II. REVIEW OF STRUCTURAL ASPECTS OF FIVE-COORDINATION . . . . .	4
Factors Which Determine Coordination Numbers	
Factors Which Determine Confirmation of Five-Coordinate Complexes	
Survey of Five-Coordinate Complexes	
III. REVIEW OF SPECTRAL ASPECTS OF FIVE-COORDINATION . . . . .	24
Crystal Field Theory	
Spectra of Transition Metal Complexes	
IV. INSTRUMENTATION . . . . .	39
X-Ray Studies	
Magnetic Studies	
Spectral Studies	
V. EXPERIMENTAL . . . . .	43
Preparation of Complexes	
X-Ray Diffraction Studies	
Magnetic Moment Determinations	
Spectral Studies	
VI. CALCULATIONS . . . . .	69
Structure Determination	
Qualitative Correlation Diagrams	
VII. RESULTS AND DISCUSSION . . . . .	97
Structure	

## Table of Contents (continued)

Spectral Properties	
Magnetic Properties	
VIII. CONCLUSIONS . . . . .	123
APPENDIX . . . . .	125
LITERATURE CITED . . . . .	138
VITA . . . . .	145

## LIST OF TABLES

Table	Page
1. Five-Coordinate Structure Determination . . . . .	9
2. Possible Five-Coordinate Compounds . . . . .	20
3. States for $d^n$ Systems in Russell-Saunders Coupling . . . . .	26
4. Splittings of One-Electron Levels in $C_{4v}$ and $D_{3h}$ Symmetries .	28
5. Predicted and Observed Spectra of Five-Coordinated High-Spin Nickel(II) Complexes . . . . .	37
6. Calculated and Observed Transitions in $CuCl_5^{3-}$ . . . . .	38
7. Analytical Data for $M(DPP)_3X_2$ . . . . .	45
8. Analytical Data for $Co(Pyridine\ N-Oxide)_3X_2$ . . . . .	45
9. Analytical Data for $Co(Pyridine\ N-Oxide)_6CoBr_4$ . . . . .	46
10. X-Ray Powder Patterns for the Pyridine N-Oxide Complexes . .	48
11. X-Ray Powder Patterns for the Diphenylphosphine Complexes . .	49
12. Unit Cell Parameters for the $M(DPP)_3X_2$ Compounds . . . . .	50
13. Magnetic Data for $M(DPP)_3X_2$ Complexes . . . . .	53
14. Visible Mull Spectra of $Co(Pyridine\ N-Oxide)_3Br_2$ and $[Butyl_4N][CoBr_4]$ . . . . .	54
15. Values of Statistical Functions . . . . .	70
16. Structure Parameters for $Co(DPP)_3Br_2$ . . . . .	76
17. Observed and Calculated Structure Factors for $Co(DPP)_3Br_2$ . .	78
18. Structure Parameters for $Ni(DPP)_3I_2$ . . . . .	85
19. Observed and Calculated Structure Factors for $Ni(DPP)_3I_2$ . .	86
20. Transformation Properties of the Dipole Moment Integrand, $\psi^* \sum q_1 \psi'$ . . . . .	90
21. Polarization of Incident Radiation . . . . .	90

## List of Tables (continued)

Table	Page
22. Predicted Transitions for a $d^9$ Configuration in a $C_{4v}$ Environment . . . . .	91
23. Predicted Transitions for $d^8$ and $d^7$ Configuration in a Five-Coordinate Symmetry . . . . .	96
24. Selected Intramolecular Distances and Angles for $M(DPP)_3X_2$ . . . . .	101
25. Carbon-Carbon Distances of the Phenyl Groups . . . . .	105
26. Carbon-Carbon Angles of the Phenyl Groups . . . . .	106
27. Assignment of Observed Transitions for the [Cu(dipyridyl) $_2$ I]I Complex . . . . .	113
28. Assignment of Observed Transitions for the Ni(DPP) $_3X_2$ Complexes . . . . .	116
29. Assignment of Observed Transitions for the Co(DPP) $_3X_2$ Complexes . . . . .	119



## LIST OF ILLUSTRATIONS

Figure	Page
1. Strong Field Splittings of the d-Orbitals in the Five-Coordinate Symmetries . . . . .	30
2. Polarizing Microspectrophotometer . . . . .	42
3. Mull Spectra of Tris(Pyridine N-Oxide)Cobalt(II) Chloride and Bromide . . . . .	55
4. Spectra of $\text{CoCl}_2$ in DMF with Increasing Concentrations of Pyridine N-Oxide . . . . .	57
5. Absorption Spectra of $\text{Co(DPP)}_3\text{X}_2$ in Dichloromethane . . . . .	58
6. Absorption Spectra of $\text{Ni(DPP)}_3\text{X}_2$ in Dichloromethane . . . . .	59
7. Solution and Solid Spectra of $[\text{Cu(dipyridyl)}_2\text{I}]\text{I}$ . . . . .	60
8. Crystal Spectra of $\text{Co(DPP)}_3\text{X}_2$ . . . . .	61
9. Crystal Spectra of $\text{Ni(DPP)}_3\text{X}_2$ . . . . .	62
10. Polarized Spectra of $[\text{Cu(dipyridyl)}_2\text{I}]\text{I}$ . . . . .	64
11. Polarized Spectra of $\text{Ni(DPP)}_3\text{Br}_2$ . . . . .	65
12. Polarized Spectra of $\text{Ni(DPP)}_3\text{I}_2$ . . . . .	66
13. Polarized Spectra of $\text{Co(DPP)}_3\text{Br}_2$ . . . . .	67
14. Polarized Spectra of $\text{Co(DPP)}_3\text{I}_2$ . . . . .	68
15. Distribution of Intensities for $\text{M(DPP)}_3\text{X}_2$ ; Compared with Theoretical Curves for 1 and $\bar{1}$ . . . . .	71
16. Patterson Projection of the HOL Zone of the $\text{Co(DPP)}_3\text{Br}_2$ Crystal	73
17. Electron-Density Projection of the HOL Zone of the $\text{Co(DPP)}_3\text{Br}_2$ Crystal . . . . .	74
18. Correlation Diagram for a $d^9$ Configuration in $D_{3h}$ Symmetry . .	88
19. Correlation Diagram for a $d^9$ Configuration in $C_{4v}$ Symmetry . .	89
20. Correlation Diagram for a $d^8$ Configuration in $D_{3h}$ Symmetry . .	92

## List of Illustrations (continued)

Figure	Page
21. Correlation Diagram for a $d^8$ Configuration in $C_{4v}$ Symmetry . . .	93
22. Correlation Diagram for a $d^7$ Configuration in $D_{3h}$ Symmetry . . .	94
23. Correlation Diagram for a $d^7$ Configuration in $C_{4v}$ Symmetry . . .	95
24. A Perspective Drawing of One Molecule of $Co(DPP)_3Br_2$ as Viewed Down the $b$ -Axis of the Crystal . . . . .	102
25. Splitting of the d-Orbitals of Copper in Various Possible Symmetries . . . . .	111
26. Spectroscopic States Arising from a Descent in Symmetry from $D_{3h}$ to $C_s$ in a $d^8$ Configuration . . . . .	115
27. Spectroscopic States Arising from a Descent in Symmetry from $D_{3h}$ to $C_s$ in a $d^7$ Configuration . . . . .	118
28. The Splitting of d-Orbitals in $D_{3h}$ and $C_s$ Symmetries . . . . .	122

## SUMMARY

The structural, spectral and magnetic properties of five-coordinate transition metal complexes have been investigated. These properties have been qualitatively interpreted in terms of ligand field theory.

In order to apply the ligand field approach to the five-coordinate system, energy level correlation diagrams have been constructed for the trigonal bipyramid and the square pyramid symmetries for d-orbital configurations of seven, eight and nine. This approach is based mainly on the fact that eigenfunctions are bases for an irreducible representation of the symmetry group; this allows qualitative calculations using symmetry arguments. From these diagrams, it is possible to predict the possible electron transitions. The principal absorption bands are expected to be spin allowed (same multiplicity for the ground and excited states) and one-electron transitions. It is also possible to qualitatively decide whether a transition is electronically allowed or vibronically allowed (experimentally the electronically allowed are expected to be 10 to 100 times more intense than the vibronically allowed bands). This results from the non-centric nature of the two possible five-coordinate stereochemical forms, which allows the possibility of mixing p-character into the d-states and thereby relaxing the electronic selection rules which make the d-d transitions forbidden. Also in both stereochemical forms, the z-axis of the molecule belongs to a different representation than the other two axes and therefore, transitions are expected to be strongly polarized.

The structure of dibromotris(diphenylphosphine)cobalt(II) has been determined from three-dimensional X-ray data. The two bromine and three phosphorus atoms form a bipyramid about the cobalt atom with two phosphorus atoms in the axial positions and the base plane of the bipyramid made up of the third phosphorus ( $P_3$ ) and the two bromine atoms. The structure does not have a regular trigonal bipyramidal conformation, but can be thought of as intermediate between the trigonal bipyramidal and the square pyramidal conformations.

The two bromine atoms, one phosphorus atom ( $P_3$ ) and the cobalt are essentially coplanar, the dihedral angle between the plane defined by the cobalt-bromine-bromine and the planes defined by the cobalt-phosphorus( $P_3$ )-bromine are approximately  $2^\circ$ . The angles between the equatorial groups and each axial group are approximately  $90^\circ$ . The angles between groups in the equatorial plane range from  $98^\circ$  to  $136^\circ$ , instead of the  $120^\circ$  required for trigonal symmetry. The orientation of the two phenyl groups on each diphenylphosphine ligand of the axial phosphorus atoms show dihedral angles close to  $90^\circ$ . This may suggest that the phenyl groups are entering into d-p  $\pi$ -bonding with the phosphorus atoms; however, the equatorial phosphine does not show such orientation. Steric crowding would certainly be greater in the vicinity of the equatorial phosphine and could affect the orientations of the phenyl groups.

The related diphenylphosphine complexes of cobalt iodide, nickel bromide and nickel iodide have also been investigated. X-ray powder patterns show that the two bromide structures are identical. Similar results are also obtained for the two iodide structures. Slight differences are observed both in intensities and in d-spacings between the

bromide and iodide compounds. However, the successful refinement of the heavy atom coordinates using two zones of intensity data from the nickel iodide crystal shows that the iodide and bromide structures are essentially identical, the only differences appear related to the difference in size of the bromine and iodine atoms.

The structures of tris(pyridine N-oxide)cobalt(II) chloride and bromide have been investigated. These complex compounds have a five-coordinate stoichiometry but do not have a five-coordinate conformation. The solid spectra of these compounds suggest that they contain the tetrahalocobaltate(II) anion and that the compound should be formulated as a mixed complex  $[\text{CoL}_6][\text{CoX}_4]$  (where L represents the ligand, pyridine N-oxide, and X represents a halide ion). To check such a possibility, cadmium was substituted for the tetrahedral cobalt to give  $[\text{CoL}_6][\text{CdBr}_4]$ . X-ray powder patterns for the  $\text{CoL}_3\text{Br}_2$  and the  $[\text{CoL}_6][\text{CdBr}_4]$  were found to be almost identical in both peak position and intensity. Studies of the solution spectra of these complexes indicate that the cobalt(II) ions are probably present as various tetrahedral species.

The polarized crystal spectra of the diphenylphosphine complexes mentioned above and the five-coordinate iodobis(dipyridyl)copper(II) iodide have been investigated. In order to obtain the single crystal polarized spectra, a single beam microspectrophotometer was constructed.

The polarized spectra of iodobis(dipyridyl)copper(II) iodide have been interpreted in terms of the  $C_{2v}$  symmetry of the coordination sphere. The spectral assignments, order of d-orbitals and the extent of splittings seem reasonable in terms of the structure of this complex.

The polarized spectra of the diphenylphosphine complexes have been interpreted in terms of the  $C_s$  symmetry of the coordination sphere. The observed spectra agree well with the predictions of ligand field theory; the spectral assignments and the extent of d-orbital splittings seem reasonable.

The diiodotris(diphenylphosphine)nickel(II) compound has an unusual magnetic moment. Five-coordinate complexes of nickel(II) which contain phosphorus or arsenic ligands are usually diamagnetic; however, the nickel iodide complex exhibits paramagnetism (1.29 B.M.). Since the nickel iodide and nickel bromide complexes have identical structures this difference can be attributed to a difference in field strengths. Therefore, the unusual paramagnetism is probably due to thermal population of a low-lying triplet state.

## CHAPTER I

### INTRODUCTION

The coordination numbers six and four are the ones usually observed for transition metal complex compounds; however, recent investigations indicate many more "five-coordinate" complexes than previously suspected. The investigation of five-coordination presents a few problems normally not encountered in a study of the coordination numbers four and six. A major difficulty is the limited number of definitely established five-coordinate complexes; many complexes that possess a penta-coordinate stoichiometry are not five-coordinate. Harris and co-workers (1) have investigated the dihalobis(o-phenylenebisdimethylarsine) metal(II) complexes (metal = nickel, palladium and platinum). They reported on the basis of conductivity and spectrometric studies that all these metals gave presumably five-coordinate cations of the type  $[M(\text{Diarsine})_2X]^+$ . However crystal structure determinations by Stephenson (2, 3) have revealed an octahedral configuration for the  $\text{Ni}(\text{Diarsine})_2\text{I}_2$  complex and a square planar configuration for the  $\text{Pt}(\text{Diarsine})_2\text{Cl}_2$  complex. The pentacyanocobalt(II) anion has been found to be dimeric (4) in the solid state with metal-metal bonding and in aqueous solution (5) has been reported to exist as a monohydrate. Sacco and Freni (6) found that the cobalt(II) complex  $(\text{Co}(\text{CNCH}_3)_5(\text{ClO}_4)_2)$  could be obtained in two forms, one light blue and paramagnetic and the more stable one red and diamagnetic. Cotton and co-workers (7) have determined the structure of the red form and have found it to contain dinuclear cations  $[(\text{CH}_3\text{CN})_5\text{Co}-\text{Co}(\text{CNCH}_3)_5]^{+4}$ .

Two ideal stereochemical forms are energetically possible for a coordination number of five, the square pyramid ( $C_{4v}$  coordination symmetry) and the trigonal bipyramid ( $D_{3h}$  coordination symmetry). This is analogous to the four-coordinate system where two stereochemical forms are possible; however, a sufficient number of four-coordinate systems have been investigated to allow a reasonable assignment of the stereochemistry of a particular complex on the basis of spectral and magnetic properties. A number of examples must be available before such assignments are possible; in five-coordinate systems, reliable assignments are not presently possible due to limited knowledge of the structure and properties of such complexes.

Many five-coordinate complexes in the solid state are extensively dissociated in solution while others are rapidly decomposed; therefore solution data in many cases are of little value. Also five-coordinate symmetries appear to be non-rigid and in solution the vibrations may completely change the symmetry; therefore spectral data will probably represent an average over the various possible conformations.

Muetterties (8) has pointed out that to neglect the effects of dynamics on stereochemistry and simply treat the molecule as a rigid point group can lead to serious misconceptions. If the time scale for a permutation between two stereochemical forms were comparable to or shorter than that of the laboratory observation, then the systems would have to be considered as a non-rigid structure. Berry (9) has pointed out that the two five-coordinate stereochemical forms, the trigonal bipyramid ( $D_{3h}$  symmetry) and the square pyramid ( $C_{4v}$  symmetry), should undergo interconversion easily through vibrational excitation. Mahler and



Muetterites (10) have recently reported two phosphorane molecules which they characterize as non-rigid molecules. Certainly with bulky ligands and particularly multidentate ligands, the symmetries will be more rigid than those of the phosphoranes; however, the value of solution data is still questionable.

In this thesis the author will report on the structural, spectral and magnetic properties of five-coordinate transition metal compounds. He will attempt to correlate these properties with the predictions of ligand field theory. He will report the verification of a series of five-coordinate diphenylphosphine complexes by an X-ray structure determination. The spectral and magnetic properties of these complexes and others already known to be five-coordinate will be correlated with the predictions of ligand field theory. Also a survey of five-coordinate structures will be given along with a discussion of the factors which stabilize a coordination number of five and the factors which are expected to affect the stereochemical form of a complex. The approach in presenting this thesis will be to discuss the structural, spectral and magnetic properties separately; this approach is employed rather than a separate discussion of each complex. The structures will be discussed first, since this information is necessary to interpret the spectral and magnetic properties. In the spectral discussion correlation diagrams will be developed for the ideal five-coordinate symmetries ( $D_{3h}$  and  $C_{4v}$ ). The complexes under investigation do not possess ideal symmetries but may be treated as distorted from ideal symmetry. Therefore, correlation diagrams for lower symmetries can be derived from the correlation diagrams of the ideal symmetries.

## CHAPTER II

### REVIEW OF STRUCTURAL ASPECTS OF FIVE-COORDINATION

#### Factors Which Determine Coordination Numbers

The most important factors (11) which determine the coordination number of a metal atom in a complex compound appear to be: (a) the oxidation state of the metal; (b) the nature of the ligand; (c) the particular metal atom chosen; (d) the type of bonding; and (e) steric effects.

In recent years, examples of five-coordinate complexes have appeared more frequently. The preparation of these complexes have required, however, a particular combination of ligand and metal. Several recent reports (12, 13, 14) of five-coordination have presented arguments that the stability arises from intermolecular blocking of the unused octahedral site. However a combined effect of the ligand (its electronegativity and synergic bonding capabilities) and the metal (its oxidation state and electron configuration) may very well play an important role in producing a five-coordinate configuration.

#### Factors Which Determine Conformation of Five-Coordinate Complexes

Probably an even more perplexing question associated with five-coordination is whether the square pyramidal or the trigonal bipyramidal configuration would be preferred by a particular combination of metal ion and ligand. Recently, several discussions (15, 16) have been presented concerning the stereochemistry of five-coordination. Zemann (15) has pursued the problem from the point of view of electrostatic and non-coulombic

repulsive forces. He indicated that the most favorable conformation was the trigonal bipyramidal arrangement, but only a little less favorable was a distorted square pyramid with an angle (apex-central-base atoms) of  $104^{\circ}4'$ . He also indicated that the transition between the trigonal bipyramid and the above distorted pyramid was easily obtained.

A consideration of the ligand field stabilization energy (17) alone showed that, for every case from  $d^1$  through  $d^9$ , a square pyramidal arrangement with the metal in the base was more favorable than a trigonal bipyramidal arrangement. Gillespie (16) has discussed the stereochemistry of five-coordination in terms of the theory of valency-shell electron pair repulsion. He indicated that for symmetrical  $d^0$  and  $d^{10}$  configurations the trigonal bipyramidal arrangement was preferred (determined by the interaction between the five bonding electron pairs in the valency shell). For the less symmetrical d-configurations he found it necessary to consider the interaction between the valency-shell electron pairs and the non-bonding d-shell electrons. When the interaction between the ligand electron-pairs is more important than the interaction with the non-bonding d-electrons, a trigonal bipyramidal arrangement would be preferred (highly covalent complexes); when the interaction between the bonding and non-bonding electron-pairs predominates, then a square pyramidal arrangement would be preferred (ionically bonded complexes); when the interactions are comparable an intermediate arrangement would be expected.

Gillespie has indicated that the unsymmetrical d-configurations may be regarded as having an ellipsoidal shape of either an oblate or prolate orientation. He has pointed out that the tetragonal distortion of octahedral complexes can most often be associated with a prolate ellipsoidal

d-shell; therefore yielding longer bonds along the tetragonal axis than along equatorial bonds. A prolate ellipsoidal d-shell interacting with the valency-shell electron-pairs would tend to cause the valency-shell electron-pairs to avoid the ends of the ellipsoidal (area of greatest repulsion). This would destabilize the trigonal bipyramidal arrangement more than the square pyramidal arrangement and could well favor the square pyramidal configuration. Regardless of which stereochemical form, the axial bond(s) would be longer than the basal bonds. An oblate ellipsoidal d-shell would further stabilize the trigonal bipyramid arrangement and would possibly cause the equatorial bonds to be longer than the axial bonds. Double-bond character increases the repulsions between the bonds, and by removing electrons from the non-bonding d-shell it reduces the interaction between the d-shell and the bonding-electron pairs. Hence this interaction between the bonding-electron pairs predominates over the interaction with the d-shell and the trigonal bipyramidal structure is preferred. Gillespie had an insufficient number of examples to test his theory; however some were consistent and others which did not conform to the general rule were accounted for in terms of the steric requirements of the ligands.

Muetterties and co-workers (18, 19) have reported on a number of molecules which contained five-coordinate central atoms which were not transition metal ions; a trigonal bipyramidal geometry prevailed at least for the liquid or solution state and the more electronegative ligands preferred the axial positions.

Ballhausen and Gray (20) have recently formulated a rule that is pertinent to five-coordinate complexes with  $\pi$ -bonding ligands. The rule

was stated as follows:

for distorted octahedral complexes with tetragonal symmetry ( $ML_5X$ ), nearly all the  $\pi$ -bonding is axially directed and involves the metal  $d_{xz}$  and  $d_{yz}$  orbitals. The stronger axial  $\pi$ -bonding may be either M-X or M-L depending on whether the  $\pi$ -orbital energies of X or L more closely approximate the metal  $d\pi$  orbital energies. It is a good approximation to neglect planar  $\pi$ -bonding and approximate the metal  $d_{xy}$  orbital as non-bonding.

They have indicated that the trans-effect results from the desire of the best  $\pi$ -bonding ligand in a metal complex to have exclusive rights to the metal  $d\pi$  orbitals. They argued that for the vanadyl complexes (21) an axial elimination of a hypothetical ligand had taken place, thus resulting in a square-based pyramidal structure, in which the V-O group had the exclusive right to the two metal  $d\pi$  orbitals.

### Survey of Five-Coordinate Complexes

#### Complexes for Which Structures Have Been Established by X-Ray Diffraction

Ibers (22) has presented a review article on molecular structure in which he devotes a section to the discussion of five-coordinate structure determinations. Although this article is recent, a number of structure articles on five-coordinate complexes have appeared in the literature since this article was published. In the following section the author will summarize what little is known with certainty about five-coordinate transition metal structures. A discussion of the three-dimensional five-coordinate complexes such as  $V_2O_3$  is less meaningful than the isolated complexes and these will not be discussed. Also the carbonyl complexes and the delocalized  $\pi$ -bonded complexes will be omitted from this discussion.

Table 1 is a synopsis of the twenty-seven independent five-coordinate structure determinations. They will be briefly discussed

following Table 1 in the order  $d^7$ ,  $d^8$ ,  $d^9$ ,  $d^{10}$ ,  $d^6$ ,  $d^5$ , and  $d^1$ .

DiVaria and Orioli (23) have very recently reported the preparation of a series of divalent 3d-metals with the general formula  $M(\text{denMe})X_2$ , where  $M = \text{Mn, Fe, Co, Ni, Cu, Zn}$ ;  $\text{denMe} = \text{bis}(2\text{-dimethylaminoethyl})\text{methylamine}$ ; and  $X = \text{Cl, Br, I, NCS}$ . All were high-spin complexes and have been proposed to be five-coordinate on the basis of molecular weights, spectral and magnetic properties. They have determined the crystal structure of the  $\text{Co}(\text{denMe})\text{Cl}_2$  complex and have reported that the cobalt atom is in an environment of five ligands. The arrangement of the ligands was reported as an intermediate structure, not easily described in terms of either a square pyramidal or trigonal bipyramidal geometry. They indicated that steric repulsions appeared to play an important role in determining the distribution of the ligands about the cobalt.

Alderman and co-workers (24, 25) have determined the structure of nitroso(dimethyldithiocarbamato)cobalt(II) and have found the structure to be that of a tetragonal pyramidal arrangement with the four sulfur atoms at the corners of the base. The N-O bond was inclined at  $139^\circ$  to the pyramidal axis, forming an unsymmetrical  $\pi$ -complex with the cobalt atom. The complex was essentially diamagnetic and its formulation as cobalt(II) has been questioned (26).

Nyholm and co-workers (28) have reported a series of compounds using diphenylmethylarsine oxide as a ligand. They have prepared complexes of the general formula  $M(\text{II})(\text{Ph}_2\text{MeAsO})_4(\text{ClO}_4)_2$  where  $M = \text{Mn, Fe, Co, Ni, Cu, Zn}$ . X-ray powder patterns have indicated that these are all isostructural. They have reported that the infrared spectra of the

Table 1. Five-Coordinate Structure Determinations

Complexes used in structure det.	Conf.	d shell	Other Metal ions	Struct. ref.	Prep. and chem. ref.	Additional notes
1. $\text{Co}(\text{denMe})\text{Cl}_2$	1	7	Mn, Fe Ni, Cu Zn	23	-	high spin Co
2. $\text{Co}(\text{L}^1)\text{NO}$	DSP	7?	-	24,25	26	oxidation state questionable
3. $\text{Co}(\text{Ph}_2\text{MeAsO})_4(\text{ClO}_4)_2$	DSP	7	Mn, Ni Zn	27	28	high spin Co, Mn all isostructural
4. $(\text{Co}(\text{CNCH}_3)_5)\text{ClO}_4$	DTB	8	-	29	30	-
5. $\text{Ni}(\text{triarsine})\text{Br}_2$	DSP	8	Co	31	32,33	diamagnetic
6. $\text{Ni}(\text{L}^2)_2$	DSP	8	Co	34	35	high spin, isomorphous
7. $\text{trans-PdI}_2(\text{L}^3)_2$	DSP	8	-	12	-	octahedral possibility
8. $\text{PdBr}_2(\text{L}^4)_3$	DSP	8	Pt, Co	36	37,38	not isomorphous
9. $(\text{PtI}(\text{QAS}))(\text{BPH}_4)$	DTB	8	Pd, Ni	39	40,41,42	-
10. $(\text{PH}_3\text{P}(\text{CH}_3))_3(\text{Pt}(\text{SnCl}_3)_5)$	DTB	8	-	45	46	-
11. $(\text{Cu}(\text{dipyridyl})_2\text{I})\text{I}$	DTB	9	-	47	48	1,10 phenanthroline complexes are probably analogous
12. $(\text{Cr}(\text{NH}_3)_6)(\text{CuCl}_5)$	TB	9	-	49	50	-

Table 1 (continued)

13. $\text{Cu}(\text{L}^5)\text{H}_2\text{O}$	DSP	9	-	51	52,53	-
14. $\text{Cu}(\text{dimethylglyoxime})_2$	DSP	9	-	54	-	dimer
15. $\text{Cu}(\text{salicylaldehydato})_2$	DSP	9	-	55	-	dimer
16. Copper formate	DSP	9	-	56	-	dimer
17. $\text{Cu}(\text{L}^5)$	DSP	9	-	57	-	dimer
18. $\text{Cu}(\text{L}^6)_2$	DSP	9	-	58	-	dimer
19. $\text{Cu}(\text{L}^7)$	DSP	9	-	59	-	dimer
20. $\text{Zn}(\text{AA})_2\text{H}_2\text{O}$	I	10	-	60,61	-	-
21. $\text{Zn}(\text{terpyl})\text{Cl}_2$	DTB	10	Cu,Cd	62	63	isostructural?
22. $\text{Zn}(\text{L}^8)\text{H}_2\text{O}$	DSP	10	-	64	-	Zn 0.34 Å above plane
23. $\text{Zn}(\text{sal-Me})_2$	DTB	10	Co,Mn	66	67	dimer
24. $\text{Ru}(\text{PH}_3\text{P})_3\text{Cl}_2$	DSP	6	Os	13	14	octahedral possibility probably isostructural
25. chlorohemin	DSP	6	-	68	-	Fe slightly above plane
26. Iron(III)porphyrin	DSP	5	-	69	-	Fe slightly above plane
27. $\text{VO}(\text{AA})_2$	DSP	1	-	21	-	V at center of gravity



Note: DTB = distorted trigonal bipyramid  
 DSP = distorted square pyramid  
 TB = trigonal bipyramid  
 I = intermediate configuration  
 denMe = bis(2-dimethylaminoethyl)methylamine  
 triarsine =  $(\text{CH}_3)_2\text{As}(\text{CH}_2)_3\text{AsCH}_3(\text{CH}_2)_3\text{As}(\text{CH}_3)_2$   
 QAS = tris(o-diphenylarsenophenyl)arsine  
 AA = acetylacetonate  
 terpyl = 2:6-di-2'pyridylpyridine  
 sal-Me = N-methylsalicyldiminato  
 L<sup>1</sup> = dimethyldithiocarbamate  
 L<sup>2</sup> =  $\text{ClC}_6\text{H}_3(\text{OH})\text{CH}=\text{NC}_2\text{H}_4\text{N}(\text{C}_2\text{H}_5)_2$   
 L<sup>3</sup> = dimethylphenylphosphine  
 L<sup>4</sup> = 2-phenylisophosphophindoline  
 L<sup>5</sup> = bis(salicylaldehyde)isopropylenedi-imine  
 L<sup>6</sup> = N,N-di-n-propyldithiocarbonate  
 L<sup>7</sup> = acetylacetonato-o-hydroxyanilato  
 L<sup>8</sup> = N,N'-disalicylideneethylenediamine

manganese, cobalt, nickel and zinc complexes indicated both coordinated and uncoordinated perchlorate groups. Pauling and co-workers (27) have reported a structure analysis of the cobalt complex by single crystal X-ray diffraction techniques. The cobalt atom was found in a distorted square pyramidal arrangement with the arsine oxides in the plane and the perchlorate nearly on the four-fold axis in the axial position. The manganese and cobalt complexes were reported to have high spin electronic configurations.

Sacco and Freni (30) have reported the preparation of some isonitrile complexes of cobalt which have a five-coordinate stoichiometry. Cotton and co-workers (29) have determined the crystal structure of the pentakis(methylisonitrile)cobalt(I) perchlorate. The  $[\text{Co}(\text{CNCH}_3)_5]^+$  ion was found to have a slightly distorted trigonal bipyramidal configuration.

Barclay and Nyholm (32) have prepared the complexes  $\text{Ni}(\text{triarsine})\text{X}_2$  ( $\text{X} = \text{Br}, \text{I}$ ) and  $\text{Co}(\text{triarsine})\text{I}_2$  where triarsine represents the potentially tridentate ligand  $(\text{CH}_3)_2\text{As}(\text{CH}_2)_3\text{AsCH}_3(\text{CH}_2)_3\text{As}(\text{CH}_3)_2$ . Mair and co-workers (31) have found the molecular configuration of the  $\text{Ni}(\text{triarsine})\text{Br}_2$  to be a distorted square pyramid. They found the square plane to contain the three arsine atoms and depressed about  $20^\circ$  below the plane the bromide atom. The additional bromide at the apex was found to be at nearly right angles to the plane of the nickel-arsenic bonds.

Sacconi and co-workers (34) have reported the structure of the first high spin nickel(II) complex with a five-coordinate configuration. The ligand of general formula  $\text{XC}_6\text{H}_3(\text{OH})\text{CH}=\text{NC}_2\text{H}_4\text{N}(\text{C}_2\text{H}_5)_2$  gave complexes with nickel(II) and cobalt(II) of the general formula

$[X-C_6H_3(OH)CH=NC_2H_4N(C_2H_5)_2]_2M$ . They determined the structure of the bis[N- $\beta$ -diethylamineethyl-5-chlorosalicylaldehyde]nickel(II); they also found that the analogous high spin cobalt(II) complex was isomorphous with the nickel complex. They have described the geometry as a distorted square pyramid. The basal set consisted of one ligand (three coordination sites) and an oxygen from the other ligand which lie in a plane within  $0.1\text{\AA}$ . The nickel atom was found  $0.36\text{\AA}$  above this plane along with the axial nitrogen at  $1.93\text{\AA}$  from the nickel and the non-bonded nitrogen at a distance  $4.96\text{\AA}$  from the nickel atom.

Bailey and co-workers (12) have reported the structure of trans-di-iodobis(dimethylphenylphosphine)palladium(II). The coordination of the palladous ion was found to be a distorted square pyramid with Pd-P bond lengths of  $2.34\text{\AA}$ , two Pd-I bond lengths of  $2.63\text{\AA}$  and an axial Pd-I bond length of  $3.28\text{\AA}$ . They indicated that the coordination was really a distorted octahedron, the sixth site occupied by a hydrogen atom on the  $\beta$ -carbon atom of the phenyl ring. The metal to hydrogen bond length was  $2.8\text{\AA}$ .

Collier and co-workers (36) have found that 2-phenylisophosphindoline combines with transition metal halides to form complexes in which the metal has a five-coordinate geometry. The crystal structure (36) of the red form of tris(2-phenylisophosphindoline)dibromopalladium has shown the geometry of the palladium atom to be a distorted square pyramid. The basal plane consisted of the three phosphine ligands and a bromide which was depressed about  $10^\circ$  below the plane. The analogous platinum dibromide and di-iodide compounds were not isomorphous with the palladium dibromide; however, Mann (37) has suggested

that the platinum(II) compounds are also five-coordinate. Collier (38) has also reported the preparation of the tris(2-phenyliso-phosphindoline) dihalide complexes of cobalt(II). No structure evidence has been reported for the cobalt(II) complex.

Two tetradentate ligands which have been reported to form five-coordinate complexes are tris-(o-diphenylarsinophenyl)arsine or QAS (41) and tris-(o-diphenylphosphinophenyl)phosphine or QP (40). An X-ray structural investigation (39) of the  $[\text{PtI}(\text{QAS})][\text{BPh}_4]$  has shown that the configuration around the platinum is trigonal bipyramidal. The central arsenic atom is located at an apex, the three remaining arsenic atoms in the trigonal plane and the iodide at the other apex.

Cramer and co-workers (46) have reported that the addition of methyltriphenylphosphonium chloride to a solution of chloroplatinic acid and stannous chloride gave a crystalline material of formula  $[(\text{C}_6\text{H}_5)_3\text{PCH}_3]_3[\text{Pt}(\text{SnCl}_3)_5]$ . A crystal structure determination (45) has revealed the  $[\text{Pt}(\text{SnCl}_3)_5]^{-3}$  anion to be a trigonal bipyramid.

Harris and co-workers (48) reported the preparation and properties of a series of five-coordinate copper(II) complexes by the reaction of bis(2-2'-dipyridyl)copper(II) and bis(1,10-phenanthroline)-copper(II) perchlorate with various neutral and negatively charged ligands. The structure of the iodobis(2-2'-dipyridyl)copper(II) iodide has been determined by Barclay and co-workers (47). They have reported the complex to be an ionic structure of iodide ions and trigonal bipyramidal iodobis-(dipyridyl)copper(II) ions. They indicated that the copper was surrounded by four nitrogen atoms and an iodine atom at the corners of a distorted trigonal bipyramid. Two nitrogen atoms from two different

dipyridyl molecules and an iodine were in the trigonal plane; the other two nitrogens were located at the apexes of the trigonal pyramid. A line passing through the apexes and the copper atom made an angle of  $9^\circ$  with the normal to the trigonal plane. The ligand 1,10-phenanthroline appeared to form analogous complexes.

Mori (50) has reported the preparation of a hexamminechromium(III) pentachlorocuprate(II) salt which contains a penta-coordinate anion. Mori and co-workers (49) have done the X-ray structure determination and have reported the anion to have a trigonal bipyramidal configuration around the copper ion. The copper to chlorine distances were found to be of the same order of magnitude ( $2.32 - 2.35\text{\AA}$ ).

Llewellyn and Waters (51) have shown by a two-dimensional X-ray analysis of bis(salicylaldehyde)isopropylenedi-imine-copper(II)monohydrate that the copper is penta-coordinate. The ligands were arranged in a square pyramidal configuration with four planar bonds and a fifth Cu-O bond perpendicular to this plane with a length of  $2.53\text{\AA}$ .

There have been several dimeric copper(II) complexes reported in which the copper was five-coordinate and invariably square pyramidal. Frasson and co-workers (54) have reported the crystal structure of copper-dimethylglyoxime dimer. In addition to the four nitrogen atoms in the plane surrounding the copper atom they found a fifth coordinated oxygen from a nearby molecule lying at the apex of a tetragonal pyramid. Bevan and co-workers (55) have reported two dimeric structures analogous to the one mentioned above. The anhydrous bis-(salicylaldehydato)copper(II) and bis(8-hydroxyquinalinato)copper(II) were found to contain copper atoms surrounded by a tetragonal pyramidal arrangement. Barclay and

Kennard (56) have reported that royal blue anhydrous copper(II) formate consist of copper atoms joined together by formate groups in a bridging arrangement such that each copper atom has a distorted tetragonal pyramidal coordination. Hall and Waters (57) have shown that bis-(salicylaldhyde)ethylenedi-imine copper(II) is dimeric and similar to copper dimethylglyoxime (54) with a distorted configuration around each copper atom. Pignedoli and Peyronel (58) have reported that bis(N,N-di-n-propyldithiocarbamate)copper(II) is dimeric and that each copper atom is penta-coordinate with a distorted square pyramidal geometry. Barclay and co-workers (59) have indicated that in acetylacetonato-o-hydroxyanilato copper(II) one of the two nonequivalent copper environments is that of a distorted square pyramid. The other copper environment has a square planar configuration.

Lippert and Truter (60) have reported the preparation and crystal structure of monoaquobis(acetylacetonato)zinc. The structure determination has shown that the complex is five-coordinate with a trigonal bipyramidal configuration. The water molecule and one oxygen atom from each acetylacetone group lay in the trigonal plane; the other two oxygen of the chelating groups were at the apexes of the bipyramid. Montgomery and Lingafelter (61) have also published a crystal structure of the monoaquobis(acetylacetonato)zinc. They indicated some errors present in the previous determination; however, the main features were as described previously. They insisted, however, that the oxygen configuration was intermediate between a tetragonal pyramidal and a tetragonal bipyramidal structure, although somewhat nearer to the former.

Morgan and Burstall (53) have prepared a number of complexes of

the type  $M(\text{terpyl})X_2$  where  $M$  = metal; terpyl = 2:6-di-2'-pyridylpyridine; and  $X$  is an univalent anion. Corbridge and Cox (62) have reported the crystal structure of the  $Zn(\text{terpyl})Cl_2$  compound which they found to be five-coordinate. They also reported that the corresponding cadmium and copper compounds were isomorphous with the zinc compound. (Ibers (22) has questioned their judgement that the compounds were isostructural.) The zinc atom was found to be in a distorted trigonal bipyramid with the central nitrogen atom and the two chlorides in the trigonal plane. The distortion consisted mainly of a deflection of the two axial bonds of the bipyramid to accomodate the terpyridyl molecule.

The monohydrate of  $N,N'$ -disalicylideneethylenediaminezinc(II) has been found by Hall and Moore (64) to have a five-coordinate configuration. The two nitrogen and two oxygen atoms of the ligand were found in a plane and the zinc atom was  $0.34\text{\AA}$  above this plane on a line perpendicular to the center of the square plane.

Vaska (14) has prepared the dibromotris-(triphenylphosphine)-osmium(II) and the dichlorotris-(triphenylphosphine)ruthenium(II) complexes. A preliminary X-ray examination indicated that they were probably isostructural. LaPlaca and Ibers (13) have reported the crystal structure of the dichlorotris-(triphenylphosphine)ruthenium(II) complex. The structure consisted of individual monomers with the ruthenium located at the center of a distorted square pyramid, trans-chlorine atoms and trans-phosphorous atoms in the base and an apical phosphorous atom. They have indicated that the stability probably arises from intramolecular blocking of the unused octahedral site by the phenyl ring. The closest approach to the ruthenium atom was made by a hydrogen atom on a  $\beta$ -carbon atom

(Ru-H distance = 2.59Å). Chatt and Underhill (65) have presented some evidence of five-coordination in the bromo-1-naphthylbis-(diethylphenylphosphine)rhodium(III) complex. They also postulated that the stability of their complex resulted from a shielding of the metal atom by the bulky ligand.

Sacconi and co-workers (67) have recently prepared a series of five-coordinate complexes with the general formula bis(N-methylsalicyldiminato)metal(II) where metal represent Mn, Co and Zn. They found all to be mutually isostructural. Orioli and co-workers (66) have examined the zinc complex by a three dimensional X-ray analysis. The molecule consisted of dimers formed by sharing two oxygen atoms. The individual zinc atoms were five-coordinated and were in a distorted trigonal bipyramidal environment of two nitrogen and three oxygen atoms. The magnetic properties indicated a high spin complex for the manganese and cobalt complexes.

Two iron porphyrins have been examined by X-ray diffraction methods. These were ( $C_{34}H_{32}N_4O_4FeCl$ ),  $\alpha$ -chlorohemin, (68) and methoxy-iron(III)mesoporphyrin-IX-dimethyl ester (69). In both structures the iron was in an environment of a square pyramid with the iron slightly above the basal plane in both instances.

As a last example, Dodge and co-workers (21) have determined the crystal structure of vanadyl bisacetylacetonate. They found each vanadium atom to exist in a five-coordinate environment with five oxygen neighbors at the corners of a nearly square pyramid. The vanadium atom was found near the center of gravity of the pyramid rather than at the center of the basal plane.



### Complexes Suspected of Being Five-Coordinate

There are many reports of five-coordination that are based on spectroscopic, magnetic or other indirect measurements. Some are very interesting and certainly worthy of additional investigation. The following section will be devoted to some of the more promising examples which are suspected of being five-coordinate; Table 2 is a synopsis of those to be briefly discussed.

Two isomers of cobalt(II)bromide with diphenylphosphine (abbreviated DPP) have been prepared by Issleib and Wenschuh (71). They have suggested a trigonal bipyramidal structure for the brown isomer. Hayter (72) has prepared the dibromo- and diiodotris(diphenylphosphine)nickel(II) complexes analogous to the cobalt complex (brown isomer). He has postulated a square pyramidal structure and based this conclusion on a similarity of the solution spectra to that of the solution spectra of the  $\text{NiX}_2(\text{triarsine})$  complexes (33). The structures of these complexes (70) will be reported in detail in Chapter VII as a part of this thesis.

Jensen and Nygaard (73) reported in 1949 the isolation of the compound  $\text{NiBr}_3(\text{Et}_3\text{P})_2$ . They found the compound to be monomeric in benzene, to have a magnetic moment of 1.8 B.M. (low spin  $d^7$  configuration), and to have a dipole moment of about 2.5 D in benzene. On the basis of the dipole moment, they proposed a square pyramidal structure. This complex has been cited in most texts as a stereo-chemical example of a square pyramid. However, in 1963 Jensen(74) reported that the analogous cobalt complex ( $\text{CoCl}_3(\text{Et}_3\text{P})_2$ ) had a zero dipole moment in a pentane solution. This ruled out the earlier postulated configuration and indicated a structure more in accordance with a trigonal bipyramidal configuration.

Table 2. Possible Five-Coordinate Compounds

complex	d-shell	references	additional notes
1. $M(DPP)_3X_2$	7,8	70,71,72	low spin, $M = Co, Ni$ , $X = Br, I$
2. $(MX(QP))^+$	6,7,8	40,41,42 43,44	discussed in structure section, $(PtI(QAS))^+$ $M = Fe, Co, Ni, Rh, Pd, Pt$
3. $MBr_3(PEt_3)_2$	6,7	73,74,75 76	$Co(III), Ni(III)$
4. $(Ni(P(o-C_6H_4SCH_3)_3X))^+$	8	77,78	also neutral ligand complex $X = I, Br, Cl, NCS$ $L = thiourea, PH_3P, PH_2PCH_3$
5. $(Ni(TAP)X)^+$	8	79	also hydrate $(Ni(TAP)H_2O)^{++}$
6. $Pd(DPP)_3X_2$	8	80	-
7. $(M(trenMe)X)X$	7,8,9	81	$M = Co, Ni, Cu$
8. $M(dienMe)X_2$	5-10	82	$M = Mn-Zn$
9. $(Cu(NO_2)_5)^{-3}$	9	83	-
10. $Co(MNT)_2L$	6	84	$L = PH_3P, pyridine$
11. $Fe(L^1)_3X_2$	6	85	-
12. $(MnCl_5)^{-2}$	4	86	-
13. $VCl_3(OPR_3)_2$	2	87	-
14. $MCl_3(NMe_3)_2$	1,2	88,89	$M = Ti(III), V(III)$

note: TAP = tris(3-dimethylarsinopropyl)phosphine  
 TrenMe = tris(2-dimethylaminoethyl)amine  
 dienMe = bis(2-dimethylaminoethyl)methylamine  
 MNT =  $(N \equiv C) - C \equiv C - (C \equiv N)$   
 $\begin{array}{c} | \quad | \\ S \quad S \end{array}$   
 $L^1$  = cyclohexylphosphine

Recently, Jensen and Jorgensen (76) have discussed the charge transfer spectra of the cobalt(III) complex in terms of a trigonal bipyramidal structure.

Dyer and Meek (77) have recently reported a new tetradentate ligand, tris(o-methylthiophenyl)phosphine,  $P(o-C_6H_4SCH_3)_3$ , which with nickel (II) formed a series of complexes with the stoichiometry  $[Ni\{P-(o-C_6H_4SCH_3)_3\}X]^+$  ( $X = I, Br, Cl, \text{ or } NCS$ ) or  $[Ni\{P-(o-C_6H_4SCH_3)_3\}L]^{2+}$  ( $L = \text{thiourea, triphenylphosphine or methyldiphenylphosphine}$ ). The halide complexes,  $[Ni\{P-(o-C_6H_4SCH_3)_3\}X]^+$ , were all diamagnetic and 1:1 electrolytes in nitromethane. The intensity of the lowest energy transition indicated a non-centrosymmetric structure. Dyer and Meek have postulated a trigonal bipyramidal structure based on the visible and ultraviolet solution spectra. They (78) have also indicated that two tridentate ligands, phenylbis(3-dimethylarsinopropyl)phosphine and phenylbis(o-methylthiophenyl)phosphine formed five-coordinate complexes with nickel(II).

Complexes (79) of the type  $[Ni(TAP)X]^+$  and  $[Ni(TAP)H_2O]^{2+}$  (where TAP = tris(3-methylarsinopropyl)phosphine) appeared to exhibit five-coordination on the basis of their diamagnetism, conductivity and absorption spectra. The author reported that the phosphine apparently functioned as a tetradentate ligand. From the absorption spectra they postulated three possible isomers of trigonal bipyramidal geometry.

Hayter (80) has reported the isolation of a complex of formula  $(Pd(DPP)_3Br_2)$  from a reaction of diphenylphosphine with palladium(II) bromide. The molecular weight and conductivity data indicated partial dissociation in solution; however, the dark red color in solution may

have indicated the presence of the non-ionic five-coordinate complex. At the present time no additional work has been reported on this system.

The quadridentate ligand tris(2-dimethylaminoethyl)amine (trenMe) with cobalt, nickel and copper(II) formed high spin complexes (81) which were reported to be five-coordinate. Conclusions concerning the stereochemistry of these complexes were based on absorption spectra. The authors reported that the spectra approached more nearly that predicted for a trigonal bipyramidal complex.

Complexes with the bivalent transition ions from manganese to zinc having the formula  $[M(\text{dienMe})X_2]$  (where  $\text{dienMe} = \text{bis}(2\text{-dimethylaminoethyl})\text{methylamine}$ ) have been reported by Crompolini and Speroni (82). The complexes are all of the high spin type and experimental data indicated a coordination number of five. The spectra of these complexes have been given in evidence of a distorted trigonal bipyramidal configuration.

Bernal (83) recently has reported electron spin resonance measurements on potassium pentanitrocuprate(II),  $K_3Cu(NO_2)_5$ . The data demonstrated only that the complex had to be axially elongated and no further information was derived about the conformation from the results.

In acetone solutions the square planar complex  $Co(MNT)_2^-$  ( $MNT = (N \equiv C)C \equiv C(C \equiv N)$ ) has been reported (84) to add a monodentate ligand such as pyridine or triphenylphosphine and become five-coordinate. The following two complexes have been reported  $[(M-C_4H_9)_4N][Co(MNT)_2C_5H_5N]$  and  $[(M-C_4H_9)_4N][Co(MNT)_2(PPh_3)]$ . The complexes were diamagnetic and a square pyramidal geometry has been suggested.

Issleib and Roloff (85) have prepared a tris(cyclohexylphosphine) iron(II) dibromide complex which has a five-coordinate stoichiometry.

The complex was found to be a non-electrolyte and monomeric in solution. It exhibited an unusually high magnetic moment of 3.48 B.M. On the basis of this data they have predicted a five-coordinate species with a trigonal bipyramidal configuration.

A deep green manganese(III) complex with the empirical formula  $(\text{Et}_4\text{N})_2(\text{MnCl}_5)$  has been reported by Gill (86). He was not able to determine the molecular weight of the compound because of its instability; therefore he has proposed either a monomeric five-coordinate or a dimeric six-coordinate structure for the manganese(III) ion.

Issleib and Bohn (87) have prepared vanadium(III) complexes of the type  $\text{VCl}_3(\text{OPR}_3)_2$  where the ligand was either a phosphine or phosphine oxide. These showed non-electrolyte behavior and were postulated to have a coordination number of five.

Complexes of the type  $\text{MCl}_3(\text{NMe}_3)_2$  have been reported (88,89) for both titanium(III) and vanadium(III). These were somewhat difficult to prepare and were not very stable; however, some chemical evidence was presented which indicated a five-coordinate species.

## CHAPTER III

## REVIEW OF SPECTRAL ASPECTS OF FIVE-COORDINATION

Crystal Field Theory

Becquerel (90) was the first to formulate the basic idea of crystal field theory which was that the metal ion in a complex was subjected to an electric field originating from the ligand. Bethe (91) formulated these ideas into a theory which in part was concerned with the qualitative consequence of the symmetry of the surrounding ligands in the crystalline lattice. He showed that the degenerate free ion states arising from a particular electronic configuration must split into two or more states when the ion was introduced into a crystalline lattice. He employed group theory in order to determine just what states resulted when an ion of particular electronic configuration was introduced into a particular symmetry environment. Bethe also calculated the magnitude of the splittings of the free ion states by assuming that the surroundings affected these splittings in a purely electrostatic manner. This electrostatic treatment was the defining feature of crystal field theory. Van Vleck (92, 93) later indicated that Bethe's symmetry arguments were valid even if the change was made from a purely electrostatic treatment to one which considered covalent bonding between the metal ion and its ligands. A combination of Van Vleck's and Bethe's ideas along with molecular-orbital (94) theory essentially defined the more sophisticated ligand field approach.

### Electronic Configuration of Free Ion

For a given  $d^n$  configuration several terms are possible and these are characterized by the quantum numbers  $L$ ,  $S$  and  $J$ . These terms are all degenerate if electron-repulsion and spin-orbit interaction are neglected. However, this approximation is unrealistic. But, if spin-orbit interaction is ignored, then  $L$  commutes with the Hamiltonian operator and is quantized. Thus, electron repulsion splits the degeneracy to give terms characterized by  $L$  and  $S$  (95). If now spin-orbit interaction is introduced as a small perturbation, through a  $\vec{L} \cdot \vec{S}$  term in  $H$ , then states with given  $L$  and  $S$  which are still degenerate are split and each final state is properly characterized by  $J$ . The notion of  $jj$  coupling refers to inclusion of  $\vec{l} \cdot \vec{s}$  for each electron before electron-repulsion such that the latter is introduced as a small perturbation. Actually, the only rigorous quantum number is  $J$  and the transition from  $L, S \rightarrow jj$  coupling is a smooth one with states of different  $L$  and  $S$  but same  $J$  mixing.

However, the  $L, S$  coupling scheme is a useful approximation and is employed for the ions of the first and second transition series. The more complex  $jj$  scheme is employed in general with the third transition series as well as with the lanthanide and actinide series.

For more than one electron beyond the closed shells,  $L$  is given by the vectorial sum:  $L = l_1 + l_2 + \dots + l_n$  where the  $l$ 's refer to the  $l$  quantum number of the individual electrons in the unfilled valence shell. The value of total spin angular momentum is given by the vectorial sum of the  $S$  values for the separate valence electrons, however, subject to the Pauli Exclusion Principle. The states which may arise by  $L, S$  coupling from all  $d^n$  configurations are listed in Table 3.





The L,S coupling scheme indicates which terms arise from a particular electronic configuration, but, in addition to the nature of the states, we must decide upon their relative energies. These energies have been determined experimentally for a large number of ions and standard tabulations are available (97). Normally those states of greatest multiplicity and largest L value will lie lowest in energy (Hund's rule).

### Splitting of Terms in a Chemical Environment

Weak Field Treatment. In the weak field approach (98) the crystal field (perturbation) is assumed small with respect to the separation of free ion terms. In the weak-field case, the L and S quantum numbers for the central ion are valid and the problem is to determine how a given L,S term is split by a particular ligand symmetry without considering the possibility of the different levels interacting. The qualitative features of the crystalline field splittings are obtained by group theory. In a particular environment the orbitals will transform in a manner which will be characterized by the irreducible representations of the symmetry group determined by the crystal field. The character ( $\chi$ ) of the representation (a character is the sum of the diagonal elements of a square matrix) based on the set of  $(2L + 1)$  wave functions with quantum number L in a particular point group may be found from the following formulas (99) which indicate the character of a rotation about an arbitrary axis through the angle  $\alpha$ ,

$$\chi(\alpha) = \frac{\sin(L + \frac{1}{2})\alpha}{\sin(\alpha/2)}$$

and reflection through an arbitrary plane  $\sigma$ ,

$$\chi(o) = +1.$$

This set of  $(2L + 1)$  degenerate basis functions may give matrices which are reducible or irreducible in the crystal field group. If the representation is reducible (indicating splitting in the crystal field ion), it may be reduced to a set of irreducible representations corresponding to the ion states which are produced by this field.

The splittings of the various atomic states in various symmetries have been determined for the more common point groups. The author has derived the splittings in the  $C_{4v}$  symmetry from the correlation tables found in Wilson, Decius and Cross (100). This was possible because  $C_{4v}$  is a subgroup of the common  $O_h$  point group. McClure (101) has derived the corresponding states in  $D_{3h}$  symmetry; this point group is not a subgroup of the common  $O_h$  point group. Table 4 lists the splittings of the free ion terms in field of  $C_{4v}$  and  $D_{3h}$  symmetries.

Table 4. Splittings of One-Electron Levels in  $C_{4v}$  and  $D_{3h}$  Symmetries

Type of Atomic Term	$C_{4v}$	$D_{3h}$
S	$A_1$	$A'_1$
P	$A_1 + E$	$A''_2 + E'$
D	$A_1 + B_1 + B_2 + E$	$A'_1 + E' + E''$
F	$A_1 + B_1 + B_2 + 2E$	$A'_1 + A'_2 + A''_2 + E' + E''$
G	$2A_1 + A_2 + B_1 + B_2 + 2E$	$A'_1 + A'_1 + A''_2 + E'' + 2E'$
H	$2A_1 + A_2 + B_1 + B_2 + 3E$	$A'_1 + A'_2 + A''_2 + 2E'' + 2E'$
I	$2A_1 + A_2 + 2B_1 + 2B_2 + 2E$	$2A'_1 + A'_2 + A'_1 + A''_2 + 2E'' + 2E'$

The states into which a particular free ion term is split have the same spin multiplicity as the parent term because the chemical environment is assumed not to interact directly with the electron spins.

Strong Field Treatment. In the strong field approach (102) the crystal field splitting is assumed so large that the torques exerted on the orbital motions of the electrons are determined by the lattice site symmetry, rather than by the correlative interactions between the electrons. The perturbation due to the external field is considered larger than electron repulsion and the atomic orbitals are first split according to the field symmetry, then used as bases for the ion configuration. The quantum numbers  $L$  and  $S$  are no longer significant. The electronic state of the ion is now determined by the configuration and the specified occupation numbers. In the cases of interest, the lowest state for the  $D_{3h}$  symmetry arises by the  $e''$  state filling first to a maximum of four electrons, then the less stable  $e'$  state fills to a maximum of four electrons, then the  $a_1'$  which is highest in energy accomodates the two additional electrons. The order of filling for the  $C_{4v}$  is  $e$ ,  $b_2$ ,  $a_1$  and  $b_1$  respectively from lowest to highest energy. Figure 1 shows the strong field splittings of the d-orbitals in the five-coordinate environments; the octahedral splittings are also given as a comparison of the relative energies involved (17).

For a specified configuration several terms may arise due to electron repulsion. These terms may be found by reducing the direct product representations corresponding to the configuration with suitable considerations of the restrictions imposed by the Pauli Exclusion Principle.

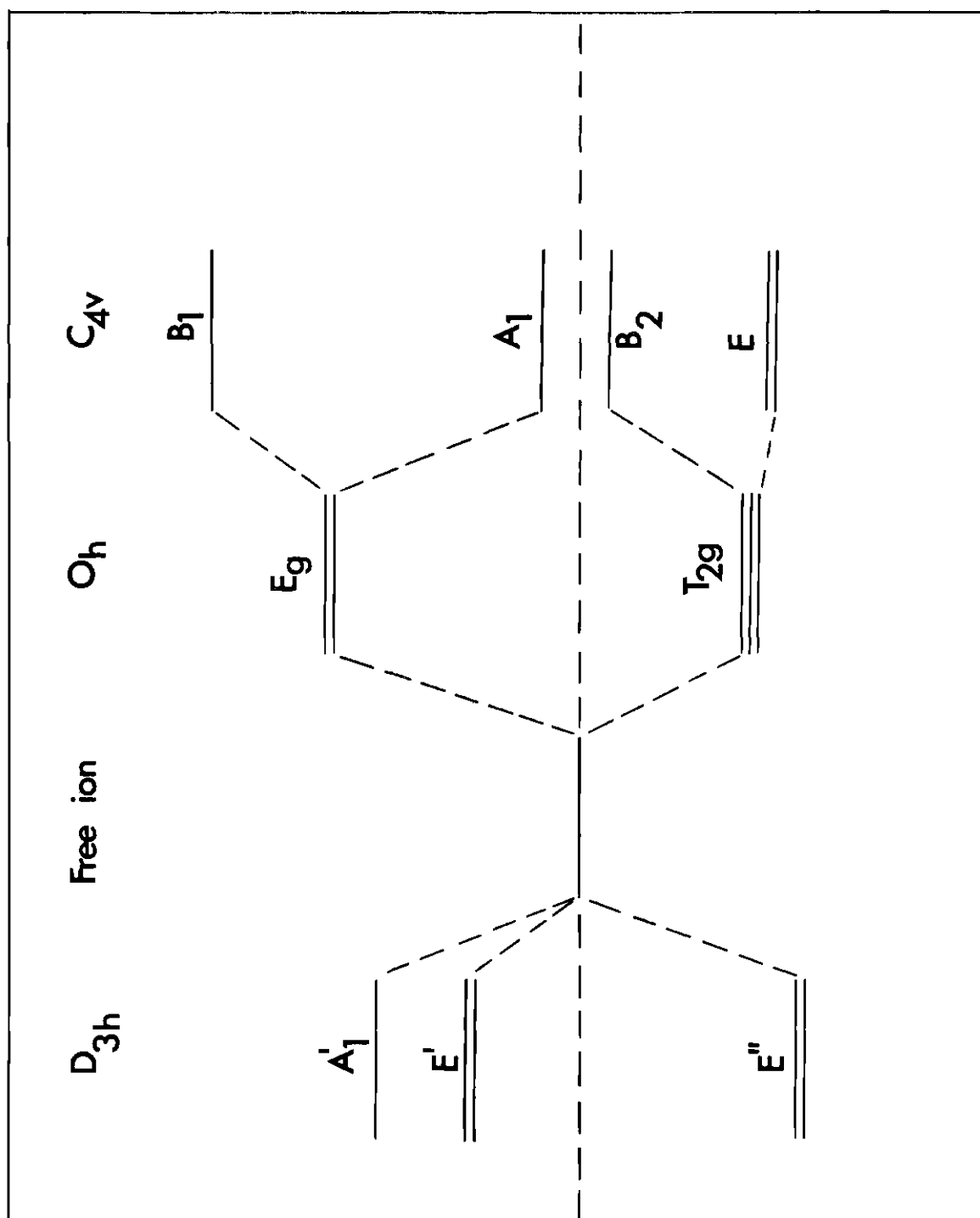


Figure 1. Strong Field Splittings of the d-Orbitals in the Five-Coordinate Symmetries

Intermediate Field. The fields of intermediate strength may be approached either from the weak-field or from the strong-field limits. The two approaches must yield identical results if each is solved exactly. As the interaction with the environment goes from weak to strong, the symmetry properties of the ionic states in the field do not change in any way; therefore there must exist a one-to-one correspondence between the states at the two extremes (96).

#### Correlation Diagrams

The correlation diagram is a combination of the weak-field and the strong-field approach; it shows how the energy levels behave as a function of the strength of interaction. Normally the diagrams are constructed so that the right side corresponds to the strong-field limit and the left side to the weak-field limit. The two sides of the diagram can then be correlated since a one-to-one correspondence of states of the same symmetry must exist and states of the same spin degeneracy and symmetry cannot cross (96).

The Hole Formalism. According to the hole formalism, a  $d^{10-n}$  configuration will behave, at all points along the abscissa of the energy diagram, in the same way as the corresponding  $d^n$  configuration, with the exception that all energies of interaction with the environment will have the opposite sign. Therefore  $n$  holes in a  $d$ -shell may be treated as  $n$ -positrons and will correspond to  $n$ -electrons in an inverted arrangement.

#### Spectra of Transition Metal Complexes

An important use of correlation diagrams is in the interpretation of spectral and magnetic properties of complexes. The near infrared,

visible and near ultraviolet spectra of transition metal ions are due in part to d-d transitions from a stable ground state to various excited states illustrated on the correlation energy level diagrams (Chapter VI). The following section will be devoted to a discussion of selection rules and mechanism which allow these d-d transitions.

### d-d Transitions

The intensity of a transition between the ground state  $\psi$  and some excited state  $\psi'$  is proportional to the square of the transition moment,  $Q$ , defined by:

$$Q = \int \psi^* \sum q_i \psi' d\tau = \int \psi_{\text{space}}^* (\sum q_i) \psi'_{\text{space}} d\tau_{\text{space}} \int \psi_{\text{spin}}^* \psi'_{\text{spin}} d\tau_{\text{spin}}$$

where  $\sum q_i$  is the electric dipole operator and where the factoring is possible only if spin-orbit interaction is ignored. The integral will vanish unless the spin functions  $\psi_{\text{spin}}$  and  $\psi'_{\text{spin}}$  are identical (no change in multiplicity). However, spin allowed d-d transitions are forbidden by an electric dipole mechanism because of Laporte's Rule. This rule stems from the fact that d-orbitals are symmetric with respect to inversion through the center of symmetry; the d-orbitals are even functions. However, the electric dipole operator is an odd function and changes sign upon inversion. Therefore, the transition moment integral between two d-orbitals will change sign upon inversion, but the values of the integral must be independent of the choice of the coordinate systems; it follows then that it must vanish.

However, such d-d transitions are observed and can be classified into two types.

### Electronic Allowed d-d Transitions. Electronic allowed

transitions occur in noncentrosymmetric complexes and are due to a mixing by the external field of the d- and p-states. The d-states are no longer pure (even) functions but are mixed with p- (odd) functions. This causes Laporte's rule to be weakened and results in transitions of oscillator strength less than expected for even-odd transitions.

Vibronic Allowed d-d Transitions. Transitions occur by an electric dipole mechanism for centrosymmetric complexes, but these transitions have much lower oscillator strengths than those of the electronic allowed transitions. These oscillator strengths are too large to be due to either electric quadrupole and/or magnetic dipole radiation. Also symmetry arguments have been used to eliminate electric quadrupole and magnetic dipole mechanisms for the 3d complexes; these mechanisms do not predict all the transitions that are observed. These transitions are, therefore, electric dipole in character and the g-character of the states must be removed to a small extent in either the excited or ground state by vibration-electronic interaction. An ungerade perturbing vibration is superimposed on the electronic wave function. Such transitions depend, therefore, upon the extent to which the perturbing vibrations can distort the electronic wavefunction.

### Symmetry Selection Rules

Since the eigenfunctions for the molecule are bases for irreducible representations of the symmetry group to which the molecule belongs, integrals of the form  $\int \psi^* \sum q_i \psi' d\tau$ , can be different from zero only if the integrand is invariant under all symmetry operations of the group. The direct product,  $\psi^* \sum q_i \psi'$ , must then form a basis for the totally symmetric representation of the group. Therefore, one of the irreducible representations occurring in the direct sum (derived from the reducible

representation which resulted from the direct product) must be the totally symmetric one; otherwise the integral will have a value of zero. From symmetry arguments, one can investigate whether the integral has a finite magnitude along a particular axis corresponding to the x, y or z component of  $\sum q_i$ . For the less symmetrical point groups such as  $C_{4v}$  and  $D_{3h}$ , the x, y and z axes do not all belong to the same representation; therefore the phenomenon of polarized absorption will be encountered.

#### Site-Symmetry Approach

The usual inorganic approach to the problem of solid state absorption spectra is based on a symmetry group determined by the site-symmetry. The selection rules used in this approach are determined by the symmetry of the complex ion and the orientation of the other complex ions within the unit cell. The more sophisticated approach to the problem is the exciton (103) approach, which takes into consideration intercomplex interactions. In this approach the selection rules are no longer determined by the site group symmetry but by the factor group, which represents the symmetry of the entire unit cell.

Winston and Halford (104) have discussed the relations between the factor group and the site group analysis of vibrational spectra. The approach that they have recommended to the interpretation of the infra-red spectrum of a crystal is:

"to carry out first a site analysis (which often does not require a map of the unit cell). This will yield an adequate interpretation for the grosser, if not all, the details of the spectrum. If finer details remain to be explained, resort may then be had to the unit cell analysis."

The following statements were made about the differences between the site group and the factor group analysis. These differences correspond



essentially to the coupling of vibrations between occupants of different sites in the unit cell.

1. A motion which is a member of a degenerate set under the site group (S) will still be a member of a degenerate set in the factor group (F); the motion cannot go into a representation of F which has smaller dimensionality than its representation in S.

2. A motion will not be assigned spectral activity in F and inactivity in S; the dipole moment and polarizability character are the same for the common elements of S and F.

3. A depolarized motion in S will not become polarized in F.

4. Motions may become more degenerate in F than in S; may lose spectral activity or become depolarized.

5. A band from S may become several times duplicated under F. Most of these relations are the consequence of the site group being necessarily isomorphous with some subgroup of the factor group. Therefore, the presence of an effect predicted from the site analysis seems to be valid; however, the absence of a predicted effect might require careful consideration.

#### Detailed Treatment of Splittings

Many theoretical treatments have been made for the energy levels of six- and four-coordinate complexes; however, no detailed treatment has been reported for five-coordinate systems. Recently, a point dipole treatment (105) has been performed on the  $d^8$  high-spin (weak field) configuration in a five-coordinate environment. Also a molecular orbital treatment (106) and a point dipole treatment (107) have been made on the  $d^9$  configuration in a trigonal bipyramidal environment. The following

section will be devoted to a brief discussion of these treatments.

Ciampolini (105) has calculated the splitting of the terms of the free nickel(II) ion in fields of five point dipoles arranged in  $D_{3h}$  and  $C_{4v}$  environments. He employed the weak-field scheme with interaction of configurations in his calculations. He compared the spectra of two high-spin nickel(II) complexes (35, 67) of approximately  $C_{4v}$  and  $D_{3h}$  stereochemistries with those predicted from the point dipole model. He found the agreement to be satisfactory. The predicted and calculated values are listed in Table 5.

Hatfield, Bedon and Horner (106) have used a molecular orbital approach (modified Wolfsberg-Helmholz method) to calculate the energy levels in the pentachlorocuprate(II) ion. Their predicted transitions agreed rather well with the observed spectrum. The assignments of the bands and energies of transitions are indicated in Table 6.

Day (107) has applied the point-charge crystal field model to the pentachlorocuprate(II) ion. He reported only one band ( $9,500\text{ cm}^{-1}$ ) in the single crystal spectrum, however, Hatfield (106) resolved this band into two bands ( $8,200$  and  $10,400\text{ cm}^{-1}$ ) at liquid nitrogen temperatures. Day (107) calculated the energy of the  ${}^2A'_1 \longrightarrow {}^2E''$  transitions (excited state assignment appears wrong, a transition to the  $E'$  state was allowed but to the  $E''$  state was forbidden by dipole selection rules) to be  $9,500\text{ cm}^{-1}$  as compared to his observed band at  $9,500\text{ cm}^{-1}$ .

Table 5. Predicted and Observed Spectra of Five-Coordinated High-Spin Nickel(II) Complexes

symmetry	reference	predicted trans.	calc. freq.(cm <sup>-1</sup> )	obs. freq.(cm <sup>-1</sup> )
D <sub>3h</sub>	71	<sup>3</sup> E' → <sup>3</sup> E''	7,000*	7,500
		→ <sup>3</sup> A <sub>1</sub> '', <sup>3</sup> A <sub>2</sub> ''	13,000	14,400
		→ <sup>3</sup> A <sub>2</sub> ''	14,900	
		→ <sup>3</sup> E''	22,500	
		→ <sup>3</sup> A <sub>2</sub> '**	26,200	
<hr/>				
C <sub>4v</sub>	32	<sup>3</sup> B <sub>1</sub> → <sup>3</sup> E	7,200***	7,700
		→ <sup>3</sup> A <sub>2</sub>	10,800	9,900
		→ <sup>3</sup> B <sub>2</sub>	12,300	12,600
		→ <sup>3</sup> E	17,300	16,500
		→ <sup>3</sup> A <sub>2</sub> **	26,400	
		→ <sup>3</sup> E	28,400	

\* dipole strength assumed to be 5.20 D.

\*\* two electron transition.

\*\*\* dipole strength assumed to be 4.85 D.

Table 6. Calculated and Observed Transitions in  $\text{CuCl}_5^{3-}$ 

obs. freq. ( $\text{cm}^{-1}$ )	orbital assignment	calc. freq. ( $\text{cm}^{-1}$ )
8,200	$a_1' \longrightarrow e'$	7,700
10,400	$\longrightarrow a_2''$	9,400
	$\longrightarrow e'$	9,500
	$\longrightarrow e'$	10,200
24,000	$\longrightarrow a_2''$	21,300
26,000	$\longrightarrow e'$	26,400

## CHAPTER IV

### INSTRUMENTATION

#### X-Ray Studies

##### Powder Diffraction

X-Ray powder patterns were obtained with a Phillips diffractometer, using Cu K $\alpha$  radiation. Several packings were run, and some preferred orientation was observed. The intensities of the pattern were evaluated in terms of very strong, strong, medium and weak.

##### Single Crystal Equipment

The reciprocal lattice data were recorded photographically using a precession camera, MoK $\alpha$  radiation, and a Picker X-ray generator.

#### Magnetic Studies

Magnetic susceptibilities were determined by the Gouy method. The Gouy balance used consisted of a Newport Instruments electromagnet equipped with a Mettler Type H 16 microbalance. In order to eliminate errors due to air drafts, a glass jacket was fitted between the poles of the electromagnet and was extended to the base of the balance. The power supply was capable of supplying current up to 9.0 amperes, which corresponded to a magnetic field range of zero to 12,000 gauss. Several readings at different magnetic fields were recorded for each sample. Diamagnetic corrections were obtained by addition of tabulated atomic diamagnetism corrections (108).

All of the magnetic measurements were made on solid samples which were finely ground with a mortar and pestle. The mercury

tetrathiocyanatocobaltate(II) complex (109) was used as a standard for tube calibration; a value of  $16.44 \times 10^{-6}$  c.g.s. was employed as the gram susceptibility of the standard.

### Spectral Studies

#### Solution and Mull Spectra

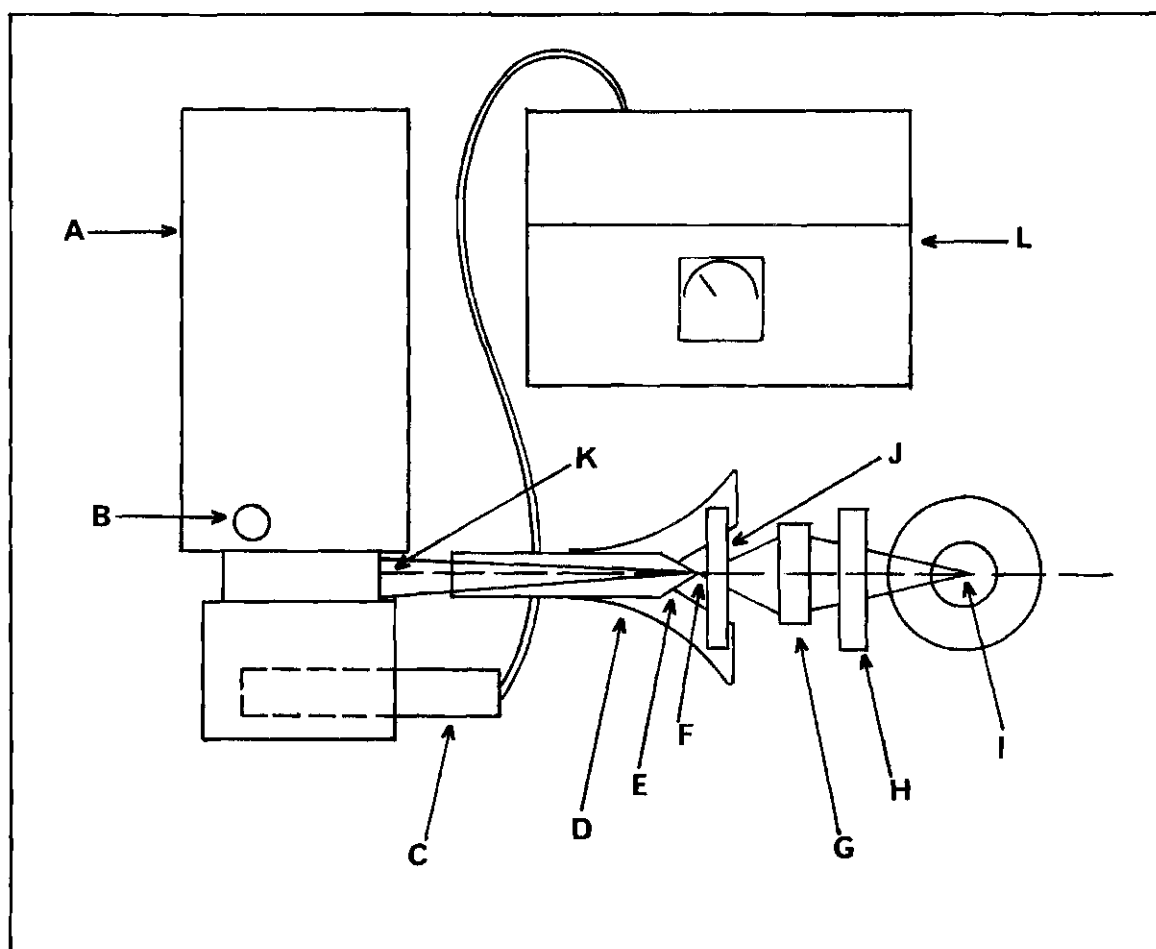
The absorption spectra were obtained on a Cary Model 14 spectrophotometer and on a Bausch and Lomb Spectronic 505 spectrophotometer. Solution spectra in the visible and near infrared were obtained with a 1 cm pair of matched cells. Solid spectra were obtained by the mull technique using hexachlorobutadiene as the mulling liquid.

#### Microspectrophotometer

Single crystal spectra were obtained with a single beam spectrophotometer constructed from a Beckman DU monochromator and a Photovolt 520-M photometer. A type 21-C photomultiplier tube was used for the visible region and a 71-D photomultiplier tube was used for the near infrared region. The light source employed was a Pointolite lamp of 100 c.p. A microscope was used to focus an enlarged image of the crystal on the slit of the monochromator. Polaroid linear polarizers were employed when polarized spectra were desired. Polaroid type HN38 was employed for the range 400-850 mμ and type HR for the range 800-1100 mμ.

The single crystals were mounted on a glass slide, the slide was placed on the microscope stage, and the optics were adjusted to focus an image of the crystal on the entrance slit of the monochromator. The microscope stage was then rotated to align the polarization of the crystal with the polarizer. The polarizer was capable of a 90° rotation so that both polarizations of the crystal could be recorded without moving

the crystal. A program of exit slit settings was determined over the workable wavelength range with continuous radiation in order to employ a horizontal base line. A diagram of the instrument is given in Figure 2.



- A = Beckman DU monochromator
- B = Exit slit control
- C = Photomultiplier tube assembly
- D = Microscope
- E = Objective lens (focal length of 16mm and magnification of X10 with numerical aperture of 0.25)
- F = Sample mounted on glass slide
- G = Lens (4 cm diameter and 9 cm focal length)
- H = Polarizer
- I = Pointolite lamp (100 c.p.)
- J = Microscope stage
- K = Entrance slit
- L = Photovolt 520-M photometer

Figure 2. Polarizing Microspectrophotometer



## CHAPTER V

## EXPERIMENTAL

Preparation of ComplexesDiphenylphosphine Complexes

Issleib and Frohlick (110) have reported the preparation of diphenylphosphine by the hydrolysis of potassium diphenylphosphide. The author has utilized a technique very similar to the one outlined by Issleib and Frohlick for the preparation of diphenylphosphine.

Into a three-neck flask (250 ml) were added, in the following order: 13.1 gm of triphenylphosphine, 100 ml of absolute dioxane, and 3.9 gm of potassium metal which was cut into small pieces under toluene. The flask was fitted with a condenser, a glass inlet tube, and stirrer. The reaction mixture was brought to reflux temperature and maintained for five to six hours with constant stirring under a nitrogen atmosphere. The reaction flask was then cooled and distilled water was added slowly with stirring under nitrogen until the potassium diphenylphosphide was hydrolyzed and all the excess potassium consumed. A solution of 1:1  $\text{HCl} \cdot \text{H}_2\text{O}$  was then added until the solution was acidic (checked with litmus). The diphenylphosphine was then extracted from the acidified solution with ether. The extracted ether layer was then stored under nitrogen and over anhydrous sodium sulfate. Five preparations were performed as indicated and combined. The solution was distilled under vacuum at a pressure of 12 mm. Approximately 13 gm of diphenylphosphine was obtained over a temperature range of 149–155°C. Wittenberg and Gilman (111) had previously

reported the boiling point of diphenylphosphine to be 150-154°C at 11 mm pressure.

A technique similar to the one reported by Hayter (72) for the preparation of the nickel complexes was employed to prepare the bromide and iodide complexes of both nickel and cobalt. Anhydrous cobalt halides were prepared by heating in vacuum at 135°C; however, the anhydrous nickel halides were prepared by refluxing the hydrates with 2,2-dimethoxypropane (112). The anhydrous metallic halides and diphenylphosphine dissolved in methylene chloride in mole ratios of one to four were refluxed for a short time with constant stirring. The intensely colored solutions were then filtered under nitrogen to remove any residual metallic halide. After filtration, n-hexane was added slowly over several hours until the complexes began to crystallize. After crystallization the complexes were separated by filtration through a sintered glass funnel, washed with n-hexane and dried in a vacuum desiccator over sulfuric acid. Analytical data are summarized in Table 7. All of the compounds except the cobalt iodide complex have been reported previously (71, 72). All of the complexes were easily recrystallized by first dissolving in methylene chloride and then adding n-hexane. The carbon and hydrogen analyses of these and subsequent compounds were performed by Galbraith Laboratories, Inc., Knoxville, Tennessee.

#### Pyridine N-Oxide Complexes

Tris(pyridine N-oxide)cobalt(II) Halides. The preparation of the tris(pyridine N-oxide)cobalt(II) bromide and chloride have been reported in the literature (113, 114). The author has followed a procedure similar to the preparation outlined by Quagliano and co-workers

Table 7. Analytical Data for  $M(DPP)_3X_2$ 

M	X	% Carbon		% Hydrogen	
		Calcd.	Found	Calcd.	Found
Co	Br	55.62	55.85	4.28	4.39
Co	I	49.62	49.83	3.82	4.02
Ni	Br	55.64	53.25	4.28	4.05
Ni	I	49.64	49.80	3.82	3.94

(113). The complexes were prepared by mixing absolute ethanol solutions of the anhydrous cobalt(II) halide and pyridine N-oxide in mole ratios of one to four respectively. The green solids were separated by filtration, washed with absolute ethanol and dried in a vacuum desiccator over sulfuric acid. Analytical data are summarized in Table 8.

Table 8. Analytical Data for  $Co(pyridine\ N\text{-}oxide)_3X_2$ 

X	% Carbon		% Hydrogen	
	Calcd.	Found	Calcd.	Found
Cl	43.39	43.45	3.64	3.89
Br	35.74	35.98	3.00	3.08

Hexakis(pyridine N-oxide)cobalt(II) Tetrabromocadmiate. A hot ethanol solution of anhydrous cobalt(II) bromide, anhydrous cadmium bromide and pyridine N-oxide in mole ratios of 1:1:6 was prepared and

allowed to cool (115). The blue solution yielded an orange-red solid on standing. The solid was separated by filtration, washed with absolute ethanol, and dried in a vacuum desiccator over sulfuric acid. Analytical data are summarized in Table 9.

Table 9. Analytical Data for  $\text{Co}(\text{pyridine N-oxide})_6\text{CdBr}_4$

% Carbon		% Hydrogen		% Cobalt	
Calcd.	Found	Calcd.	Found	Calcd.	Found
33.94	33.88	2.85	2.95	5.55	5.50

The cobalt content was determined spectrophotometrically using the tetra-n-butylammonium tetrabromocobaltate(II) complex (116) as a standard.

#### Iodobis(dipyridyl)copper(II) Iodide

This compound (48) was prepared by mixing copper nitrate, dipyridyl and potassium iodide in mole ratios, respectively, of one-two-two in a water-acetone mixture. A yellow-green solid immediately separated. The solid, after filtration, was easily recrystallized from nitromethane. From this was obtained long brown needles of iodobis(dipyridyl)copper (II) iodide.

#### X-Ray Diffraction Studies

#### Tris(pyridine N-oxide)cobalt(II) Halide Complexes

X-ray powder patterns are given for the tris(pyridine N-oxide)

cobalt(II) bromide and hexakis(pyridine N-oxide)cobalt(II) tetrabromocadmiate complexes. A comparison of intensities and interplanar spacings for these two complexes is presented in Table 10. A comparison of the powder patterns reveals that they are almost identical in both peak position and intensity, and the compounds, thus, appear to be isomorphous.

#### Tris(diphenylphosphine)metal(II) Halide Complexes

X-Ray Powder Patterns. X-ray powder patterns are given in Table 11 for the tris(diphenylphosphine)metal(II) halide complexes. A comparison of the patterns for the  $\text{Ni(DDP)}_3\text{I}_2$  and  $\text{Co(DDP)}_3\text{I}_2$  yield essentially identical intensities and interplanar spacings. Also a comparison of the  $\text{Ni(DDP)}_3\text{Br}_2$  and  $\text{Co(DDP)}_3\text{Br}_2$  yield almost identical patterns. Therefore the bromide pair and the iodide pair are isomorphous; however, there are slight differences both in intensities and in the d-spacings between the bromides and iodides. Therefore, the patterns do not prove conclusively that the bromides and iodides are isomorphous.

Unit Cell Determination. Single crystal data were recorded photographically using a precession camera and  $\text{MoK}\alpha$  radiation. A crystal, which appeared to be a single crystal when viewed under stereoscopic and polarizing microscopes, was chosen for mounting. The crystal was glued to a glass fiber which in turn was cemented to a metal pin; the metal pin was locked into the goniometer head and the crystal was visually aligned by adjusting the goniometer arcs. Final orientation was carried out on the precession camera using unfiltered radiation (117).

Data to determine space group and unit cell dimensions were obtained from zero level and upper level photographs of the two principal zones using filtered radiation. Unit cell determinations for the

Table 10. X-Ray Powder Patterns for the Pyridine N-Oxide Complexes

$(\text{CoL}_6)(\text{CdBr}_4)$		$\text{CoL}_3\text{Br}_2$	
d, Å	I*	d, Å	I
14.243	m	14.243	m
8.665	w	8.665	w
7.431	s	7.493	s
6.857	v s	6.857	v s
6.320	w	6.276	w
6.021	m	5.981	m
5.862	m	5.862	m
5.273	w	5.273	w
4.818	s	4.818	s
4.149	m	4.149	m
4.055	s	4.037	s
3.966	s	3.948	m
3.218	w	3.206	w
3.162	m	3.129	m
3.066	s	3.046	m

\*The symbols used to designate intensities are: s, strong; m, medium; w, weak; and v, very.

Table 11. X-Ray Powder Patterns for the Diphenylphosphine Complexes

Ni(DPP) <sub>3</sub> I <sub>2</sub>		Co(DPP) <sub>3</sub> I <sub>2</sub>	
d, Å	I*	d, Å	I
13.586	s	13.586	s
13.181	s	13.181	s
10.394	v s	10.394	v s
8.664	s	8.644	s
8.339	s	8.261	s
7.755	m	7.755	w
4.870	s	4.870	m
4.525	s	4.548	s
4.149	w	4.149	w
4.037	s	4.037	s
3.897	s	3.880	s
3.751	m	3.751	m
3.463	w	3.463	w
2.873	w	2.864	w
2.761	w	2.761	w
2.453	w	2.460	w

---

Ni(DPP) <sub>3</sub> Br <sub>2</sub>		Co(DPP) <sub>3</sub> Br <sub>2</sub>	
d, Å	I*	d, Å	I
13.586	m	13.586	m
13.181	m	13.181	m
10.273	v s	10.273	v s
9.710	w	9.710	w
8.499	s	8.499	s
8.185	s	8.185	m
7.755	w	7.755	w
7.557	w	7.557	w
6.411	w	6.411	w
5.063	w	5.063	w
4.818	w	4.844	m
4.436	v s	4.458	s
4.092	m	4.110	m
4.037	s	4.055	s
3.814	w	3.798	w
3.675	m	3.675	w
3.398	w	3.398	w
2.864	w	2.910	w
2.712	w	2.712	w

\*The symbols used to designate intensities are: s, strong; m, medium; w, weak; and v, very.

four diphenylphosphine compounds showed almost identical triclinic unit cells. These results along with the densities, which were obtained by the flotation method, are summarized in Table 12.

Table 12. Unit Cell Parameters\* for the  $M(DPP)_3X_2$  Compounds

M	X	a	b	c	$\alpha$	$\beta$	$\gamma$	d <sub>obs</sub>	d <sub>calc</sub>
Co	Br	11.05	11.47	15.41	98.0	82.9	118.5	1.51	1.52
Co	I	11.16	11.93	15.53	100.8	81.7	118.3	1.62	1.62
Ni	Br	11.05	11.47	15.41	98.0	82.9	118.5	1.51	1.52
Ni	I	11.16	11.93	15.53	100.8	81.7	118.3	1.62	1.62

\*All cell dimensions were obtained from measurements of precession photographs; the interaxial angles are accurate to about 5 minutes and the cell edges are accurate to about 0.2%.

Real cell constants were calculated from reciprocal cell constants using relationships given by Buerger (118). A computer program, written by the author, was used to evaluate the real cell constants and the calculated density (see appendix).

The densities calculated for two molecules per unit cell were 1.52 and 1.62 gm/cc for the bromide and iodide respectively, as compared to observed densities of 1.51 and 1.62 gm/cc.

Intensity Data. Photographs for determining intensities were recorded photographically with a precession camera using  $MoK\alpha$  radiation. A series of accurately timed exposures were taken at 2.4, 12, and 60 hours



for each layer. All exposures of a particular layer were developed simultaneously. The intensities were estimated visually using a calibration wedge prepared from the same crystal. Lorentz-polarization corrections were determined from templates (119, 120). No absorption corrections were made.

For the  $\text{Co(DPP)}_3\text{Br}_2$  crystal, data were collected for the  $h k x$  and  $x k l$  ( $x = 0-3$ ) zones. From a series of timed exposures, 1566 unique reflections were estimated visually. The observed structure factor data (square root of the corrected intensities) are reported along with calculated structure factors in Table 17 (located in Chapter VI).

For the  $\text{Ni(DPP)}_3\text{I}_2$  crystal, data for the  $h k 0$  and  $0 k l$  zones were collected and treated in the same manner as described for the  $\text{Co(DPP)}_3\text{Br}_2$  crystal. A total of 371 unique reflections were obtained. The observed structure factors are reported in Table 19 (located in Chapter VI).

### Magnetic Moment Determinations

#### Calculations

Tube Calibration. The calculation procedure and nomenclature for obtaining the tube calibration constant at given force field strengths are given below.

A = weight of empty sample tube, zero current.

B = weight of empty sample tube, at a given current.

C = weight of filled tube, zero current.

D = weight of filled tube, at a given current.

V = volume of tube in cc.

$\beta$  = tube calibration constant, at a given field strength.

$\gamma$  = temperature independent paramagnetism per metal ion.

T = absolute temperature.

$\chi_g$  = gram susceptibility.

$\chi_m$  = molar susceptibility.

$\mu_e$  = effective magnetic moment.

S = B - A = apparent mass change for empty tube.

E = D - C = apparent mass change for filled tube.

F = E - S = apparent mass change corrected for the diamagnetic character of the sample tube (mg).

$$\beta = \frac{(16.44)^*(C-A) - (0.029)**V}{F}$$

\* gram susceptibility (109) of standard  $\text{Hg}(\text{Co}(\text{CNS})_4) \times 10^6$   
 \*\* volume susceptibility of air

Effective Magnetic Moment of Sample. The procedure for obtaining the effective magnetic moment of the sample is given below. None of the values were corrected for temperature independent paramagnetism ( $\gamma$ ).

$$\chi_g = \left[ \frac{(0.029)V + \beta F}{(C-A)} \right] (10^{-6})$$

$$\chi_m = \chi_g (\text{molecular weight of sample}) + \text{diamagnetic corrections}$$

$$\mu_e = 2.84((\chi_m - \gamma)T)^{1/2}$$

A computer program written by the author, was used to evaluate the susceptibilities and magnetic moments (see appendix).

#### Magnetic Moments of Diphenylphosphine Complexes

The results of the magnetic studies of the diphenylphosphine complexes are summarized in Table 13.

The magnetic moments of the cobalt bromide and the cobalt iodide

Table 13. Magnetic Data for  $M(DPP)_3X_2^*$  Complexes

M	X	amp.	$\chi_g \times 10^6$	diamag. corr.	$\chi_m \times 10^6$	$\mu_e$ (B.M.)
Co	Br	4	2.991	248	2573	2.49
		6	2.854	248	2467	2.43
		8	2.798	248	2423	2.41
					mean	= 2.43
Co	I	4	2.078	280	2091	2.24
		6	2.062	280	2077	2.23
		8	2.023	280	2051	2.22
					mean	= 2.23
Ni	Br	diamagnetic				
Ni	I	4	0.514	280	728	1.32
		6	0.473	280	692	1.29
		8	0.450	280	672	1.27
					mean	= 1.29

\* temperature = 298 C°

complexes (2.43 and 2.23 B.M., respectively) are consistent with the presence of one unpaired electron. Although the values are above the spin-only value of 1.73, the difference is probably due to an orbital contribution.

The magnetic moment (1.29 B.M.) of the nickel iodide complex is

considerably below the value for one unpaired electron. However, two unpaired electrons would be present in a spin-free nickel(II) complex. The origin of this unusual magnetic moment will be discussed in a later chapter.

### Spectral Studies

#### Mull Spectra

The visible spectra of the solids of tris(pyridine N-oxide)-cobalt(II) chloride and bromide were obtained as mulls in hexachlorobutadiene. These spectra are given in Figure 3 and were found to be almost identical with those of the corresponding tetrahalocobaltate(II) anions (116). Table 14 is given as a comparison of the solid spectra of the cobalt bromide complex with the tetra-n-butylammonium tetrabromocobaltate(II) complex.

Table 14. Visible Mull Spectra of  $\text{Co}(\text{pyridine N-oxide})_3\text{Br}_2$  and  $[\text{Butyl}_4\text{N}][\text{CoBr}_4]$

$\text{Co}(\text{pyridine N-oxide})_3\text{Br}_2$	$[\text{Butyl}_4\text{N}][\text{CoBr}_4]$
$\mu$ (abs. peak position)	$\mu$
643	644
658 (sh)*	660 (sh)
668	669
698	699
717 (sh)	720 (sh)
729 (sh)	-
* (sh) = shoulder	

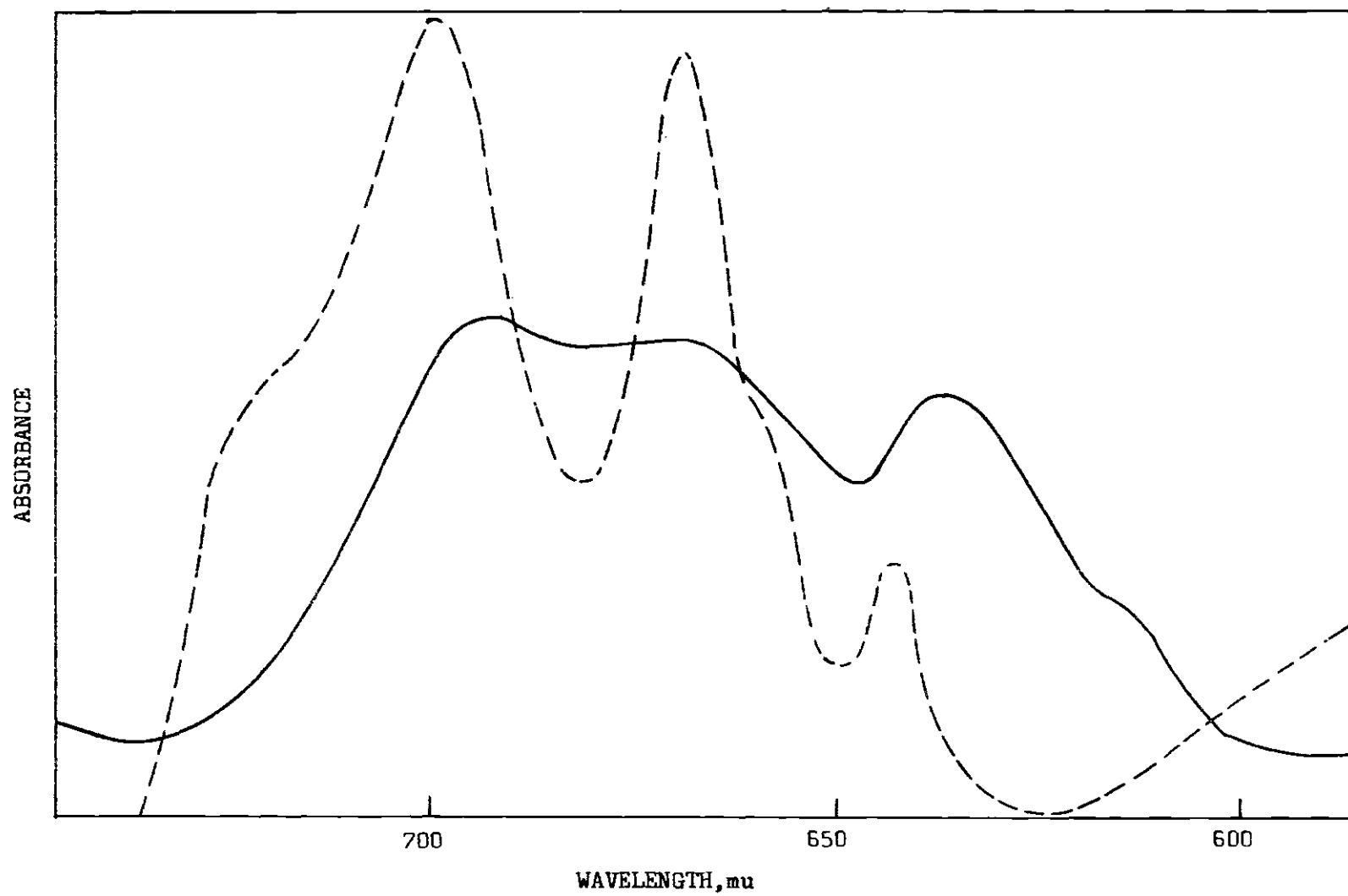


Figure 3. Mull Spectra of Tris(Pyridine N-Oxide)Cobalt(II) Chloride and Bromide (Dashed line represents the bromide complex and the solid line the chloride complex)

### Solution Spectra

The spectrum of cobalt(II) chloride in dimethylformamide (DMF) was observed as the concentration of pyridine N-oxide was increased; these spectra are given in Figure 4.

The absorption spectra of  $\text{Co(DPP)}_3\text{X}_2$  (Figure 5) and  $\text{Ni(DPP)}_3\text{X}_2$  (Figure 6) were measured in dichloromethane.

The solution spectrum of iodobis(dipyridyl)copper(II) iodide in nitromethane is shown in Figure 7.

### Single Crystal Spectra

The crystal spectrum of iodobis(dipyridyl)copper(II) iodide is shown in Figure 7. The extinction coefficients are only approximations since the crystal thickness was difficult to measure accurately and since it was necessary to correct for scattering by the crystal. A correction for background scattering was made by assuming 100% transmission at the point of lowest absorption.

The crystal spectra of  $\text{Co(DPP)}_3\text{X}_2$  and  $\text{Ni(DPP)}_3\text{X}_2$  are shown in Figures 8 and 9 respectively. Again, the extinction coefficients were only approximate; correction for background scattering was made as indicated above.

### Polarized Spectra

Dipyridyl Complexes. The crystals of iodobis(dipyridyl)copper(II) iodide that were used for the spectral studies exhibited well-developed 100 faces. Observation of the crystal in polarized light showed red light transmitted perpendicular to the c-axis and very little light transmitted parallel to the c-axis. The structure determination (47) showed the iodide ion in the trigonal plane and the four nitrogens completing a slightly distorted trigonal bipyramid. The Cu-I vector was approximately

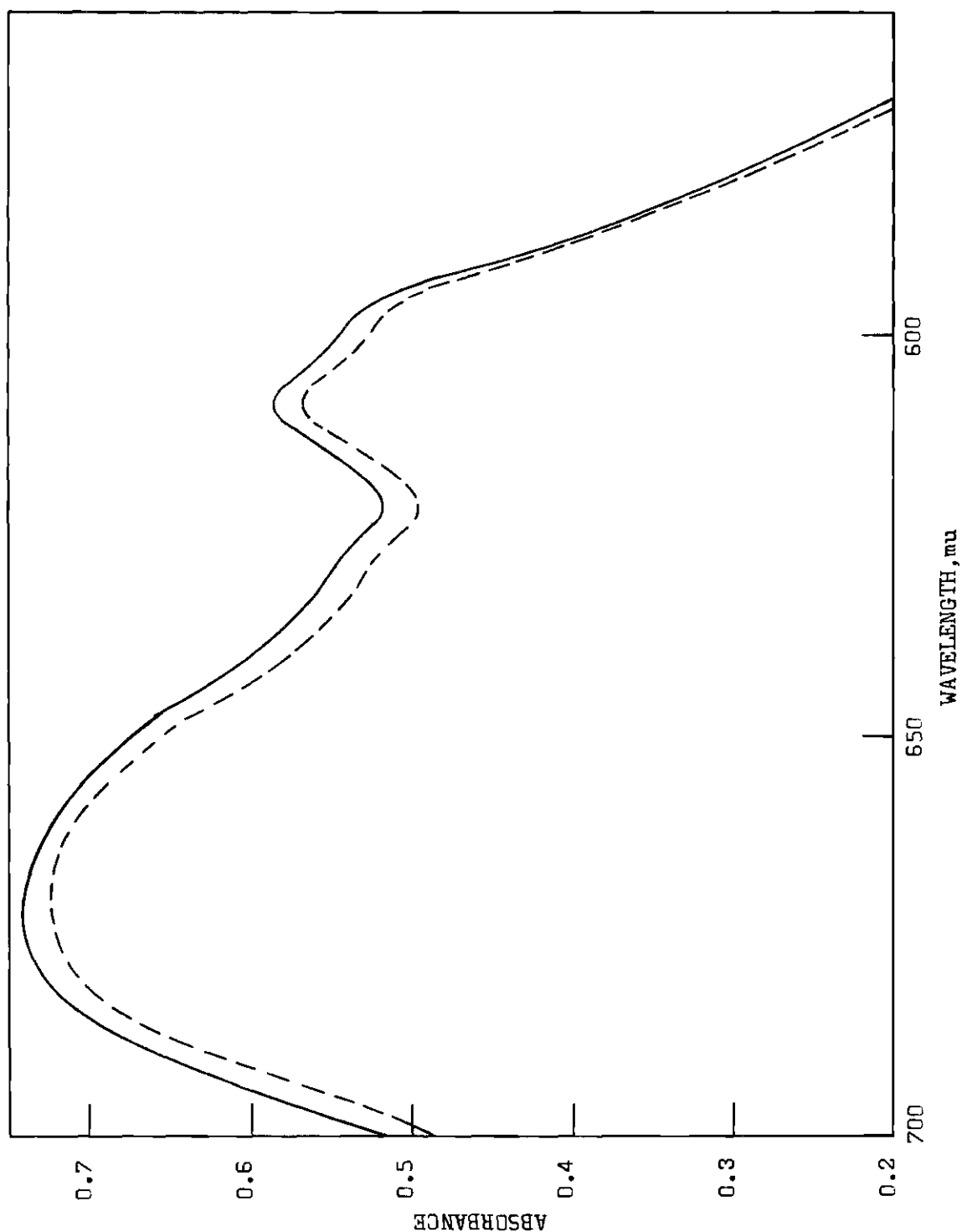


Figure 4. Spectra of  $\text{CoCl}_2$  in DMF with Increasing Concentrations of Pyridine N-Oxide (Dashed line represents mole ratios of cobalt to pyridine N-oxide of 1:0, 1:1, 1:2, 1:3 and 1:4; solid line represents 1:10)

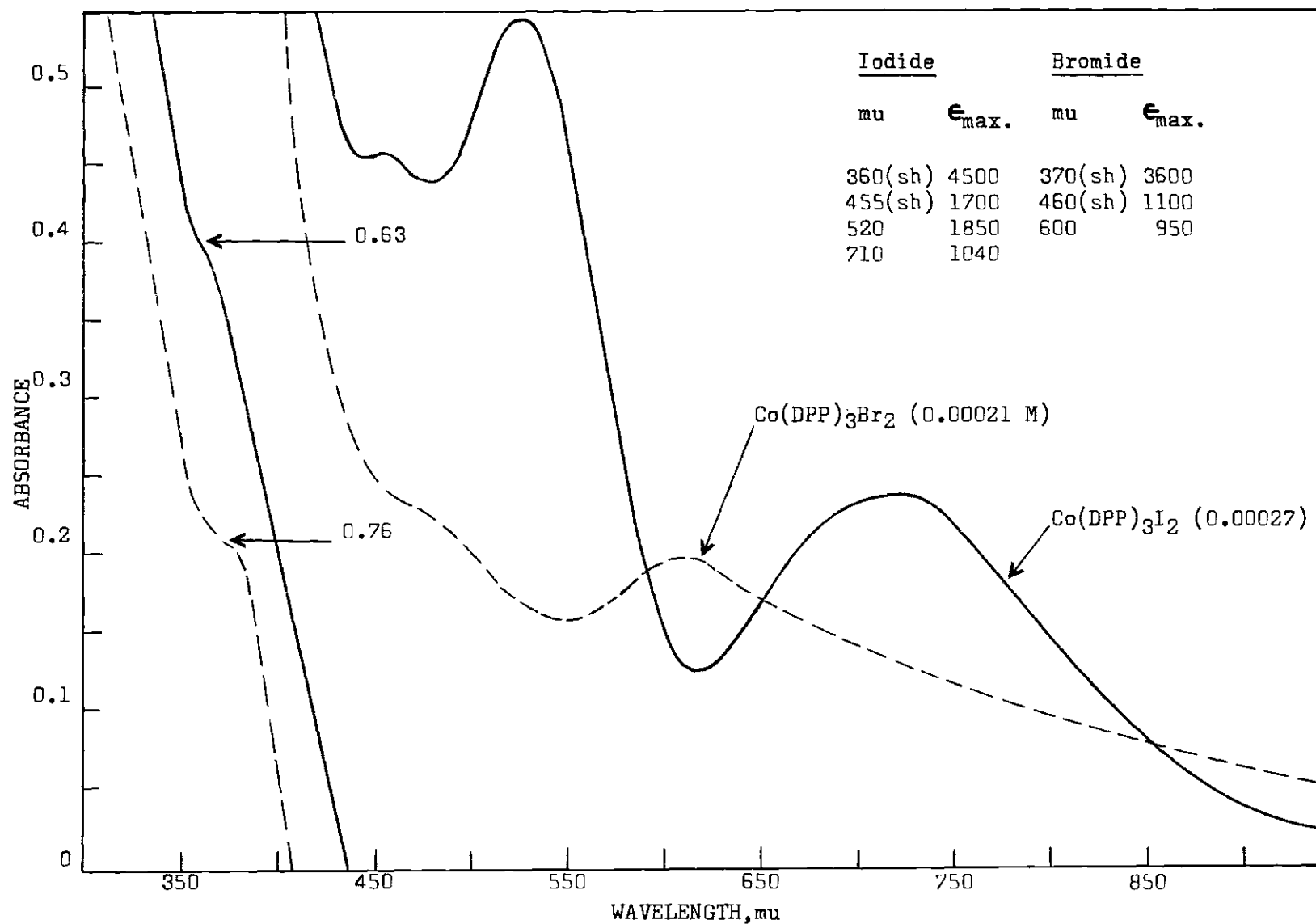
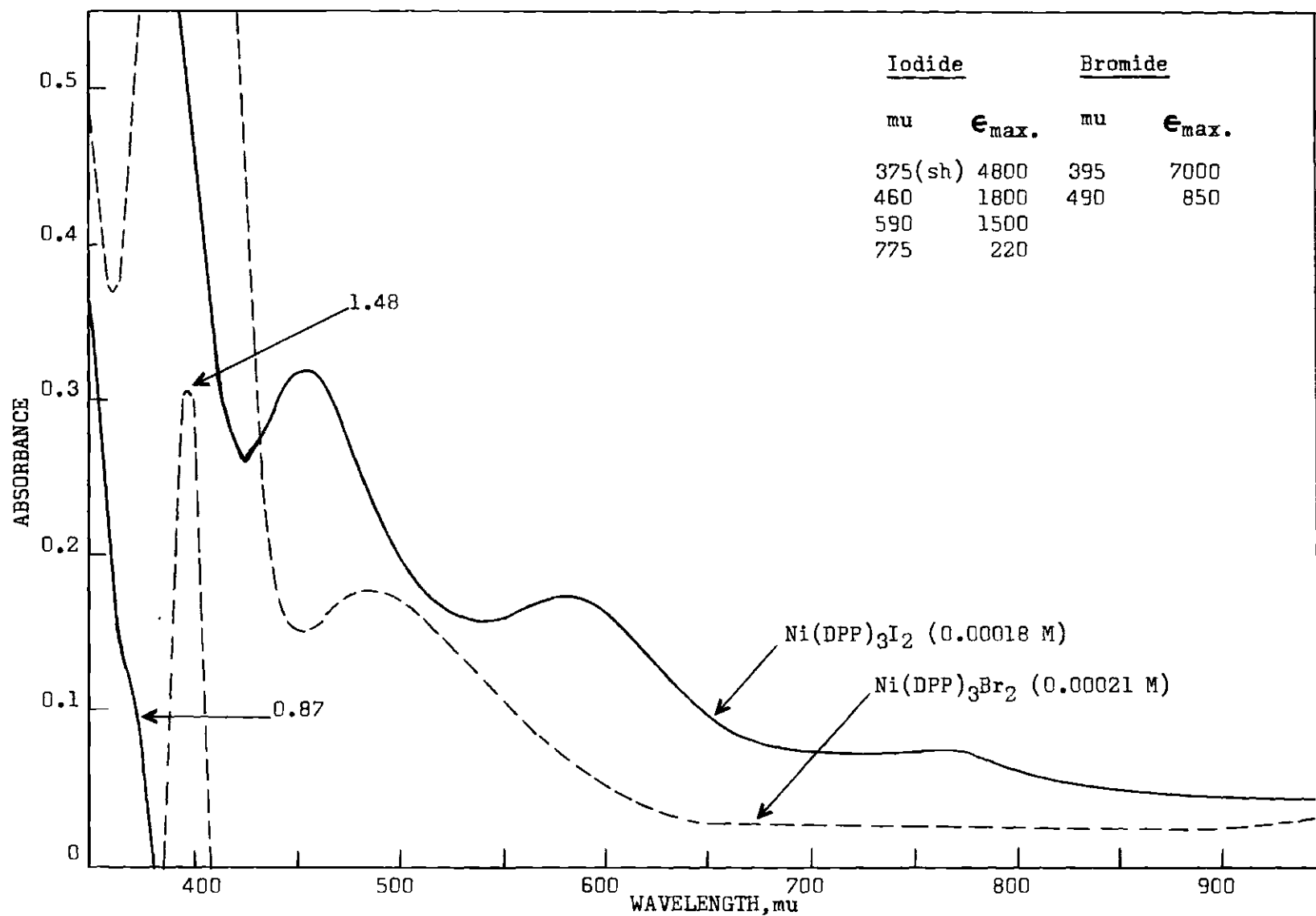


Figure 5. Absorption Spectra of  $\text{Co(DPP)}_3\text{X}_2$  in Dichloromethane





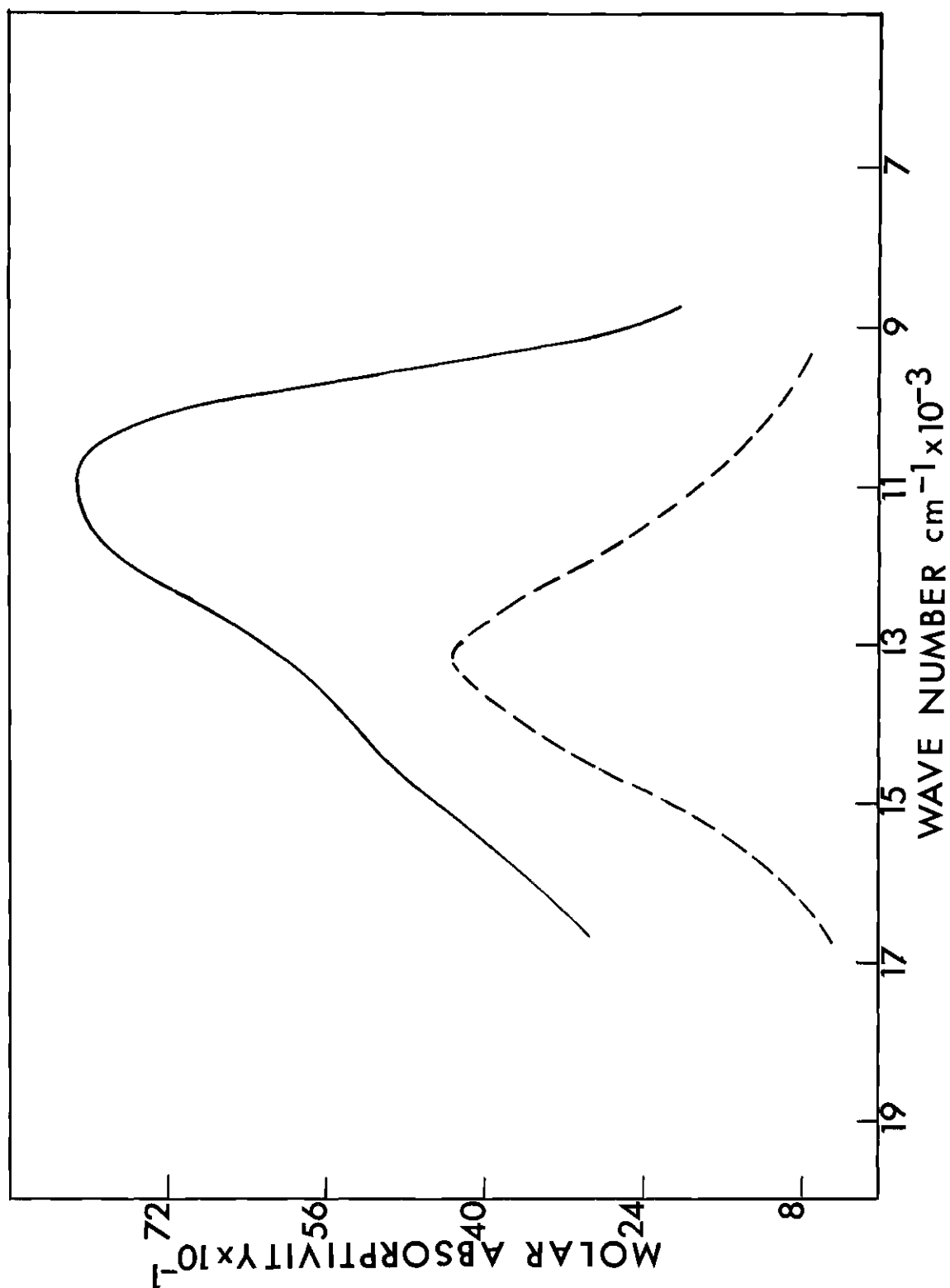


Figure 7. Solution and Solid Spectra of  $[\text{Cu}(\text{dipyridyl})_2\text{I}]\text{I}$   
(Solution spectrum is represented as dashed line,  
the solid as a solid line)

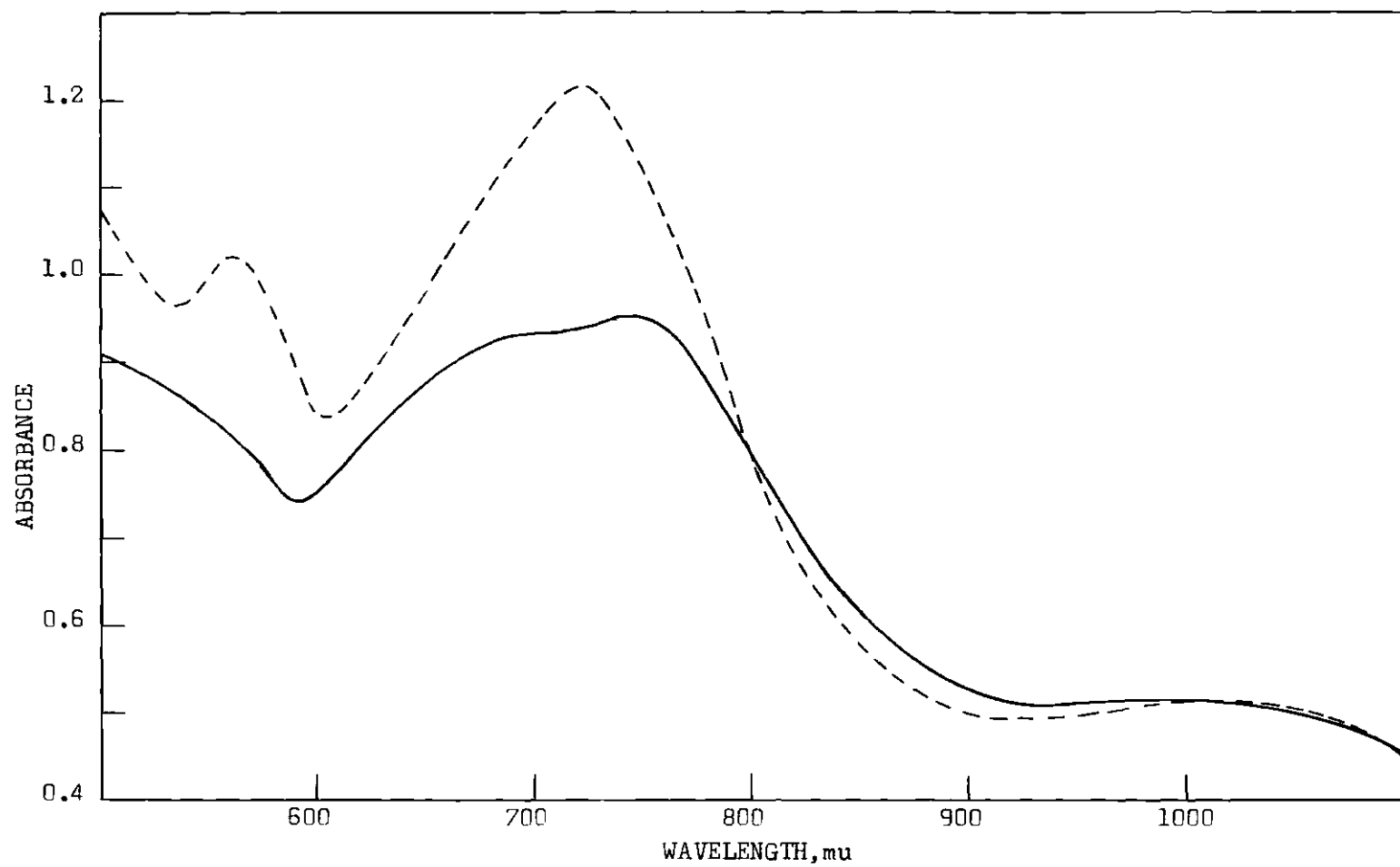


Figure 8. Crystal Spectra of  $\text{Co(DPP)}_3\text{X}_2$  (Dashed line represents the iodide complex and solid line the bromide complex)

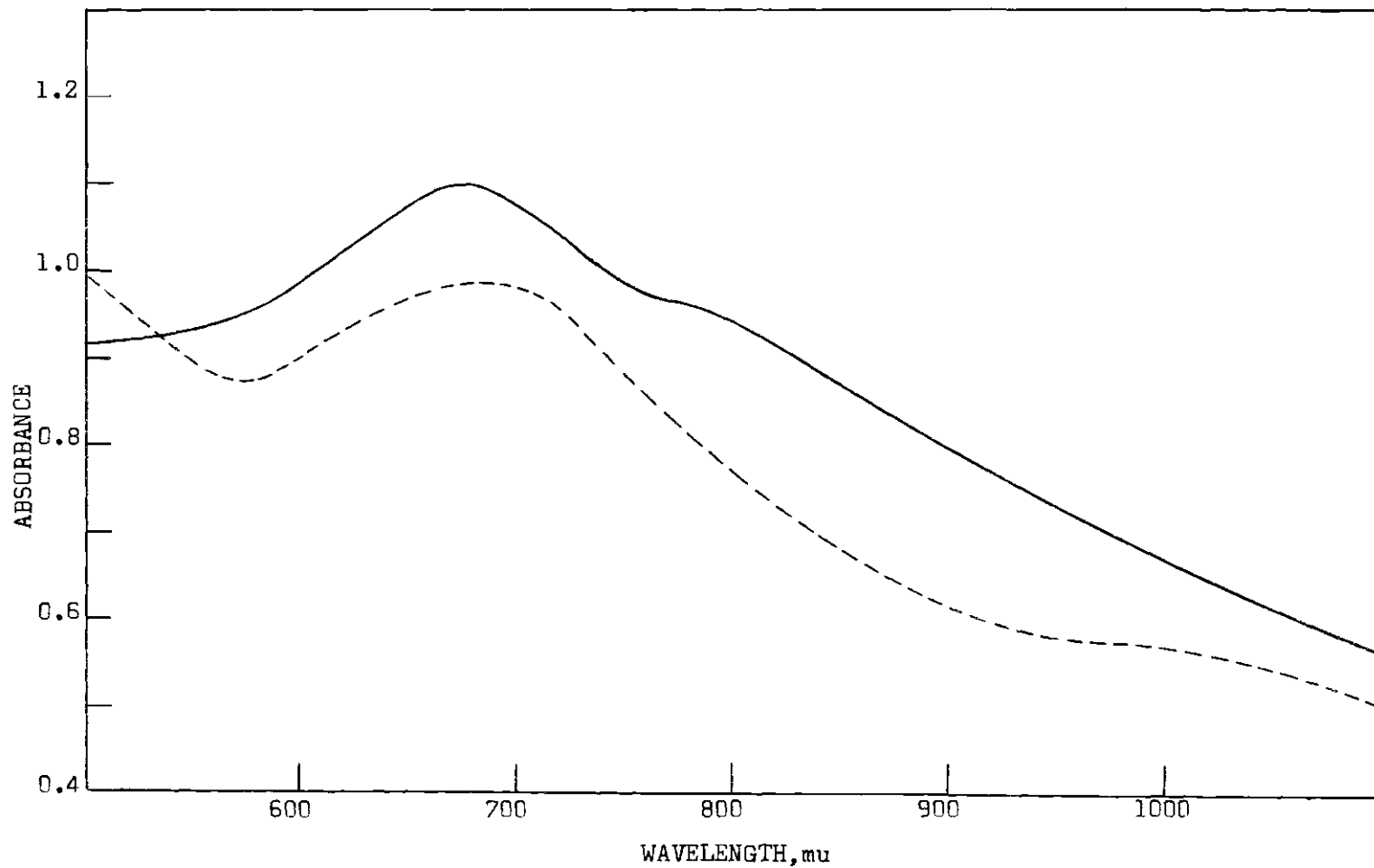


Figure 9. Crystal Spectra of  $\text{Ni}(\text{DPP})_3\text{X}_2$  (Dashed line represents the bromide complex and solid line the iodide complex)

parallel to the  $c$ -axis. Since, in either  $C_2$  or  $C_{2v}$  symmetry, the Cu-I vector represented the principal axis, the polarized spectra obtained with light incident on the 100 face were parallel and perpendicular to the principal axis of the complex. Figure 10 shows the polarized spectra of the crystal with light parallel and perpendicular to the principal axis.

Diphenylphosphine Complexes. On observation, the  $Ni(DPP)_3I_2$  crystal in polarized light shows green light transmitted approximately perpendicular to the  $\underline{c}$ -axis and appears opaque with light parallel to the  $\underline{c}$ -axis. Figures 11 and 12 show the polarized spectra of  $Ni(DPP)_3Br_2$  and  $Ni(DPP)_3I_2$  respectively with light perpendicular and parallel to the  $\underline{c}$ -axis.

The  $Co(DPP)_3I_2$  crystal in polarized light shows red light transmitted perpendicular to the  $\underline{c}$ -axis and green light parallel to the  $\underline{c}$ -axis. Figures 13 and 14 illustrate the polarized spectra of the  $Co(DPP)_3Br_2$  and  $Co(DPP)_3I_2$  respectively.

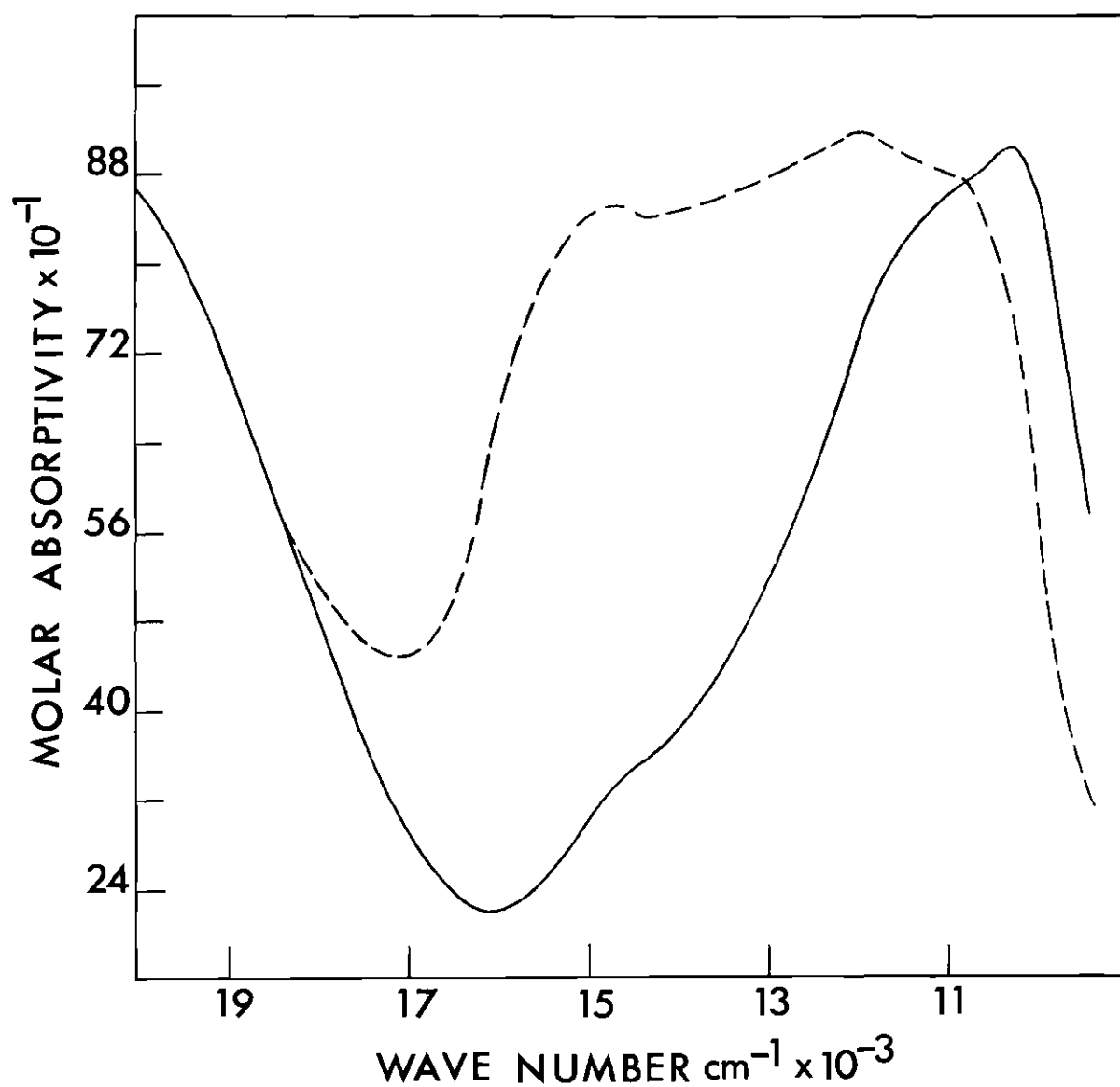


Figure 10. Polarized Spectra of  $(\text{Cu}(\text{dipyridyl})_2\text{I})\text{I}$  (Light polarized parallel to the principal axis is represented as a solid line and light perpendicular to the principal axis as a dashed line)

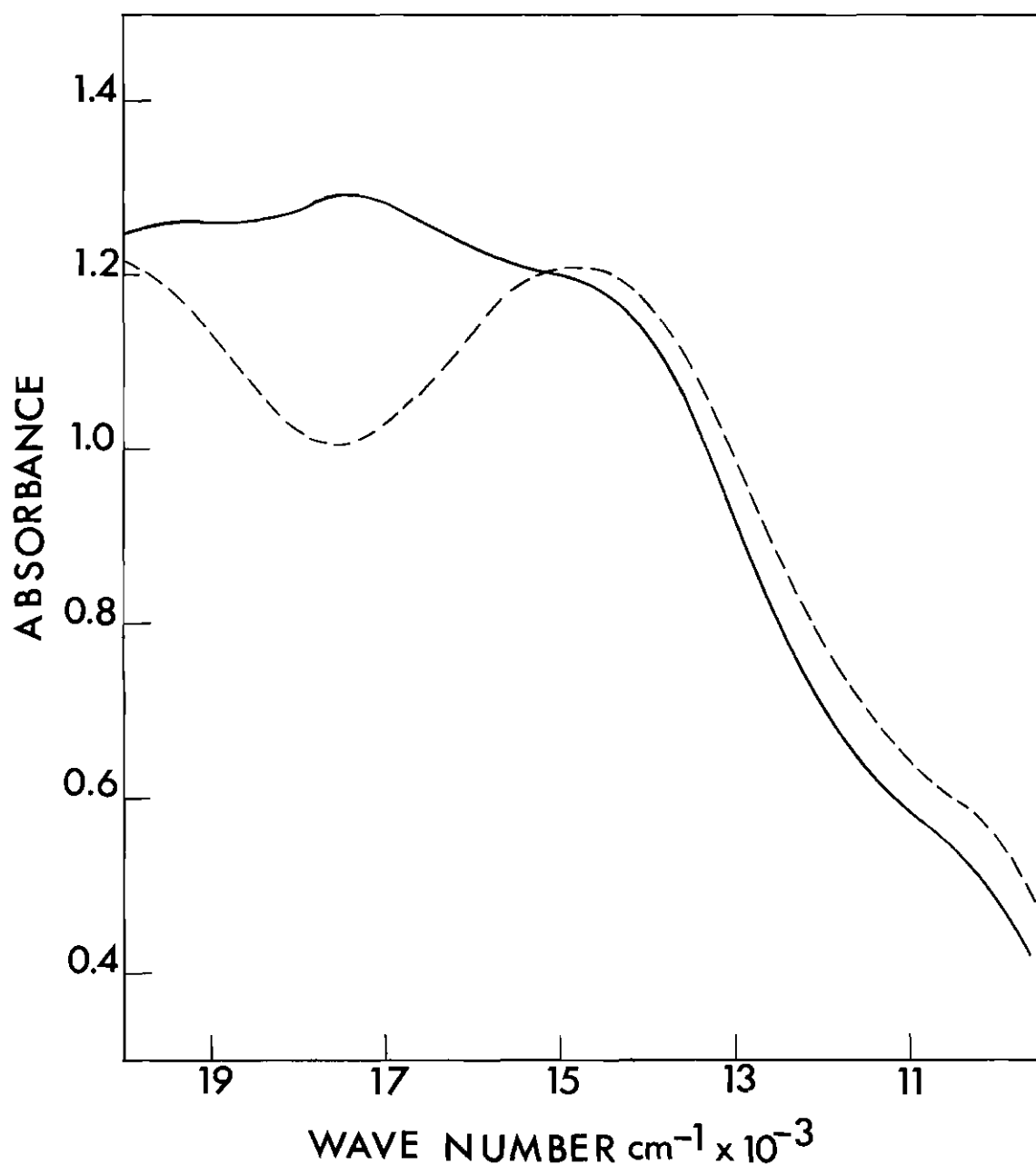


Figure 11. Polarized Spectra of Ni(DPP)<sub>3</sub>Br<sub>2</sub> (Light polarized parallel to the principal axis is represented as a solid line and light perpendicular to the principal axis as a dashed line)

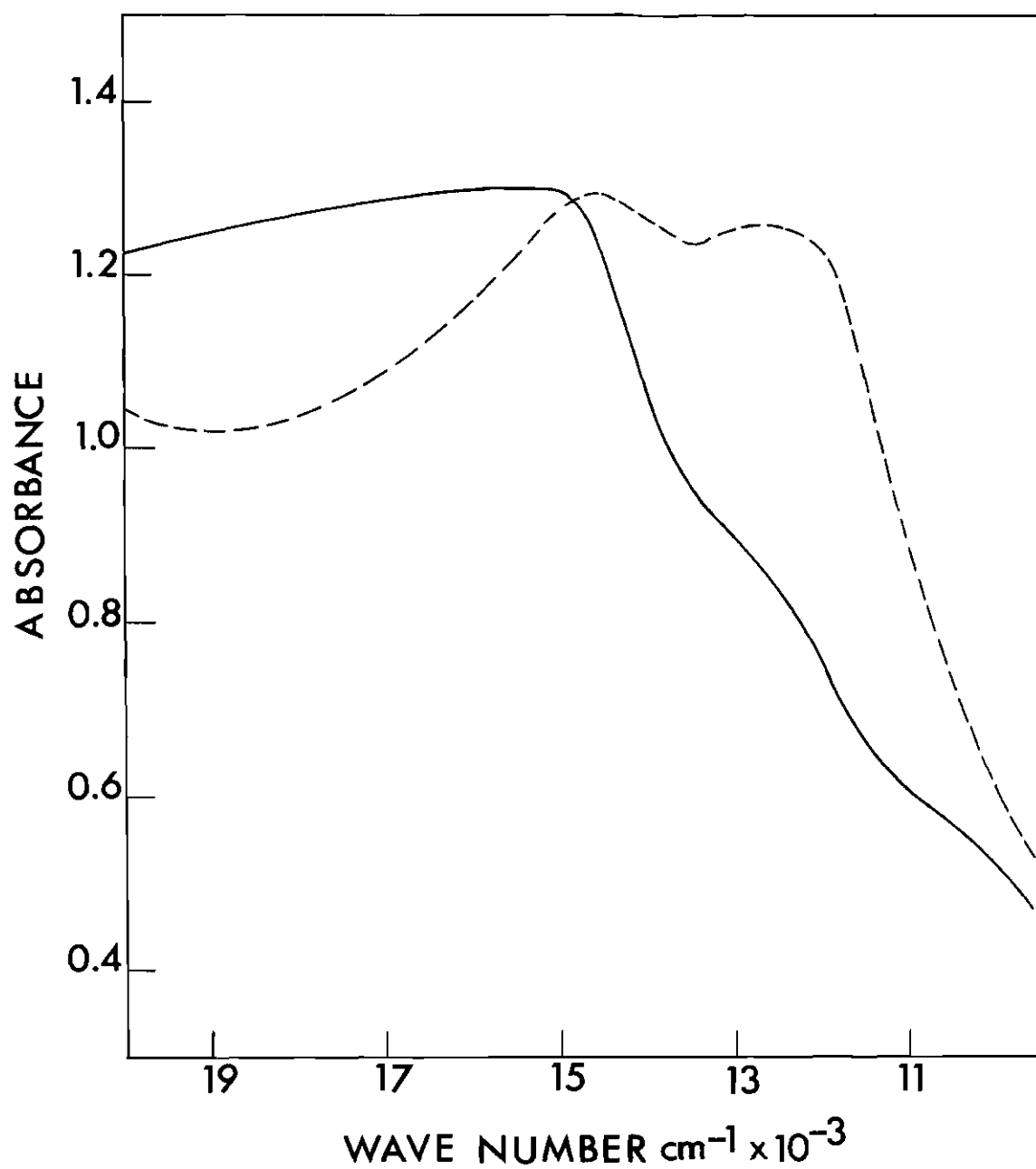


Figure 12. Polarized Spectra of  $\text{Ni}(\text{DPP})_3\text{I}_2$  (Light polarized parallel to the principal axis is represented as a solid line and light perpendicular to the principal axis as a dashed line)



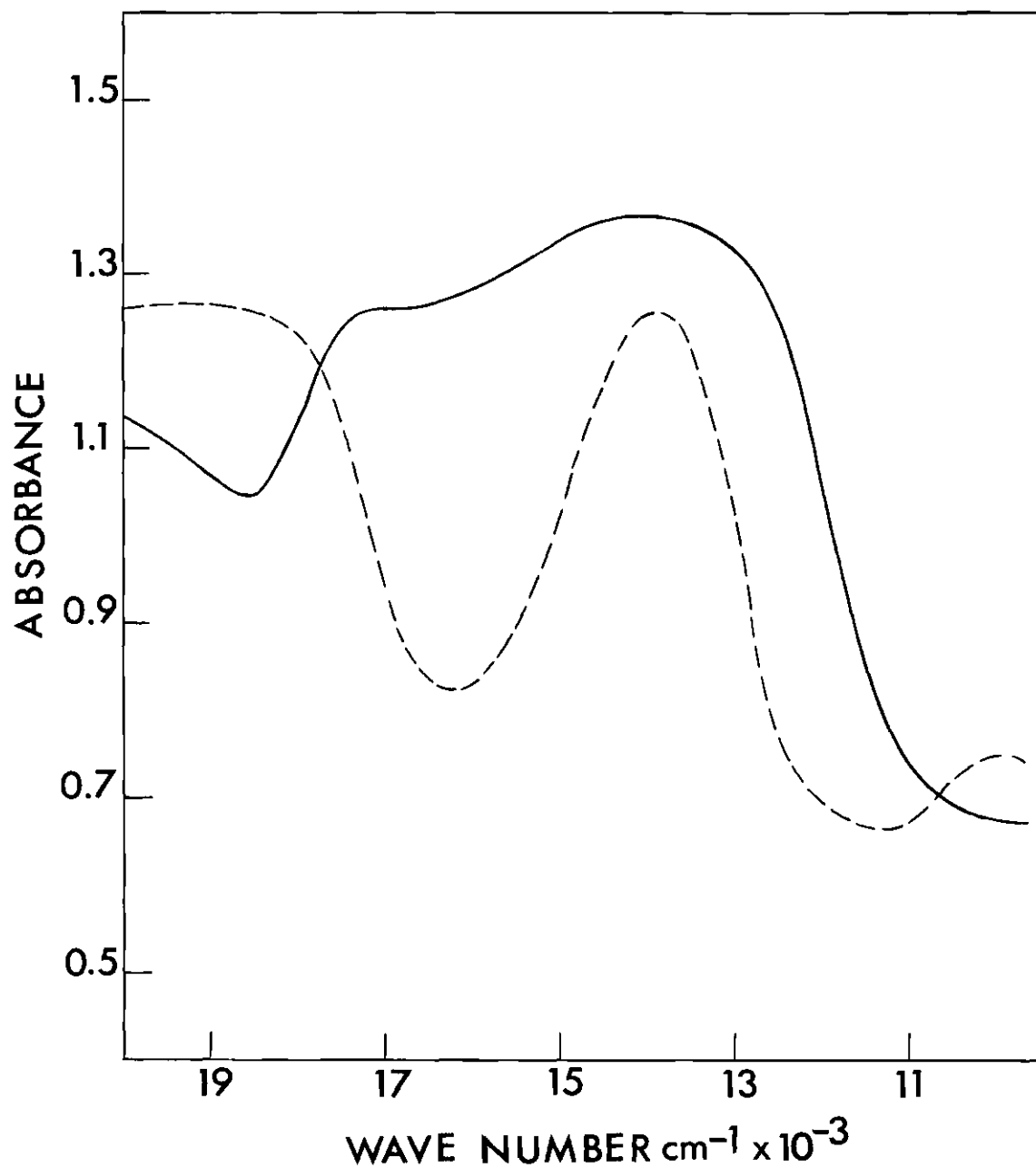


Figure 13. Polarized Spectra of  $\text{Co}(\text{DPP})_3\text{Br}_2$  (Light polarized parallel to the principal axis is represented as a solid line and light perpendicular to the principal axis as a dashed line)

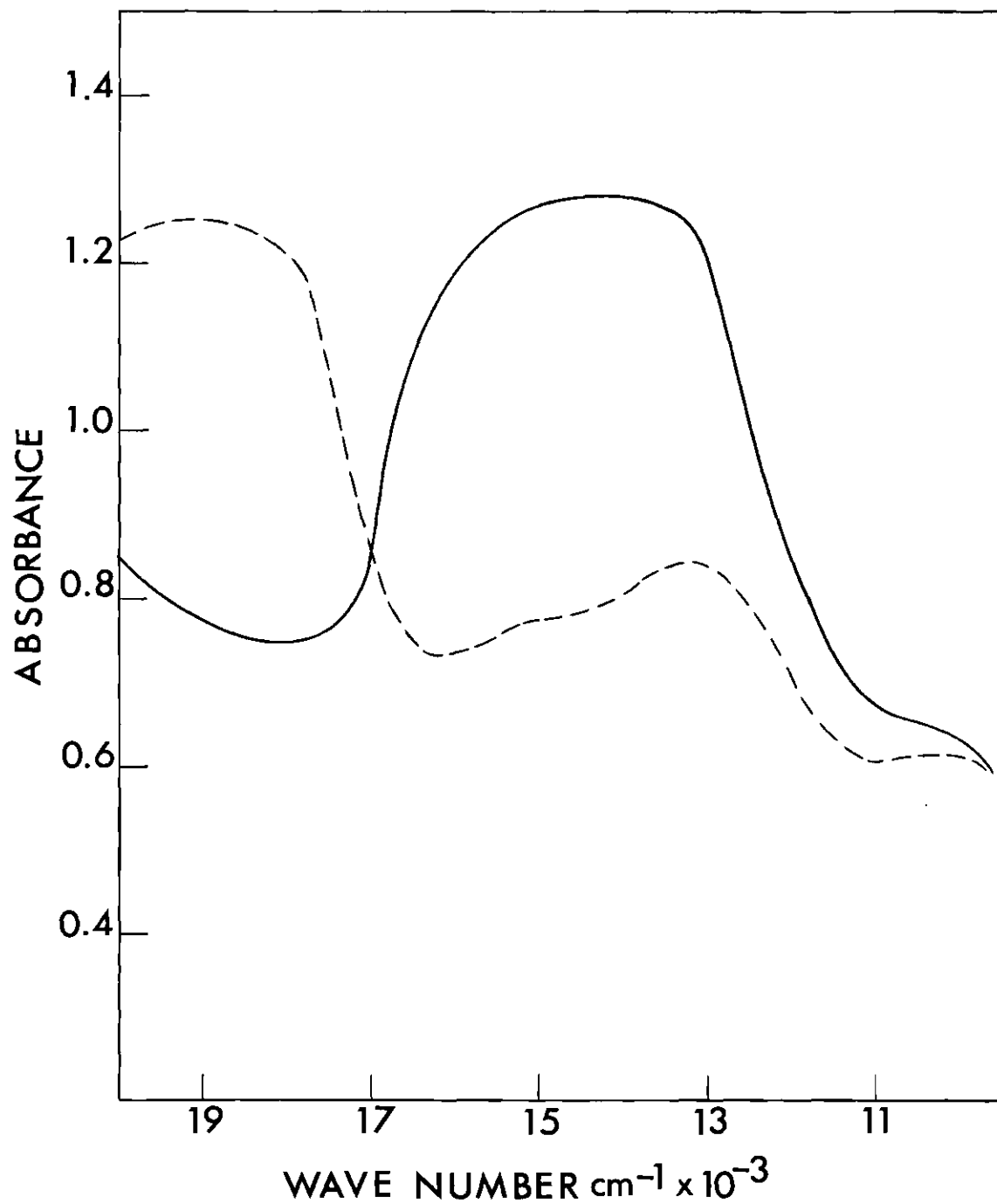


Figure 14. Polarized Spectra of  $\text{Co(DPP)}_3\text{I}_2$  (Light polarized parallel to the principal axis is represented as a solid line and light perpendicular to the principal axis as a dashed line)

## CHAPTER VI

## CALCULATIONS

Structure DeterminationStatistical Tests

Since the crystal systems ( $M(DPP)_3X_2$ ) were found to be triclinic, two space groups were possible ( $P1$  and  $P\bar{1}$ ). In order to choose between these two space groups, statistical tests were applied to the zones of reflections. Application of statistical tests to the zones of data indicated a centric structure and the space group  $P\bar{1}$  was assumed. The successful refinement of the structure confirmed this choice of space group. The statistical tests employed are discussed below.

Howells and co-workers (121) have devised a statistical test which will indicate whether a structure is centrosymmetric or non-centrosymmetric. They have shown that the fractions  $N(z)$  of reflections whose intensities were equal to or less than a fraction  $z$  of a local average are given, for a non-centrosymmetrical structure, by the function  $N(z) = 1 - \exp(-z)$  and for a centrosymmetrical structure by the function  $N(z) = \text{erf}(1/2z)^{1/2}$ . The symbol  $\text{erf}$  represented the error function of Jahnke and Emde (122). The values (123) of the two functions are tabulated in Table 15. They found that this method could often be applied satisfactorily to zones of reflections. The method of treating the zones of reflections was as follows. The data were divided into sets corresponding to  $\sin \theta$  ranges (selected so that each range contained approximately the same number of reflections).

Table 15. Values of Statistical Functions

N	N(z)									
	0.1	0.2	0.3	0.4	0.5	0.6	0.7	0.8	0.9	1.0
$1-\exp(-z)$	9.52	18.13	25.92	32.97	39.35	45.12	50.34	55.07	59.34	63.21
$\text{erf}(1/2z)^{1/2}$	24.81	34.53	41.87	47.38	52.05	56.14	59.72	62.89	65.72	68.33

The mean value intensity for each range was obtained by dividing the sum of the intensities for the range by the total number of reflections included in the range. The number of reflections were counted which possessed values less than or equal to fractions (N) of the mean values (from 10% to 100%, the mean value in increments of 10%). The number of reflections corresponding to each of these ranges were divided by the total number of reflections for the range, thus, resulting in the N(z) fraction. The complete set of results, N(z), was derived in this manner for the various ranges. The mean N(z) of the various ranges was then plotted versus the fraction N. Figure 15 illustrates the distribution of intensities for several zones of reflection of the  $\text{M}(\text{DPP})_3\text{X}_2$  crystals and compares these with the theoretical curves for 1 and  $\bar{1}$ .

#### Solution of the Structure of $\text{Co}(\text{DPP})_3\text{Br}_2$

The structural analysis involved the location of one cobalt, two bromine, three phosphorus, and thirty-six carbon atoms which corresponded to a molecular unit. The other molecule in the unit cell was related by a center of inversion. A three-dimensional Patterson (124) synthesis was computed from the corrected intensities (see appendix for computer

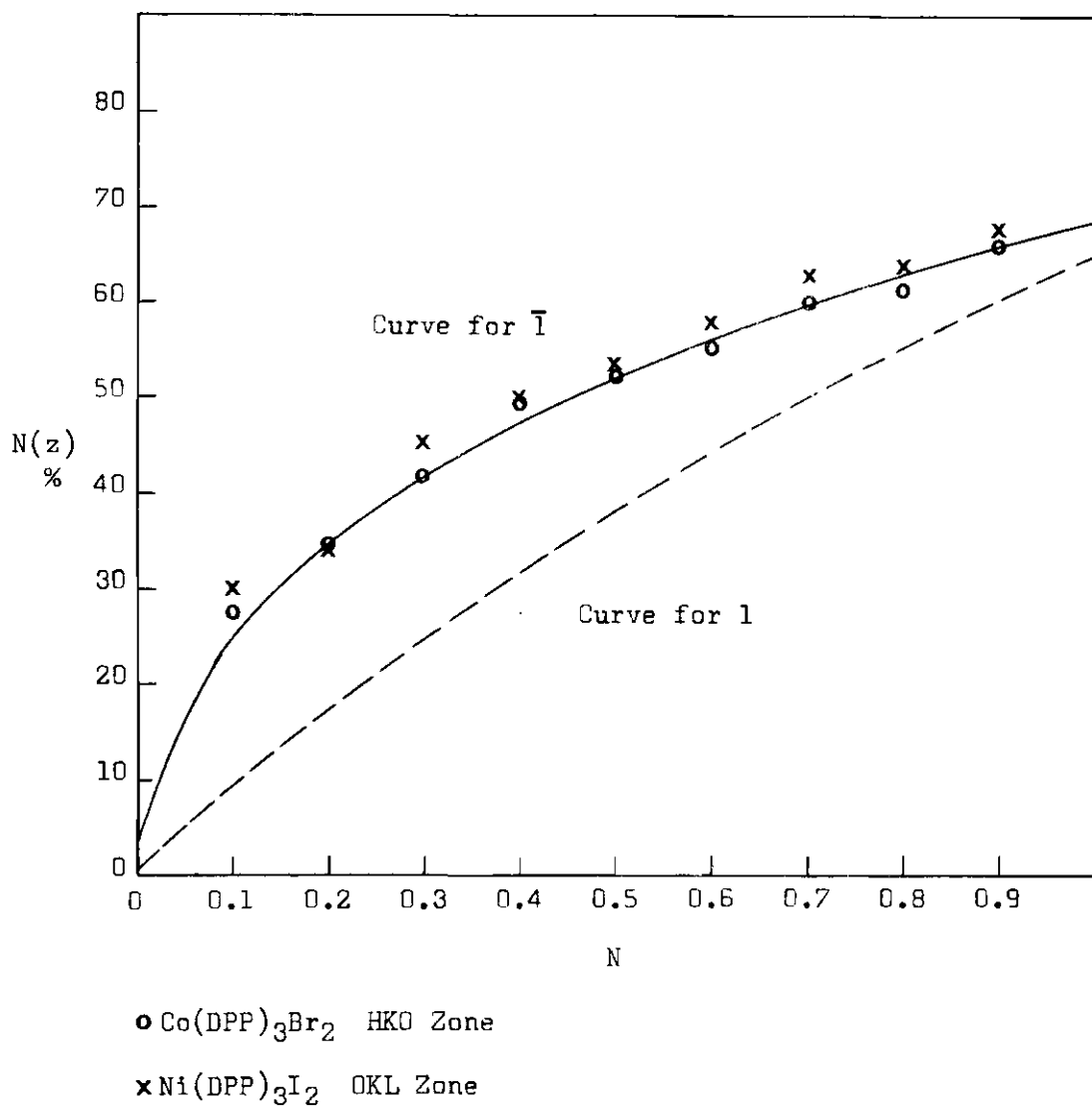


Figure 15. Distribution of Intensities for  $M(DPP)_3X_2$ ; Compared with Theoretical Curves for  $\bar{l}$  and  $l$

program information). An analysis of the Patterson map revealed the atomic positions of the two bromine atoms.

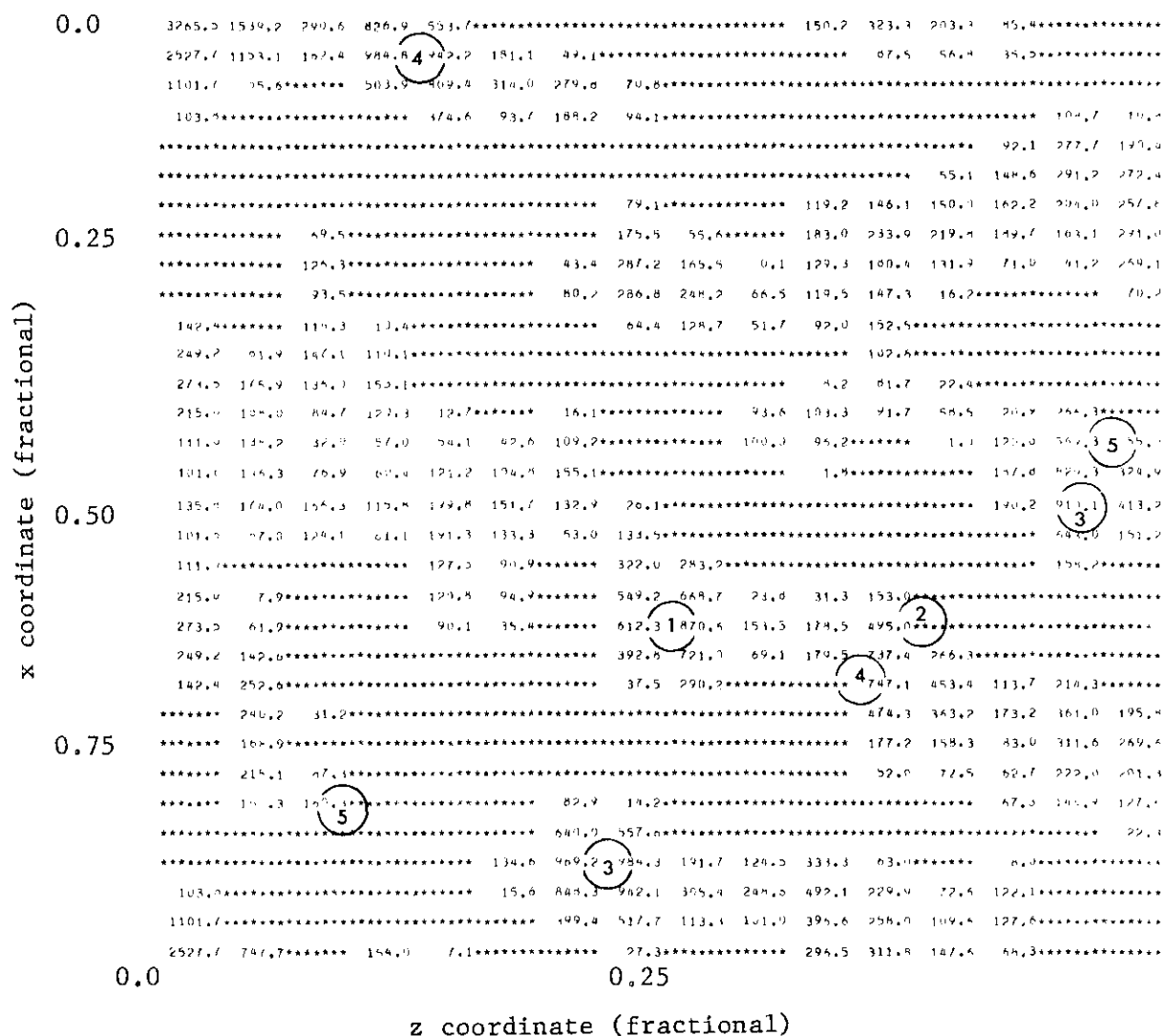
The peaks located in Patterson space represent the ends of the vectors which radiate from a common origin and these vectors are related to the differences of vectors in the electron-density function. Therefore, for the two bromine atoms labeled  $x_1, y_1, z_1$  and  $x_2, y_2, z_2$ , one expects vectors in Patterson space with peak coordinates corresponding to  $x_2 - x_1$ ,  $y_2 - y_1$ , and  $z_2 - z_1$ . Also since the other molecule is present in the unit cell with bromine coordinates of  $\bar{x}_1, \bar{y}_1, \bar{z}_1$  and  $\bar{x}_2, \bar{y}_2, \bar{z}_2$ , the additional peaks  $2x_1, 2y_1, 2z_1$  and  $2x_2, 2y_2, 2z_2$  are expected. The Patterson function is centrosymmetric and therefore each peak listed above will also have an inverse. The peaks representing the vectors for the two bromine and one cobalt atoms are shown in a Patterson projection of the HOL zone in Figure 16.

The cobalt and phosphorus atoms were located from a minimum function (124) based on the bromine atom vectors. A Fourier Synthesis based on observed structure factors and phased on the cobalt, bromine and phosphorus atoms revealed the carbon atom positions ( $R^* = 0.24$ ). A Fourier Synthesis based on all atoms should reproduce the electron density at each point of the unit cell; an electron density plot computed in this manner for the HOL projection is included, Figure 17, as an illustration.

---

\*The unweighted discrepancy factor  $R$  (125) is defined as:

$$R = \sum | |F_o| - |F_c| | / \sum |F_o|$$



vector 1 = the vector between Br<sub>1</sub> and Br<sub>1</sub>

vector 2 = the vector between Br<sub>2</sub> and Br<sub>2</sub>

vector 3 = the vector between Br<sub>1</sub> and Br<sub>2</sub>

vector 4 = the vector between Co and Br<sub>1</sub>

vector 5 = the vector between Co and Br<sub>2</sub>

Figure 16. Patterson Projection of the HOL Zone of the Co(DPP)<sub>3</sub>Br<sub>2</sub> Crystal

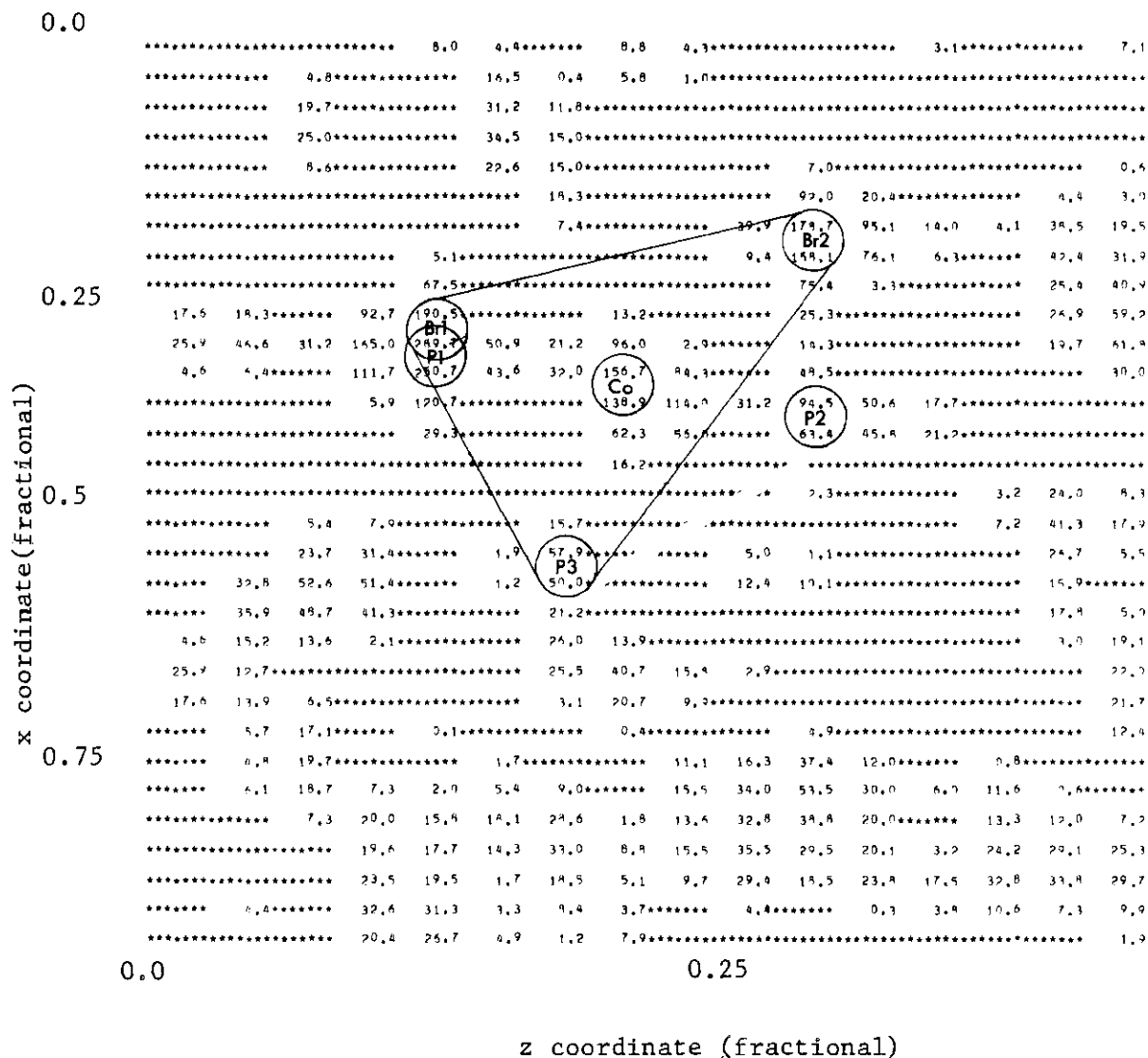


Figure 17. Electron-Density Projection of the HOL Zone of the  $\text{Co(DPP)}_3\text{Br}_2$  Crystal



Full-matrix least-squares refinement (126), using individual isotropic temperature factors for each atom, omitting hydrogen atoms, and using all reflections weighted at unity, was continued until no parameter showed any significant change between successive cycles; the final R value was 0.12. Final atomic parameters for all atoms of the asymmetric unit, except the hydrogen atoms, are tabulated in Table 16. The calculated structure factors (FC) obtained using these parameters are compared with the observed structure factors (FO) in Table 17.

#### Refinement of the Heavy Atom Coordinates of $\text{Ni}(\text{DPP})_3\text{I}_2$

The parameters from Table 16, substituting nickel for cobalt and iodine for bromine, were used with the data from the  $\text{Ni}(\text{DPP})_3\text{I}_2$  crystal. Since the amount of data was limited (371 reflections), only the parameters for nickel, iodine and phosphorus atoms were refined by least-squares refinement; a final R value of 0.16 was obtained.

Final parameters for the atoms varied are listed in Table 18. The calculated structure factors obtained using these parameters are compared with the observed structure factors (FO) in Table 19.

Table 16. Structure Parameters for  $\text{Co}(\text{DPP})_3\text{Br}_2$ 

Atom	x	y	z	B, Å <sup>2</sup>
Co	0.3606(4)*	0.0541(3)	0.2248(3)	1.98(7)
Br <sub>1</sub>	0.3151(4)	0.1774(3)	0.1184(2)	3.89(8)
Br <sub>2</sub>	0.1943(3)	0.9032(3)	0.3181(2)	3.33(7)
P <sub>1</sub>	0.3185(8)	0.8921(6)	0.1163(5)	2.2(1)
P <sub>2</sub>	0.3974(8)	0.2210(6)	0.3259(5)	2.6(1)
P <sub>3</sub>	0.5811(8)	0.1306(6)	0.1929(5)	2.5(1)
R <sub>1</sub> C <sub>1</sub>	0.152(4)	0.811(3)	0.064(3)	3.4(6)
R <sub>1</sub> C <sub>2</sub>	0.057(4)	0.859(3)	0.081(3)	4.4(7)
R <sub>1</sub> C <sub>3</sub>	0.936(5)	0.802(4)	0.030(3)	5.0(8)
R <sub>1</sub> C <sub>4</sub>	0.906(4)	0.692(4)	0.967(3)	4.2(7)
R <sub>1</sub> C <sub>5</sub>	0.994(4)	0.642(4)	0.954(3)	4.6(7)
R <sub>1</sub> C <sub>6</sub>	0.111(4)	0.693(3)	0.006(2)	2.9(5)
R <sub>2</sub> C <sub>1</sub>	0.351(3)	0.754(3)	0.133(2)	2.4(5)
R <sub>2</sub> C <sub>2</sub>	0.282(4)	0.668(3)	0.192(3)	3.6(6)
R <sub>2</sub> C <sub>3</sub>	0.320(5)	0.566(4)	0.205(3)	4.6(7)
R <sub>2</sub> C <sub>4</sub>	0.423(6)	0.567(5)	0.154(4)	6.8(10)
R <sub>2</sub> C <sub>5</sub>	0.501(5)	0.653(4)	0.096(3)	5.4(8)
R <sub>2</sub> C <sub>6</sub>	0.469(4)	0.760(4)	0.091(3)	4.3(7)
R <sub>3</sub> C <sub>1</sub>	0.512(3)	0.258(3)	0.420(2)	2.2(5)
R <sub>3</sub> C <sub>2</sub>	0.535(5)	0.171(5)	0.447(4)	6.3(9)
R <sub>3</sub> C <sub>3</sub>	0.630(5)	0.193(4)	0.508(3)	5.6(9)
R <sub>3</sub> C <sub>4</sub>	0.699(5)	0.326(4)	0.550(3)	5.4(8)

Table 16. (Continued)

Atom	x	y	z	$B_A^2$
$R_3C_5$	0.667(5)	0.416(5)	0.531(3)	6.3(10)
$R_3C_6$	0.575(5)	0.392(4)	0.460(3)	4.8(8)
$R_4C_1$	0.247(4)	0.220(3)	0.378(3)	3.0(8)
$R_4C_2$	0.201(5)	0.187(4)	0.463(3)	5.5(8)
$R_4C_3$	0.078(6)	0.178(5)	0.504(4)	7.7(12)
$R_4C_4$	0.015(5)	0.215(4)	0.453(3)	5.2(8)
$R_4C_5$	0.043(5)	0.256(5)	0.363(3)	5.7(9)
$R_4C_6$	0.180(5)	0.258(4)	0.324(3)	5.5(8)
$R_5C_1$	0.670(3)	0.047(3)	0.220(2)	3.8(7)
$R_5C_2$	0.601(4)	0.947(3)	0.288(3)	4.1(7)
$R_5C_3$	0.678(7)	0.884(6)	0.296(5)	9.7(15)
$R_5C_4$	0.802(6)	0.904(5)	0.283(4)	8.0(12)
$R_5C_5$	0.864(5)	0.992(5)	0.221(3)	7.5(11)
$R_5C_6$	0.802(5)	0.070(4)	0.183(3)	5.7(10)
$R_6C_1$	0.700(4)	0.309(3)	0.219(2)	2.7(5)
$R_6C_2$	0.681(5)	0.392(4)	0.165(3)	4.9(8)
$R_6C_3$	0.782(5)	0.531(4)	0.191(3)	5.5(9)
$R_6C_4$	0.868(5)	0.571(4)	0.254(3)	5.1(8)
$R_6C_5$	0.878(5)	0.480(4)	0.314(3)	5.1(8)
$R_6C_6$	0.792(5)	0.344(4)	0.285(3)	4.5(7)

\* Numbers in parentheses here and in succeeding tables are standard deviations in the least significant digits.

TABLE 17. OBSERVED AND CALCULATED STRUCTURE FACTORS FOR CO(DPP)3BR2

H	K	L	FO	FC	H	K	L	FO	FC	H	K	L	FO	FC	H	K	L	FO	FC
2	0	0	374	492	6	8	0	63	57	-2	6	0	257	198	1	1	1	424	321
3	0	0	300	309	2	9	0	95	79	-3	6	0	272	281	3	1	1	155	150
4	0	0	283	266	4	9	0	71	78	-4	6	0	105	108	4	1	1	141	119
5	0	0	71	66	5	9	0	63	60	-5	6	0	341	414	5	1	1	134	122
6	0	0	247	279	1	10	0	95	142	-7	6	0	200	209	7	1	1	182	201
7	0	0	118	114	2	10	0	134	142	-11	6	0	71	54	8	1	1	138	100
8	0	0	155	192	4	10	0	63	87	-1	7	0	428	352	1	2	1	537	446
10	0	0	138	119	1	11	0	134	128	-2	7	0	118	94	3	2	1	158	160
2	1	0	237	248	4	11	0	55	68	-4	7	0	114	77	4	2	1	190	192
3	1	0	63	68	1	12	0	89	85	-5	7	0	315	347	5	2	1	327	354
4	1	0	438	431	-2	1	0	219	287	-7	7	0	329	389	6	2	1	63	72
5	1	0	202	223	-3	1	0	158	182	-8	7	0	277	236	7	2	1	164	149
6	1	0	114	113	-4	1	0	63	93	-9	7	0	89	106	10	2	1	105	110
7	1	0	63	77	-5	1	0	164	167	-11	7	0	71	60	1	3	1	367	364
8	1	0	130	124	-6	1	0	249	229	-1	8	0	202	207	2	3	1	179	158
9	2	0	329	312	-7	1	0	230	237	-2	8	0	176	142	3	3	1	435	462
1	2	0	245	182	-8	1	0	89	93	-3	8	0	250	317	4	3	1	355	334
2	2	0	276	256	-10	1	0	71	31	-4	8	0	173	133	5	3	1	155	135
4	2	0	473	485	-1	2	0	200	220	-6	8	0	89	66	6	3	1	134	155
5	2	0	182	219	-2	2	0	707	707	-7	8	0	249	250	7	3	1	100	94
6	2	0	122	123	-3	2	0	122	125	-8	8	0	89	125	9	3	1	105	123
8	2	0	71	44	-4	2	0	281	287	-9	8	0	95	114	10	3	1	116	150
0	3	0	432	359	-7	2	0	176	166	-12	8	0	141	114	1	4	1	170	153
1	3	0	435	407	-9	2	0	158	148	-1	9	0	95	83	2	4	1	114	111
2	3	0	184	185	-10	2	0	95	77	-2	9	0	95	76	3	4	1	385	387
3	3	0	152	142	-11	2	0	100	76	-3	9	0	224	243	4	4	1	243	262
4	3	0	114	112	-13	2	0	95	66	-5	9	0	89	73	6	4	1	141	120
5	3	0	84	84	-1	3	0	374	359	-7	9	0	89	108	7	4	1	179	175
8	3	0	167	178	-4	3	0	134	171	-12	9	0	100	73	8	4	1	148	150
9	3	0	170	198	-5	3	0	148	126	-3	10	0	71	72	1	5	1	187	149
11	3	0	84	88	-7	3	0	245	255	-4	10	0	134	94	3	5	1	224	234
0	4	0	307	246	-8	3	0	118	130	-6	10	0	130	92	7	5	1	148	150
1	4	0	326	312	-9	3	0	253	277	-5	10	0	134	139	8	5	1	148	152
2	4	0	346	283	-10	3	0	190	175	-9	10	0	138	111	1	6	1	202	179
3	4	0	184	220	-11	3	0	71	84	-3	11	0	95	91	2	6	1	230	221
6	4	0	95	113	-13	3	0	100	103	-4	11	0	95	78	3	6	1	153	120
8	4	0	170	164	-1	4	0	324	312	-6	11	0	167	135	4	6	1	173	117
9	4	0	138	169	-3	4	0	365	368	-8	11	0	170	143	1	7	1	71	72
0	5	0	77	54	-4	4	0	182	188	-9	11	0	71	72	2	7	1	221	193
1	5	0	195	199	-5	4	0	152	120	-4	12	0	167	132	4	7	1	179	146
2	5	0	205	211	-7	4	0	245	249	-10	12	0	160	101	2	8	1	145	166
5	5	0	63	62	-8	4	0	263	250	-5	13	0	95	82	3	9	1	105	79
6	5	0	134	124	-9	4	0	197	202	-6	13	0	167	166	2	10	1	152	153
7	5	0	100	130	-10	4	0	247	211	-8	13	0	95	84	3	10	1	105	103
0	6	0	118	112	-11	4	0	71	66	-9	13	0	95	75	2	11	1	105	110
1	6	0	241	255	-2	5	0	100	72	-10	13	0	95	89	2	-1	1	212	222
2	6	0	235	222	-3	5	0	410	477	-5	14	0	130	111	3	-1	1	625	535
5	6	0	71	87	-4	5	0	241	213	-6	14	0	161	148	4	-1	1	148	132
6	6	0	100	95	-5	5	0	161	151	-8	14	0	130	142	6	-1	1	202	229
0	7	0	176	168	-6	5	0	212	178	-9	14	0	95	69	7	-1	1	118	100
1	7	0	255	253	-7	5	0	77	68	2	0	1	447	283	11	-1	1	148	127
2	7	0	184	194	-8	5	0	187	184	3	0	1	557	405	3	-2	1	251	243
6	7	0	95	77	-9	5	0	63	71	4	0	1	293	254	6	-2	1	285	253
0	8	0	120	126	-10	5	0	130	141	6	0	1	141	103	7	-2	1	114	104
1	8	0	134	127	-11	5	0	95	101	7	0	1	122	108	8	-2	1	232	247
5	8	0	134	105	-1	6	0	400	380	11	0	1	77	90	1	-3	1	285	285

TABLE 17. (CONTINUED)

H	K	L	FO	FC	H	K	L	FO	FC	H	K	L	FO	FC	H	K	L	FO	FC
2	-3	1	581	516	-5	2	1	148	169	-2	10	1	145	125	-3	-8	1	71	64
8	-3	1	385	353	-6	2	1	126	136	-4	10	1	141	168	-1	-9	1	105	66
10	-3	1	138	165	-8	2	1	173	181	-5	10	1	200	206	-3	-9	1	105	109
11	-3	1	205	223	-12	2	1	77	68	-6	10	1	173	168	-1	-10	1	105	99
2	-4	1	616	500	-1	3	1	200	172	-6	11	1	105	109	4	0	2	283	271
3	-4	1	276	283	-2	3	1	95	101	-9	11	1	71	120	5	0	2	145	138
7	-4	1	55	129	-3	3	1	279	298	-5	12	1	105	103	6	0	2	214	223
8	-4	1	148	131	-4	3	1	173	143	-9	12	1	105	120	8	0	2	134	109
10	-4	1	237	278	-5	3	1	297	309	-4	13	1	105	117	2	1	2	458	495
11	-4	1	205	228	-6	3	1	145	169	-5	13	1	152	154	4	1	2	141	133
2	-5	1	274	250	-7	3	1	192	237	-7	13	1	105	117	5	1	2	176	154
4	-5	1	170	212	-9	3	1	89	102	-8	13	1	77	65	6	1	2	89	75
7	-5	1	161	131	-12	3	1	77	105	-5	14	1	105	117	8	1	2	173	151
10	-5	1	167	165	-1	4	1	134	105	-7	14	1	105	119	4	2	2	349	349
1	-6	1	141	155	-2	4	1	286	241	-2	0	1	424	351	5	2	2	226	217
2	-6	1	355	371	-4	4	1	184	173	-3	0	1	245	228	6	2	2	207	220
3	-6	1	346	309	-6	4	1	134	158	-5	0	1	485	533	7	2	2	219	215
4	-6	1	134	145	-7	4	1	176	197	-6	0	1	286	249	2	3	2	161	144
1	-7	1	217	237	-8	4	1	84	96	-7	0	1	228	228	3	3	2	55	30
2	-7	1	509	600	-9	4	1	89	108	-8	0	1	161	158	4	3	2	471	501
3	-7	1	207	213	-5	4	1	184	210	-10	0	1	105	76	5	3	2	358	352
5	-7	1	145	89	-1	5	1	77	54	-2	-1	1	126	145	6	3	2	219	213
6	-7	1	167	182	-2	5	1	329	281	-3	-1	1	390	452	7	3	2	230	232
8	-7	1	155	166	-4	5	1	226	218	-4	-1	1	197	228	8	3	2	105	98
10	-7	1	100	122	-8	5	1	164	179	-5	-1	1	268	284	9	3	2	158	116
1	-8	1	134	104	-9	5	1	63	102	-6	-1	1	145	175	2	4	2	366	335
2	-8	1	415	432	-10	5	1	138	138	-7	-1	1	126	108	3	4	2	173	156
4	-8	1	200	220	-11	5	1	145	133	-1	-2	1	648	625	4	4	2	415	383
8	-8	1	161	154	-3	6	1	224	168	-2	-2	1	152	161	5	4	2	219	225
3	-9	1	134	110	-4	6	1	463	487	-3	-2	1	346	340	8	4	2	110	113
9	-9	1	141	178	-6	6	1	363	403	-4	-2	1	130	139	7	4	2	114	101
1-10	1	145	125	-7	6	1	265	242	-8	-2	1	100	101	2	5	2	349	292	
10-10	1	148	72	-9	6	1	130	65	-1	-3	1	321	320	3	5	2	190	181	
11-10	1	77	123	-10	6	1	167	170	-2	-3	1	224	239	4	5	2	141	98	
1-11	1	105	104	-11	6	1	145	134	-3	-3	1	173	158	7	5	2	77	86	
3-11	1	148	148	-2	7	1	152	130	-5	-3	1	63	69	2	6	2	259	221	
9-11	1	179	177	-3	7	1	243	209	-6	-3	1	130	127	4	6	2	105	97	
11-11	1	77	130	-4	7	1	377	349	-7	-3	1	138	136	5	6	2	152	134	
5-12	1	105	118	-5	7	1	145	107	-8	-3	1	179	192	7	6	2	77	96	
1-13	1	105	107	-6	7	1	506	521	-2	-4	1	249	278	2	7	2	105	81	
5-13	1	105	134	-7	7	1	339	330	-3	-4	1	84	87	3	7	2	184	139	
7-13	1	105	113	-9	7	1	164	140	-6	-4	1	71	72	5	7	2	77	91	
7-14	1	105	129	-10	7	1	138	109	-7	-4	1	176	158	4	-1	2	292	288	
9-14	1	105	126	-1	8	1	71	62	-8	-4	1	148	132	6	-1	2	130	167	
-2	1	1	230	226	-2	8	1	230	238	-1	-5	1	55	58	7	-1	2	167	169
-3	1	1	251	264	-3	8	1	89	68	-2	-5	1	298	327	8	-1	2	130	121
-4	1	1	134	128	-5	8	1	155	126	-3	-5	1	126	100	9	-1	2	100	95
-5	1	1	401	410	-6	8	1	272	284	-7	-5	1	148	136	3	-2	2	396	351
-6	1	1	187	215	-7	8	1	89	119	-1	-6	1	179	201	5	-2	2	205	188
-7	1	1	167	191	-8	8	1	187	213	-2	-6	1	130	129	6	-2	2	179	151
-8	1	1	219	248	-9	8	1	71	60	-5	-6	1	100	79	7	-2	2	363	326
-10	1	1	100	93	-1	9	1	226	74	-7	-6	1	105	109	8	-2	2	197	246
-1	2	1	114	129	-2	9	1	197	208	-1	-7	1	232	254	9	-2	2	192	227
-2	2	1	265	237	-4	9	1	95	102	-4	-7	1	105	126	10	-2	2	176	185
-3	2	1	570	512	-8	9	1	95	127	-1	-8	1	141	145	5	-3	2	324	333
-4	2	1	261	227	-9	9	1	71	48	-2	-8	1	145	142	6	-3	2	361	329

TABLE 17. (CONTINUED)

H	K	L	FO	FC	H	K	L	FO	FC	H	K	L	FO	FC	H	K	L	FO	FC
7	-3	2	308	274	-10	5	2	141	131	-3	-3	2	134	109	10	-2	3	145	145
8	-3	2	63	17	-2	6	2	322	279	-5	-3	2	239	285	6	-3	3	354	356
9	-3	2	228	261	-3	6	2	477	506	-7	-3	2	179	186	7	-3	3	257	222
10	-3	2	173	219	-5	6	2	406	399	-9	-3	2	77	96	8	-3	3	122	94
2	-4	2	55	60	-6	6	2	145	140	-2	-4	2	114	80	10	-3	3	290	244
6	-4	2	285	231	-7	6	2	148	111	-3	-4	2	170	192	11	-3	3	77	132
8	-4	2	84	107	-9	6	2	190	222	-5	-4	2	195	203	6	-4	3	625	573
9	-4	2	130	166	-10	6	2	141	139	-7	-4	2	77	88	7	-4	3	352	337
10	-4	2	100	116	-11	6	2	148	140	-2	-5	2	176	195	9	-4	3	245	185
11	-4	2	148	146	-3	7	2	395	364	-3	-5	2	130	101	10	-4	3	141	129
3	-5	2	266	239	-5	7	2	436	455	-6	-5	2	152	124	11	-4	3	77	117
7	-5	2	315	289	-6	7	2	152	163	-2	-6	2	190	222	3	-5	3	110	59
11	-5	2	105	97	-7	7	2	179	176	-3	-6	2	141	158	8	-5	3	148	141
3	-6	2	134	163	-8	7	2	130	114	-4	-6	2	148	139	9	-5	3	226	200
9	-6	2	161	206	-9	7	2	167	150	-5	-6	2	152	123	11	-5	3	77	131
2	-7	2	126	123	-11	7	2	184	187	-6	-6	2	192	199	3	-6	3	142	159
3	-7	2	385	395	-12	7	2	155	174	-3	-7	2	210	228	4	-6	3	167	170
5	-7	2	148	138	-3	8	2	95	88	-4	-7	2	187	170	9	-6	3	161	132
2	-8	2	192	196	-5	8	2	268	222	-5	-7	2	110	128	4	-7	3	187	181
3	-8	2	363	397	-7	8	2	212	240	-6	-7	2	161	164	5	-7	3	145	124
5	-8	2	158	160	-11	8	2	184	132	-2	-8	2	110	85	4	-8	3	130	149
8	-8	2	190	231	-12	8	2	110	145	-3	-8	2	190	166	5	-8	3	158	107
3	-9	2	224	265	-3	9	2	176	156	-4	-8	2	114	93	6	-8	3	130	118
4	-9	2	170	157	-7	9	2	224	233	-2	-9	2	161	136	9	-8	3	141	157
2-10	2	110	88		-9	9	2	105	108	4	0	3	192	163	4	-9	3	71	102
4-10	2	207	223		-2	10	2	155	134	5	0	3	319	279	5	-9	3	100	109
10-10	2	184	223		-3	10	2	239	251	6	0	3	141	105	9	-9	3	205	228
2-11	2	158	161		-2	11	2	114	122	7	0	3	179	196	10	-9	3	105	80
4-11	2	155	153		-3	11	2	221	226	3	1	3	387	365	3-10	3	110	108	
6-11	2	105	124		-3	12	2	114	116	4	1	3	109	79	4-10	3	105	133	
10-11	2	190	173		-2	4	2	141	112	6	1	3	89	102	5-10	3	210	227	
4-12	2	114	86		-4	4	2	293	294	8	1	3	145	164	7-10	3	105	120	
6-12	2	158	138		-5	4	2	212	204	4	2	3	77	91	8-10	3	182	167	
-3	1	2	416	456	-6	4	2	105	130	5	2	3	148	180	11-10	3	114	156	
-4	1	2	592	642	-7	4	2	114	135	6	2	3	134	127	5-11	3	221	256	
-5	1	2	155	165	-8	4	2	173	189	7	2	3	173	178	7-11	3	155	156	
-6	1	2	344	277	-3	0	2	89	82	3	3	3	247	243	11-11	3	84	127	
-7	1	2	190	225	-4	0	2	640	736	5	3	3	187	229	7-12	3	114	100	
-8	1	2	63	109	-5	0	2	399	454	6	3	3	173	209	-3	0	3	522	582
-9	1	2	170	138	-6	0	2	361	328	3	4	3	442	460	-4	0	3	276	260
-3	2	2	290	279	-7	0	2	157	226	4	4	3	190	206	-5	0	3	313	286
-4	2	2	84	108	-8	0	2	71	65	5	4	3	122	200	-6	0	3	315	280
-6	2	2	105	85	-2	-1	2	671	721	6	4	3	105	131	-8	0	3	71	82
-7	2	2	114	74	-3	-1	2	232	196	3	5	3	305	314	-9	0	3	207	190
-8	2	2	179	190	-4	-1	2	495	477	4	5	3	100	121	-10	0	3	190	186
-9	2	2	190	154	-5	-1	2	391	434	4	-1	3	245	193	-4	1	3	114	109
-2	3	2	416	421	-6	-1	2	122	34	5	-1	3	134	139	-5	1	3	371	348
-4	3	2	520	592	-7	-1	2	130	119	6	-1	3	170	184	-6	1	3	245	210
-6	3	2	77	101	-8	-1	2	141	160	7	-1	3	167	198	-7	1	3	118	118
-7	3	2	114	78	-9	-1	2	210	186	8	-1	3	95	88	-8	1	3	161	128
-2	5	2	126	96	-2	-2	2	505	440	9	-1	3	100	108	-9	1	3	173	150
-3	5	2	202	207	-3	-2	2	100	76	4	-2	3	451	398	-10	1	3	175	94
-5	5	2	212	204	-4	-2	2	300	237	5	-2	3	141	126	-12	1	3	118	119
-7	5	2	263	277	-7	-2	2	100	97	6	-2	3	179	160	-4	2	3	310	254
-8	5	2	176	192	-8	-2	2	71	79	8	-2	3	155	153	-5	2	3	134	163
-9	5	2	130	143	-9	-2	2	110	114	9	-2	3	134	114	-6	2	3	105	82

TABLE 17. (CONTINUED)

H	K	L	FO	FC	H	K	L	FO	FC	H	K	L	FO	FC	H	K	L	FO	FC
-7	2	3	202	216	-3	-6	3	145	90	0	4	8	118	84	0	1	-7	184	170
-8	2	3	126	112	-4	-6	3	152	127	0	4	9	89	77	0	1	-8	100	108
-3	3	3	416	387	-5	-6	3	158	154	0	4	12	161	137	0	1	-9	427	399
-6	3	3	182	157	-3	-7	3	187	212	0	4	13	138	130	0	1-10	251	274	
-7	3	3	114	100	-4	-7	3	158	132	0	4	15	170	193	0	1-11	145	157	
-9	3	3	134	102	-5	-7	3	164	194	0	5	2	520	429	0	1-14	130	101	
-3	4	3	355	323	-3	-8	3	161	154	0	5	3	110	99	0	2	-1	71	61
-5	4	3	170	194	-4	-8	3	118	90	0	5	5	141	120	0	2	-2	274	219
-6	4	3	152	128	0	0	3	285	254	0	5	6	84	276	0	2	-3	89	86
-7	4	3	141	132	0	0	5	387	359	0	5	8	249	288	0	2	-4	414	349
-3	5	3	274	252	0	0	6	161	185	0	5	10	184	188	0	2	-5	324	264
-4	5	3	122	105	0	0	7	63	84	0	5	11	134	119	0	2	-6	126	131
-5	5	3	130	141	0	0	8	122	135	0	5	12	95	88	0	2	-7	401	334
-7	5	3	84	116	0	0	9	477	503	0	6	1	167	125	0	2	-8	228	294
-8	5	3	155	136	0	0	10	195	222	0	6	2	221	217	0	2-12	122	118	
-4	6	3	212	240	0	0	11	237	249	0	6	3	148	166	0	3	-1	424	357
-5	6	3	114	90	0	0	12	152	150	0	6	4	84	74	0	3	-2	329	290
-6	6	3	145	122	0	0	14	130	132	0	6	8	224	257	0	3	-5	656	682
-7	6	3	176	135	0	0	16	100	90	0	6	9	95	89	0	3	-6	217	262
-8	6	3	205	225	0	1	4	335	258	0	6	10	190	170	0	3	-7	228	237
-10	6	3	202	205	0	1	5	118	151	0	6	11	95	78	0	3-10	200	225	
-11	6	3	187	173	0	1	6	89	84	0	6	13	100	99	0	3-12	126	61	
-4	7	3	152	153	0	1	8	71	83	0	7	1	197	188	0	3-14	190	187	
-6	7	3	179	185	0	1	9	217	215	0	7	3	155	140	0	3-15	100	75	
-7	7	3	184	176	0	1	11	253	285	0	7	4	155	152	0	3-16	170	182	
-8	7	3	190	174	0	1	12	152	125	0	7	5	130	142	0	4	-1	214	218
-10	7	3	205	237	0	1	16	100	71	0	7	6	161	149	0	4	-2	167	179
-11	7	3	187	175	0	2	1	89	91	0	7	7	134	149	0	4	-3	237	243
-4	8	3	134	169	0	2	2	862	973	0	7	8	164	154	0	4	-4	197	222
-5	8	3	95	106	0	2	3	95	84	0	7	9	100	108	0	4	-5	619	556
-6	8	3	192	263	0	2	4	935	972	0	7	10	195	201	0	4	-6	498	451
-4	9	3	71	139	0	2	5	179	166	0	8	1	277	235	0	4	-7	134	130
-6	9	3	100	139	0	2	6	212	214	0	8	3	95	70	0	4	-8	114	93
-7	9	3	105	81	0	2	7	100	85	0	8	4	95	101	0	4-10	170	197	
-4	10	3	155	74	0	2	8	77	92	0	8	6	134	127	0	4-11	39	116	
-4	11	3	114	147	0	2	9	77	96	0	8	10	100	91	0	4-14	192	194	
-3	-1	3	474	415	0	2	11	122	137	0	9	1	164	124	0	4-15	170	175	
-4	-1	3	303	296	0	2	12	126	101	0	9	2	95	88	0	4-16	141	124	
-5	-1	3	110	76	0	2	13	187	194	0	9	3	214	196	0	5	-2	77	73
-7	-1	3	134	151	0	2	14	71	86	0	9	4	95	93	0	5	-3	341	350
-8	-1	3	100	112	0	2	15	100	90	0	9	5	138	80	0	5	-4	134	83
-9	-1	3	110	110	0	3	1	409	316	0	9	6	100	77	0	5	-5	77	78
-10	-1	3	114	141	0	3	2	616	534	0	9	8	100	97	0	5	-6	114	82
-3	-2	3	251	247	0	3	3	286	247	0	10	2	167	155	0	5-12	161	161	
-4	-2	3	152	133	0	3	4	812	789	0	10	3	195	160	0	5-14	138	137	
-5	-2	3	84	99	0	3	5	118	122	0	10	4	95	89	0	5-15	100	87	
-6	-2	3	130	114	0	3	6	515	476	0	10	5	138	110	0	6	-1	579	477
-7	-2	3	173	108	0	3	9	141	166	0	11	2	71	74	0	6	-2	232	236
-8	-2	3	148	126	0	3	13	212	236	0	11	4	95	72	0	6	-3	219	211
-3	-3	3	187	155	0	3	15	170	205	0	11	5	134	115	0	6	-6	190	216
-4	-3	3	205	194	0	3	16	100	82	0	12	1	63	96	0	6-10	158	212	
-6	-3	3	170	138	0	4	2	71	81	0	12	5	89	63	0	6-11	161	151	
-8	-3	3	77	82	0	4	3	510	402	0	13	1	63	68	0	6-12	164	196	
-4	-4	3	245	240	0	4	4	367	307	0	1	-3	77	119	0	6-13	95	99	
-7	-4	3	110	57	0	4	5	130	146	0	1	-4	371	320	0	7	-1	292	325
-6	-5	3	110	116	0	4	6	557	542	0	1	-5	352	270	0	7	-2	214	224

TABLE 17. (CONTINUED)

H	K	L	FO	FC	H	K	L	FO	FC	H	K	L	FO	FC	H	K	L	FO	FC
U	7	-3	89	104	1	2	2	170	155	1	10	3	184	193	1	-7	9	164	152
U	7	-4	89	113	1	2	3	569	562	1	10	6	110	79	1	-7	11	221	242
U	7	-6	200	228	1	2	4	190	163	1	11	2	105	138	1	-7	12	145	117
U	7	-8	89	93	1	2	5	455	409	1	12	2	105	129	1	-8	2	164	191
U	7	-10	212	266	1	2	6	122	142	1	-1	4	537	502	1	-8	5	214	217
U	7	-11	192	246	1	2	7	130	136	1	-1	6	164	144	1	-8	9	173	182
U	8	-1	89	120	1	2	8	285	347	1	-1	7	95	74	1	-8	11	145	164
U	8	-2	130	110	1	2	10	152	164	1	-1	8	358	413	1	-8	12	100	109
U	8	-3	89	91	1	2	12	190	222	1	-1	9	77	88	1	-9	4	141	129
U	8	-4	95	93	1	2	14	200	243	1	-1	10	442	523	1	-9	7	202	182
U	8	-5	63	74	1	2	16	148	176	1	-1	12	179	190	1	-9	8	100	81
U	8	-8	164	189	1	3	2	134	149	1	-1	15	141	116	1	-9	9	145	158
U	8	-9	134	137	1	3	3	267	227	1	-2	3	110	106	1	-10	3	145	132
U	8	-10	95	142	1	3	4	358	304	1	-2	4	205	183	1	-10	5	148	167
U	8	-11	138	144	1	3	5	335	339	1	-2	5	292	293	1	-10	6	105	96
U	9	-2	134	114	1	3	6	205	198	1	-2	6	374	431	1	-10	7	182	171
U	9	-3	95	64	1	3	8	268	300	1	-2	8	322	329	1	-10	8	148	119
U	9	-5	71	83	1	3	9	152	154	1	-2	9	243	239	1	-11	5	184	174
U	9	-6	167	167	1	3	10	202	223	1	-2	10	114	154	1	-11	6	152	149
U	9	-7	158	158	1	3	13	173	163	1	-3	2	212	241	1	-11	7	152	129
U	9	-8	100	110	1	3	14	205	214	1	-3	3	283	229	1	-11	8	105	106
U	9	-9	95	94	1	3	16	152	142	1	-3	4	465	493	1	-12	3	105	107
U	10	-2	95	50	1	4	3	346	256	1	-3	6	643	674	1	-13	3	105	101
U	10	-5	167	148	1	4	4	558	292	1	-3	7	161	174	1	0	-5	245	273
U	10	-6	167	186	1	4	5	164	158	1	-3	8	310	321	1	0	-6	148	187
U	10	-7	170	190	1	4	6	118	109	1	-3	11	173	169	1	0	-8	354	396
U	11	-4	138	121	1	4	7	173	157	1	-3	15	145	108	1	0	-9	152	160
U	11	-5	167	146	1	4	9	89	67	1	-4	2	173	180	1	0	-10	313	329
U	11	-6	71	35	1	4	10	212	259	1	-4	4	531	610	1	0	-11	170	175
U	11	-7	134	129	1	4	11	138	122	1	-4	5	274	258	1	0	-15	141	158
U	12	-1	134	114	1	4	12	224	225	1	-4	6	367	384	1	1	-8	395	436
U	12	-5	95	81	1	4	13	100	127	1	-4	7	170	185	1	1	-9	77	81
U	12	-4	95	69	1	5	3	428	341	1	-4	9	219	206	1	1	-10	161	141
U	13	-1	118	108	1	5	7	158	150	1	-4	11	237	236	1	1	-11	148	122
U	13	-3	84	97	1	5	9	95	110	1	-4	13	71	103	1	2	-2	341	348
1	0	4	89	120	1	5	10	195	171	1	-4	15	205	211	1	2	-15	145	176
1	0	5	253	246	1	5	12	179	189	1	-5	2	290	248	1	2	-17	100	138
1	0	6	442	453	1	6	3	182	177	1	-5	4	421	418	1	3	-2	170	184
1	0	7	118	76	1	6	4	226	226	1	-5	5	207	190	1	3	-4	429	495
1	0	8	261	270	1	6	7	217	87	1	-5	6	310	297	1	3	-5	158	165
1	0	9	279	277	1	6	8	138	134	1	-5	9	173	150	1	3	-6	489	575
1	0	10	485	529	1	6	9	173	196	1	-5	13	100	92	1	3	-15	145	165
1	0	11	122	99	1	6	12	105	105	1	-5	15	105	122	1	3	-16	182	175
1	0	12	202	228	1	7	2	134	123	1	-6	2	412	371	1	4	-2	77	59
1	0	15	145	146	1	7	4	138	134	1	-6	3	167	174	1	4	-4	293	272
1	1	3	297	180	1	7	5	138	132	1	-6	4	145	133	1	4	-5	173	156
1	1	4	279	245	1	7	7	173	174	1	-6	7	173	146	1	4	-6	195	183
1	1	5	105	92	1	7	8	100	135	1	-6	11	192	186	1	4	-7	141	148
1	1	6	440	417	1	8	2	200	206	1	-6	12	100	108	1	5	-2	407	396
1	1	7	141	156	1	8	4	100	101	1	-6	13	100	106	1	5	-4	235	242
1	1	8	200	214	1	8	5	179	192	1	-7	2	400	365	1	5	-5	118	104
1	1	9	224	240	1	8	7	179	166	1	-7	3	179	174	1	5	-6	148	151
1	1	10	118	142	1	9	2	105	109	1	-7	4	126	101	1	5	-8	155	136
1	1	12	226	243	1	9	3	148	146	1	-7	5	257	255	1	5	-13	141	181
1	1	13	95	88	1	9	4	148	142	1	-7	7	228	206	1	5	-14	105	97
1	1	16	77	95	1	9	5	105	131	1	-7	8	134	109	1	6	-2	397	344



TABLE 17. (CONTINUED)

H	K	L	FO	FC	H	K	L	FO	FC	H	K	L	FO	FC	H	K	L	FO	FC
1	6	-3	155	163	1	-3-12	95	109		2	1	7	618	530	2	-1	10	84	93
1	6	-5	155	144	1	-3-13	100	92		2	1	8	173	167	2	-1	11	192	265
1	6	-6	89	98	1	-3-14	226	250		2	1	9	257	271	2	-1	13	95	126
1	6	-7	95	74	1	-4	-2	118	120	2	1	10	148	121	2	-1	14	141	117
1	6	-8	134	111	1	-4	-3	542	539	2	1	11	89	121	2	-1	16	110	114
1	6	-9	190	198	1	-4	-5	414	478	2	1	16	114	125	2	-2	5	182	204
1	6-10	274	311		1	-4	-6	155	150	2	2	4	527	497	2	-2	6	184	157
1	6-11	141	100		1	-4	-7	182	167	2	2	5	134	140	2	-2	7	173	204
1	7	-3	164	150	1	-4	-9	148	132	2	2	6	322	305	2	-2	8	141	165
1	7	-4	164	178	1	-4-10	158	154		2	2	7	134	139	2	-2	9	341	348
1	7	-5	134	116	1	-4-12	138	134		2	2	9	272	277	2	-2	11	122	153
1	7	-6	95	116	1	-4-14	179	204		2	2	10	89	105	2	-2	12	158	182
1	7	-8	170	153	1	-5	-2	110	102	2	2	11	95	124	2	-2	13	134	142
1	7	-9	173	159	1	-5	-3	155	124	2	2	15	110	103	2	-2	14	141	159
1	7-10	226	213		1	-5	-4	161	146	2	3	4	361	383	2	-2	15	105	86
1	7-12	148	175		1	-5	-5	412	437	2	3	6	255	251	2	-3	4	378	333
1	8	-2	200	195	1	-5	-7	387	349	2	3	8	89	82	2	-3	5	134	98
1	8	-3	100	68	1	-5	-8	89	93	2	3	10	134	121	2	-3	6	105	77
1	8	-4	224	236	1	-6	-2	145	116	2	3	11	313	322	2	-3	7	339	365
1	8	-6	100	98	1	-6	-3	173	142	2	3	12	105	75	2	-3	8	71	79
1	8	-8	100	132	1	-6	-7	277	270	2	4	3	179	175	2	-3	9	155	185
1	8	-9	105	86	1	-6	-9	367	354	2	4	4	118	96	2	-3	12	130	159
1	8-10	71	97		1	-6-10	100	83		2	4	5	84	72	2	-3	13	167	190
1	9	-2	105	110	1	-7	-2	89	69	2	4	6	283	275	2	-3	16	155	138
1	9	-4	207	193	1	-7	-3	130	90	2	4	7	205	203	2	-4	3	261	250
1	9	-6	179	205	1	-7	-4	184	159	2	4	8	164	132	2	-4	4	288	260
1	9	-7	105	114	1	-7	-5	190	180	2	4	11	182	186	2	-4	5	632	630
1	9	-8	148	122	1	-7	-7	167	179	2	4	13	110	131	2	-4	6	138	138
1	10	-4	105	112	1	-7	-8	141	148	2	5	4	261	267	2	-4	7	365	456
1	10	-6	152	183	1	-7	-9	387	351	2	5	6	167	168	2	-4	10	170	198
1	10-10	77	85		1	-7-11	145	113		2	5	7	71	40	2	-4	12	95	114
1	-1	-5	335	355	1	-8	-2	167	145	2	5	8	202	226	2	-4	14	145	136
1	-1	-6	176	183	1	-8	-5	170	138	2	5	9	105	64	2	-4	16	110	145
1	-1	-8	105	91	1	-8	-9	179	164	2	5	10	105	100	2	-5	3	257	239
1	-1	-9	155	131	1	-8-11	105	144		2	5	13	114	133	2	-5	4	100	112
1	-1-10	366	328		1	-9	-2	176	177	2	6	4	141	132	2	-5	5	460	465
1	-1-11	63	69		1	-9	-7	105	94	2	6	5	145	108	2	-5	6	110	105
1	-1-12	155	152		1	-9-11	152	83		2	6	6	105	109	2	-5	7	161	214
1	-1-10	141	116		1	-9-13	148	124		2	6	7	105	82	2	-5	8	84	113
1	-2	-3	423	535	1	-10	-2	182	146	2	6	10	110	96	2	-5	10	179	194
1	-2	-4	126	140	1	-10	-3	148	132	2	7	3	77	50	2	-5	13	100	86
1	-2	-6	134	114	1	-10	-4	237	217	2	7	6	245	244	2	-5	14	141	122
1	-2	-7	214	245	1	-10	-9	105	83	2	7	8	114	102	2	-6	3	394	368
1	-2	-9	77	61	1	-10-13	145	120		2	7	9	84	71	2	-6	4	195	273
1	-2-10	167	155		1	-11	-4	152	136	2	7	10	114	101	2	-6	5	164	176
1	-2-12	184	170		2	0	5	190	200	2	8	3	158	121	2	-6	8	89	101
1	-2-14	141	100		2	0	6	268	240	2	8	4	114	121	2	-6	9	130	135
1	-3	-2	155	130	2	0	7	469	433	2	8	6	230	233	2	-6	12	145	109
1	-3	-3	585	591	2	0	8	230	227	2	8	8	164	130	2	-6	13	148	139
1	-3	-4	130	102	2	0	10	145	116	2	9	4	118	144	2	-7	3	217	226
1	-3	-5	465	520	2	0	11	277	242	2	9	6	118	123	2	-7	5	89	103
1	-3	-6	190	182	2	0	12	63	82	2	-1	5	574	625	2	-7	6	207	229
1	-3	-7	170	175	2	0	16	155	153	2	-1	6	100	108	2	-7	8	71	75
1	-3	-8	138	139	2	1	4	122	138	2	-1	7	110	120	2	-7	9	100	71
1	-3	-9	145	146	2	1	5	45	58	2	-1	8	141	126	2	-7	10	226	228
1	-3-10	152	148		2	1	6	63	25	2	-1	9	241	239	2	-7	11	105	126

TABLE 17. (CONTINUED)

H	K	L	FO	FC	H	K	L	FO	FC	H	K	L	FO	FC	H	K	L	FO	FC
2	-7	12	148	150	2	7	-6	148	121	2	-9	-3	152	157	3	5	-7	307	241
2	-8	3	138	145	2	7	-8	77	86	2	-10	-3	228	241	3	5	-8	197	162
2	-8	6	141	148	2	7	-9	110	60	2	-10	-5	200	149	3	5	-9	145	126
2	-8	9	105	103	2	8	-3	247	240	2	-10	-12	170	154	3	5	-10	141	75
2	-8	10	152	157	2	8	-4	190	176	2	-11	-3	205	167	3	6	-4	200	131
2	-8	11	110	100	2	8	-5	155	135	2	-11	-5	167	151	3	6	-5	228	138
2	-8	12	110	109	2	8	-8	114	83	2	-11	-12	122	105	3	7	-4	217	169
2	-9	4	182	153	2	9	-3	114	94	3	0	6	253	330	3	7	-5	219	156
2	-9	6	110	99	2	9	-5	114	66	3	0	8	285	373	3	7	-7	158	113
2	-9		110	112	2	-1	-5	279	325	3	0	9	77	145	3	7	-9	161	94
2	-10	6	138	167	2	-1	-6	148	131	3	1	4	212	242	3	8	-4	164	82
2	-10	8	114	91	2	-1	-7	95	102	3	1	6	250	354	3	-1	-7	141	106
2	-11	6	164	178	2	-1	-8	100	69	3	1	7	100	123	3	-1	-8	274	231
2	-11	7	167	120	2	-1	-9	346	371	3	1	8	523	511	3	-1	-9	298	249
2	-11	8	118	95	2	-1	-10	187	234	3	2	4	239	238	3	-1	-10	184	155
2	0	-3	228	243	2	-1	-11	249	266	3	2	5	263	262	3	-1	-11	197	228
2	0	-7	297	274	2	-1	-14	100	84	3	2	6	167	203	3	-2	-6	110	112
2	0	-8	105	121	2	-2	-5	245	204	3	3	4	167	201	3	-2	-7	251	251
2	0	-9	387	369	2	-2	-8	290	245	3	3	5	176	192	3	-2	-8	145	99
2	0	-10	319	332	2	-2	-11	219	232	3	3	7	176	211	3	-2	-9	247	187
2	0	-12	130	118	2	-2	-13	141	133	3	3	8	130	179	3	-2	-10	265	240
2	0	-14	100	103	2	-3	-4	467	412	3	3	10	195	263	3	-2	-11	126	121
2	1	-9	251	229	2	-3	-5	279	276	3	4	4	122	130	3	-2	-12	210	212
2	1	-13	138	115	2	-3	-6	118	113	3	4	7	192	206	3	-3	-5	152	143
2	2	-4	253	239	2	-3	-8	352	298	3	5	4	95	102	3	-3	-6	122	98
2	2	-8	134	138	2	-3	-9	167	184	3	5	5	141	146	3	-3	-7	268	272
2	2	-10	152	123	2	-3	-13	176	184	3	6	4	148	153	3	-3	-8	105	128
2	3	-3	379	364	2	-3	-14	148	138	3	6	5	239	221	3	-3	-10	122	110
2	3	-4	303	242	2	-3	-15	105	114	3	6	7	155	164	3	-3	-12	214	213
2	3	-5	423	421	2	-4	-3	84	96	3	7	5	161	173	3	-3	-13	141	134
2	3	-6	341	330	2	-4	-4	725	670	3	7	7	232	253	3	-3	-15	110	103
2	3	-10	126	191	2	-4	-5	158	168	3	8	7	173	181	3	-4	-4	100	81
2	4	-3	387	359	2	-4	-6	130	110	3	-1	6	161	239	3	-4	-5	237	287
2	4	-4	349	318	2	-4	-9	179	201	3	0	-7	145	137	3	-4	-6	155	168
2	4	-5	141	106	2	-4	-10	95	109	3	0	-8	358	334	3	-4	-8	84	102
2	4	-6	118	119	2	-4	-13	182	210	3	0	-9	245	252	3	-4	-12	141	122
2	4	-7	192	206	2	-4	-14	110	88	3	0	-11	197	170	3	-4	-13	148	136
2	4	-12	145	138	2	-4	-15	158	136	3	0	-12	293	275	3	-4	-14	155	156
2	4	-13	148	110	2	-5	-3	100	116	3	1	-6	235	266	3	-4	-15	158	155
2	4	-15	114	114	2	-5	-4	341	355	3	1	-14	207	143	3	-5	-4	148	136
2	5	-3	245	223	2	-5	-5	55	86	3	2	-4	77	29	3	-5	-5	319	419
2	5	-4	152	142	2	-5	-6	232	240	3	2	-5	276	261	3	-5	-7	118	118
2	5	-5	126	82	2	-5	-7	122	108	3	2	-8	110	117	3	-5	-10	138	106
2	5	-6	89	47	2	-5	-10	170	168	3	2	-9	167	108	3	-5	-14	158	174
2	5	-7	265	266	2	-6	-3	190	209	3	2	-10	176	163	3	-6	-7	182	187
2	5	-8	190	175	2	-6	-6	259	284	3	2	-11	207	189	3	-7	-4	200	216
2	5	-9	195	188	2	-6	-8	167	172	3	2	-12	217	123	3	-7	-7	197	205
2	6	-5	195	179	2	-6	-9	100	112	3	3	-4	214	205	3	-7	-9	148	140
2	6	-6	197	165	2	-7	-3	184	167	3	3	-5	322	276	3	-8	-4	221	219
2	6	-7	141	127	2	-7	-4	134	136	3	3	-6	173	172	3	-8	-6	145	143
2	6	-8	71	57	2	-7	-6	100	112	3	4	-6	332	288	3	-8	-7	148	145
2	6	-9	179	169	2	-7	-8	292	313	3	4	-7	281	223	3	-8	-9	221	225
2	6	-11	187	197	2	-7	-9	105	127	3	4	-8	290	255	3	-9	-6	155	183
2	7	-3	253	237	2	-7	-10	187	199	3	4	-13	141	96	3	-11	-4	170	202
2	7	-4	207	180	2	-8	-8	266	270	3	5	-5	184	133					
2	7	-5	148	109	2	-8	-10	158	170	3	5	-6	212	207					

Table 18. Structure Parameters for  $\text{Ni}(\text{DPP})_3\text{I}_2$ 

Atom	x	y	z	$B, \text{\AA}^2$
Ni	0.359(2)	0.043(1)	0.224(1)	2.6(3)
I <sub>1</sub>	0.289(1)	0.152(1)	0.106(1)	5.2(3)
I <sub>2</sub>	0.187(1)	0.896(1)	0.324(1)	4.0(2)
P <sub>1</sub>	0.311(4)	0.879(2)	0.122(2)	2.8(6)
P <sub>2</sub>	0.394(4)	0.218(2)	0.319(2)	2.4(5)
P <sub>3</sub>	0.573(4)	0.111(3)	0.198(2)	3.4(7)

### Qualitative Correlation Diagrams

Qualitative energy level diagrams for  $d^n$ -configurations with  $n$  equal to seven, eight and nine have been constructed for the  $C_{4v}$  and  $D_{3h}$  symmetries. These were constructed as outlined in Chapter III.

The correlation diagrams for  $d^9$  are illustrated in Figures 18 and 19. It is possible to predict that for a  $D_{3h}$  symmetry there should be two transitions which are spin allowed and involve one electron ( ${}^2A'_1 \rightarrow {}^2E'$  and  ${}^2A'_1 \rightarrow {}^2E''$ ).<sup>\*</sup> From the character table for  $D_{3h}$ , one finds that the  $z$  axis belongs to the  $A''_2$  representation and the  $x, y$  axes to the  $E'$  representation. The transformation properties of the dipole moment integrand for each of these transitions are presented in Table 20.

<sup>\*</sup>Hole formalism used in all correlation diagrams.

TABLE 19. OBSERVED AND CALCULATED STRUCTURE FACTORS FOR NI(DPP)3I2

H	K	L	FO	FC	H	K	L	FO	FC	H	K	L	FO	FC	H	K	L	FO	FC
2	0	0	195	217	2	5	0	78	63	-8	3	0	26	32	-5	9	0	49	45
3	0	0	39	52	6	5	0	86	67	-9	3	0	109	120	-3	10	0	52	49
4	0	0	40	28	8	5	0	69	45	-10	3	0	42	40	-5	10	0	51	48
6	0	0	77	70	1	6	0	93	61	-1	4	0	102	112	-6	10	0	30	19
8	0	0	63	58	3	6	0	28	10	-2	4	0	73	69	-7	10	0	30	36
9	0	0	42	30	4	6	0	88	52	-3	4	0	123	126	-8	10	0	42	47
10	0	0	32	38	6	6	0	69	51	-4	4	0	77	66	-3	11	0	30	42
11	0	0	32	22	8	6	0	30	12	-7	4	0	95	93	-5	11	0	30	35
2	1	0	118	106	1	7	0	110	92	-8	4	0	58	61	-6	11	0	42	37
3	1	0	44	33	3	7	0	30	19	-9	4	0	62	88	-7	11	0	30	35
4	1	0	137	125	4	7	0	61	40	-10	4	0	41	39	-8	11	0	53	55
6	1	0	81	53	6	7	0	22	18	-11	4	0	44	46	-4	12	0	44	52
7	1	0	62	43	0	8	0	28	23	-13	4	0	22	4	-4	13	0	30	37
8	1	0	71	65	1	8	0	84	78	-1	5	0	46	37	-6	13	0	44	41
9	1	0	42	39	4	8	0	32	21	-2	5	0	83	85	-4	14	0	30	20
10	1	0	32	16	5	8	0	30	16	-3	5	0	175	181	-6	14	0	42	41
11	1	0	22	16	0	9	0	30	32	-4	5	0	98	91	-8	14	0	30	31
0	2	0	76	67	3	9	0	30	17	-5	5	0	88	84	0	0	3	52	41
1	2	0	87	74	5	9	0	42	29	-6	5	0	47	61	0	0	4	77	49
2	2	0	123	114	3	10	0	52	48	-8	5	0	53	55	0	0	5	212	188
3	2	0	42	23	5	10	0	39	22	-9	5	0	48	25	0	0	6	44	54
4	2	0	174	206	1	11	0	44	50	-10	5	0	30	30	0	0	7	62	77
5	2	0	26	15	3	11	0	49	41	-11	5	0	30	37	0	0	8	67	71
6	2	0	89	80	1	12	0	61	38	-13	5	0	45	21	0	0	9	267	224
7	2	0	40	23	3	12	0	24	17	-1	6	0	79	84	0	0	10	126	101
9	2	0	32	5	1	13	0	50	21	-2	6	0	69	40	0	0	11	65	71
0	3	0	132	152	-2	1	0	141	151	-3	6	0	120	141	0	0	14	66	61
1	3	0	101	87	-4	1	0	59	81	-5	6	0	142	173	0	1	2	212	178
2	3	0	155	143	-5	1	0	95	96	-6	6	0	35	36	0	1	3	30	25
4	3	0	130	121	-6	1	0	33	41	-7	6	0	68	77	0	1	5	160	146
5	3	0	26	21	-7	1	0	92	81	-1	7	0	93	106	0	1	8	22	30
6	3	0	49	40	-11	1	0	45	39	-2	7	0	83	69	0	1	9	173	157
8	3	0	61	51	-13	1	0	32	17	-3	7	0	45	37	0	1	10	51	61
9	3	0	32	26	-2	2	0	255	236	-5	7	0	128	141	0	1	11	93	119
10	3	0	22	12	-3	2	0	71	74	-7	7	0	118	121	0	1	12	40	37
0	4	0	136	151	-4	2	0	108	112	-8	7	0	39	52	0	1	14	52	45
1	4	0	102	87	-5	2	0	81	90	-9	7	0	50	45	0	1	16	32	26
2	4	0	152	155	-6	2	0	32	39	-12	7	0	22	21	0	2	2	410	433
3	4	0	63	51	-7	2	0	89	102	-1	8	0	94	95	0	2	3	113	101
4	4	0	81	59	-9	2	0	70	61	-3	8	0	82	75	0	2	4	339	300
6	4	0	51	36	-10	2	0	30	30	-4	8	0	47	32	0	2	5	28	21
7	4	0	22	24	-11	2	0	32	26	-5	8	0	26	20	0	2	6	30	25
8	4	0	93	81	-13	2	0	32	29	-7	8	0	79	73	0	2	7	114	96
9	4	0	32	24	-1	3	0	87	115	-9	8	0	41	41	0	2	8	54	58
10	4	0	30	23	-4	3	0	59	55	-12	8	0	44	50	0	2	10	26	24
0	5	0	93	65	-6	3	0	22	34	-1	9	0	59	63	0	2	11	87	98
1	5	0	50	39	-7	3	0	95	127	-3	9	0	87	89	0	2	12	70	69

TABLE 19. (CONTINUED)

H	K	L	FO	FC	H	K	L	FO	FC	H	K	L	FO	FC	H	K	L	FO	FC
U	2	13	30	36	U	7	2	28	42	0	2	-7	201	198	0	6-11	30	27	
U	3	1	69	85	U	7	3	40	41	0	2	-8	84	110	0	6-12	79	96	
U	3	2	292	285	U	7	4	114	113	0	2-10	44	46		0	6-13	22	13	
U	3	4	335	315	U	7	8	85	99	0	2-11	26	35		0	7 -1	162	166	
U	3	5	111	100	U	7	10	53	53	0	2-12	55	65		0	7 -2	28	28	
U	3	6	104	109	U	7	12	22	25	0	2-14	42	46		0	7 -3	55	73	
U	3	7	109	85	U	7	13	32	34	0	2-16	45	50		0	7 -5	56	58	
U	3	9	65	75	U	8	1	71	74	0	3 -1	118	136		0	7 -6	74	96	
U	3	11	28	43	U	8	2	30	39	0	3 -2	162	168		0	7 -7	20	3	
U	3	12	51	42	U	8	4	73	91	0	3 -3	37	6		0	7 -8	20	14	
U	3	13	73	79	U	8	5	22	35	0	3 -4	28	9		0	7-10	88	119	
U	3	14	32	38	U	8	6	30	35	0	3 -5	340	324		0	7-11	30	37	
U	3	15	100	47	U	8	7	30	35	0	3 -6	107	80		0	7-12	42	50	
U	4	1	44	45	U	8	8	44	42	0	3 -7	141	125		0	7-14	22	4	
U	4	2	70	70	U	8	10	44	34	0	3 -9	55	40		0	8 -1	104	87	
U	4	3	102	112	U	8	13	30	30	0	3-10	141	111		0	8 -2	41	26	
U	4	4	262	210	U	9	1	67	70	0	3-14	67	87		0	8 -3	28	46	
U	4	5	48	48	U	9	2	30	28	0	3-15	30	35		0	8 -5	41	73	
U	4	6	167	171	U	9	3	53	53	0	3-16	45	64		0	8 -8	66	80	
U	4	9	87	89	U	9	5	22	29	0	4 -1	77	90		0	8-10	42	73	
U	4	12	22	20	U	9	6	61	55	0	4 -2	67	85		0	9 -3	60	59	
U	4	13	75	83	U	9	10	22	15	0	4 -3	127	111		0	9 -5	22	19	
U	4	14	44	42	U	10	1	30	39	0	4 -5	180	261		0	9 -6	60	71	
U	4	15	45	58	U	10	3	69	72	0	4 -6	115	138		0	9 -8	68	79	
U	5	2	212	189	U	10	5	22	16	0	4 -7	41	33		0	10 -1	44	42	
U	5	3	17	3	U	10	6	30	33	0	4 -8	42	48		0	10 -3	30	29	
U	5	4	72	70	U	10	8	30	29	0	4 -9	51	35		0	10 -6	69	103	
U	5	6	146	136	U	11	3	53	45	0	4-10	65	65		0	10 -8	44	49	
U	5	7	48	52	U	11	5	20	23	0	4-12	40	35		0	10-10	22	15	
U	5	8	56	56	U	11	8	28	22	0	4-14	68	64		0	11 -1	30	36	
U	5	9	50	48	U	12	0	20	21	0	4-15	30	33		0	11 -4	44	43	
U	5	10	66	61	U	12	1	30	30	0	5 -3	205	188		0	11 -6	42	54	
U	5	11	42	48	U	12	5	20	25	0	5 -4	17	9		0	11 -7	22	19	
U	5	12	44	41	U	13	1	26	26	0	5 -5	35	43		0	11-10	30	34	
U	5	13	32	32	U	1	-2	150	124	0	5 -7	26	45		0	12 -1	30	39	
U	5	15	32	32	U	1	-3	89	98	0	5 -8	37	42		0	12 -2	22	28	
U	5	16	22	17	U	1	-4	177	133	0	5 -9	39	59		0	12 -4	42	49	
U	6	2	132	156	U	1	-5	69	79	0	5-10	20	10		0	12 -8	30	23	
U	6	4	26	22	U	1	-7	167	145	0	5-12	77	87		0	12-10	20	31	
U	6	6	69	72	U	1	-8	55	61	0	5-14	22	36		0	13 -2	28	33	
U	6	7	40	53	U	1	-9	159	140	0	6 -1	172	193		0	13 -4	20	29	
U	6	8	77	84	U	1-10	61	68		0	6 -3	172	141		0	13 -8	26	23	
U	6	10	42	38	U	1-12	55	36		0	6 -5	37	44						
U	6	11	62	53	U	1-16	22	32		0	6 -6	70	93						
U	6	12	32	32	U	2	-4	110	120	0	6 -7	66	61						
U	6	15	22	10	U	2	-5	157	165	0	6 -8	26	21						
U	7	1	39	32	U	2	-6	45	42	0	6-10	86	99						

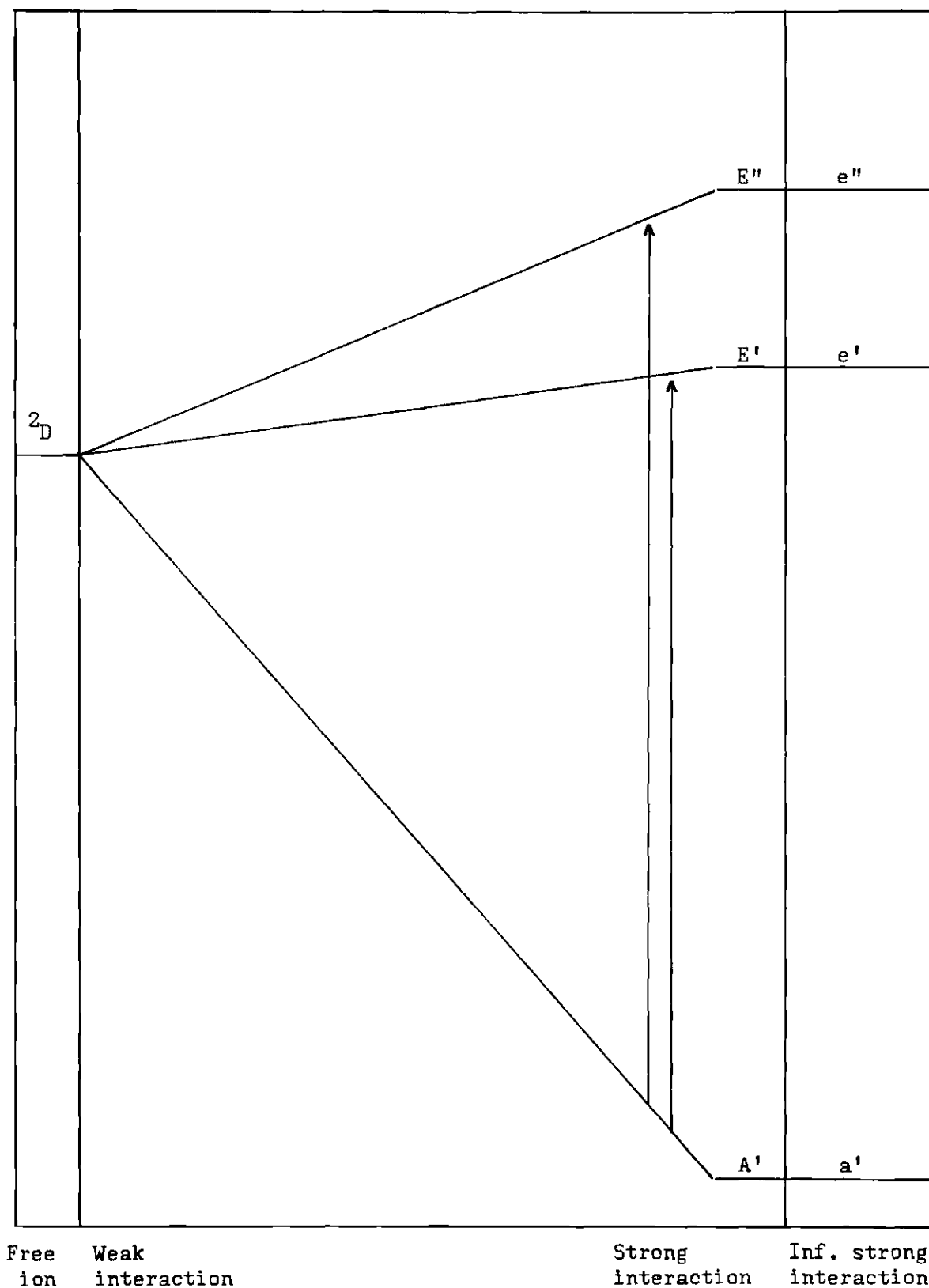


Figure 18. Correlation Diagram for a  $d^9$  Configuration in a  $D_{3h}$  Symmetry

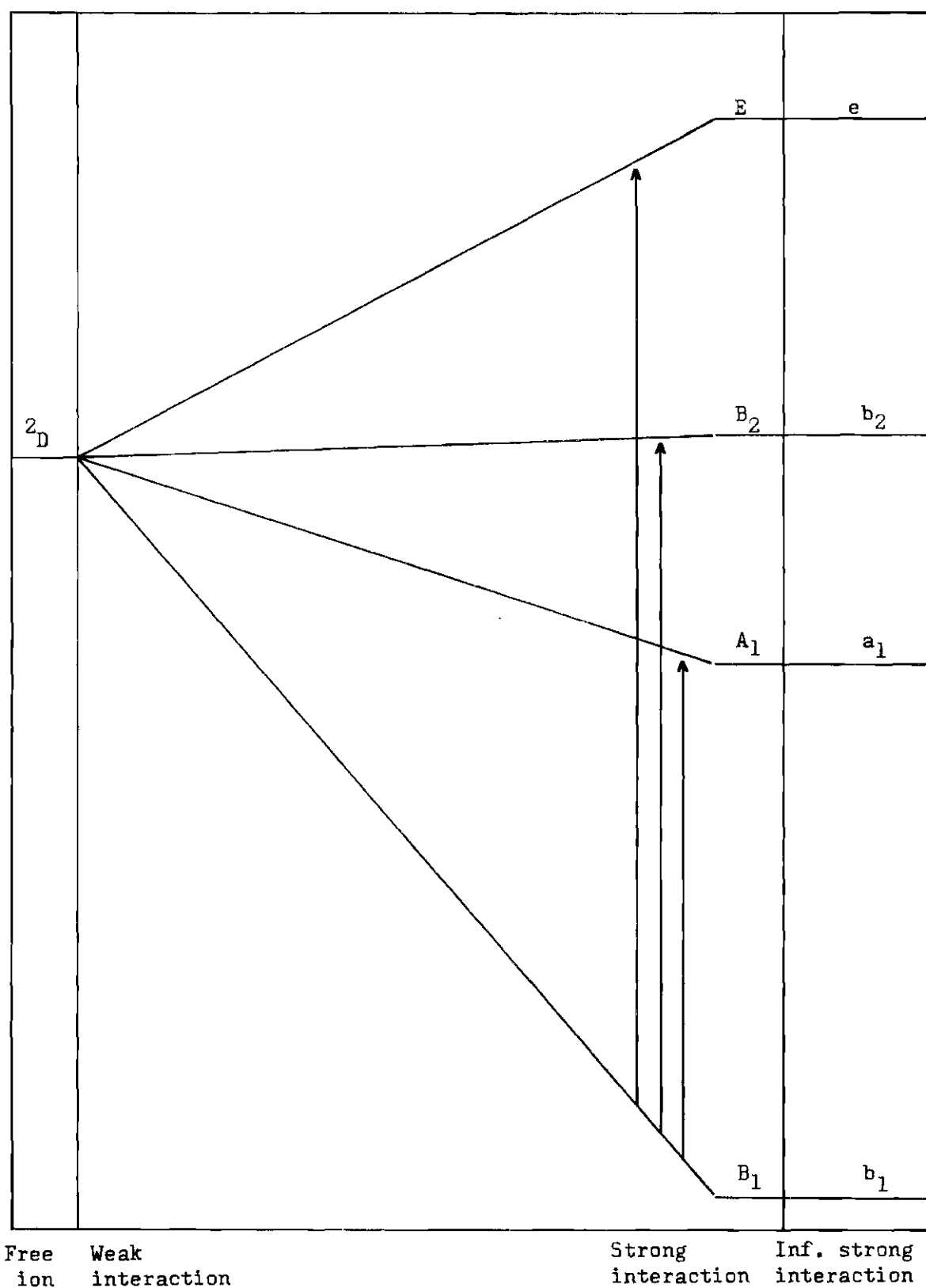


Figure 19. Correlation Diagram for a  $d^9$  Configuration in a  $C_{4v}$  Symmetry

Table 20. Transformation Properties of the Dipole Moment  
Integrand,  $\psi^* \sum q_i \psi'$

Predicted transitions	Dipole integrand	Direct products	Irred. rep.	Totally Sym- metric present
${}^2A'_1 \longrightarrow {}^2E'$	$\Gamma[\psi'(z)\psi]$	$A'_1 \times A''_2 \times E'$	$E''$	No, forbidden
	$\Gamma[\psi'(x,y)\psi]$	$A'_1 \times E' \times E'$	$A'_1 + A'_2 + E'$	Yes, allowed
${}^2A'_1 \longrightarrow {}^2E''$	$\Gamma[\psi'(z)\psi]$	$A'_1 \times A''_2 \times E''$	$E'$	No, forbidden
	$\Gamma[\psi'(x,y)\psi]$	$A'_1 \times E' \times E''$	$A''_1 + A''_2 + E''$	No, forbidden

Since the  $A'_1$  representation is present for the transition  ${}^2A'_1 \longrightarrow {}^2E'$  along the (x, y) axis, it follows that this transition is allowed by the symmetry of the purely electronic wave functions. The other transitions are vibronically allowed and whatever intensity they have must be attributed to vibronic interaction.

Transitions will be allowed only for certain orientations of the electric vector of the incident light; Table 21 is a tabulation of the polarizations (reference will normally be made to either parallel ( $\parallel$ ) or perpendicular ( $\perp$ ) to the principal axis (z) of the point group).

Table 21. Polarization of Incident Radiation

Predicted transition	z	(x,y)	Pol. with respect to principal axis
${}^2A'_1 \longrightarrow {}^2E'$	forbidden	allowed	$\perp$
${}^2A' \longrightarrow {}^2E''$	forbidden	forbidden	-



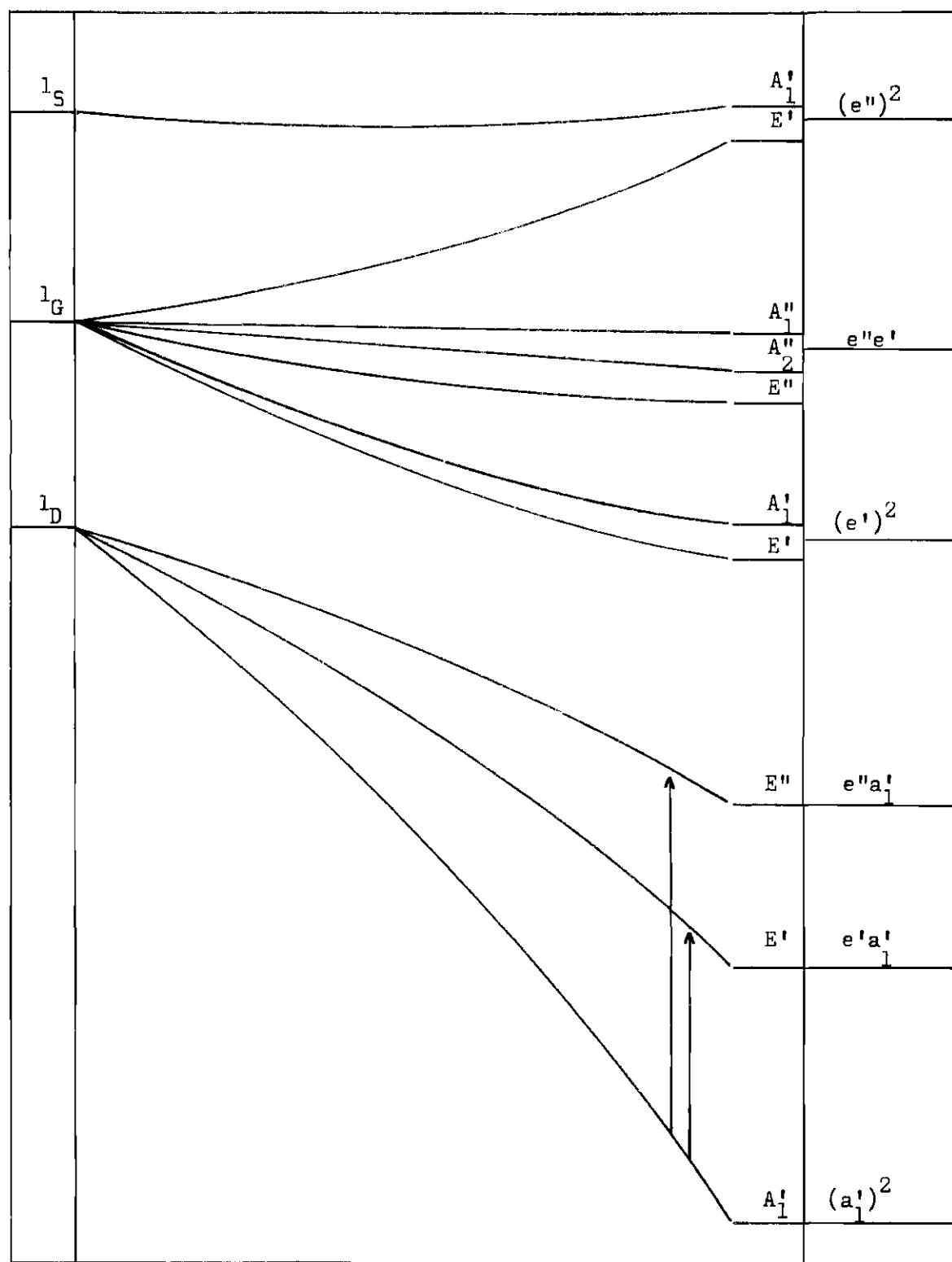
Three transitions are predicted from the correlation diagram (Figure 19) for a  $d^9$  configuration in a  $C_{4v}$  environment; these are listed in Table 22.

Table 22. Predicted Transitions for a  $d^9$  Configuration in a  $C_{4v}$  Environment

Predicted transitions	Mechanism of transition	Polarization*
${}^2B_1 \longrightarrow {}^2A_1$	vibronic	-
${}^2B_1 \longrightarrow {}^2B_2$	vibronic	-
${}^2B_1 \longrightarrow {}^2E$	electronic (x,y)	$\perp$
* Polarization with respect to principal axis (z)		

Correlations diagrams have also been constructed for  $d^8$  and  $d^7$  in  $D_{3h}$  and  $C_{4v}$  environments (the ordering of levels is based on a strong field model since the cobalt and nickel complexes of interest are low-spin). Figures 20 and 21 show, respectively, the splitting of the singlet states for a  $d^8$  configuration in  $D_{3h}$  and  $C_{4v}$  environments. Figure 22 and 23 illustrate the doublet states arising from a  $d^7$  configuration in  $D_{3h}$  and  $C_{4v}$  environments.

Table 23 is a tabulation of the predicted transitions for the  $d^8$  and  $d^7$  configurations in the two symmetries.



Free ion      Weak interaction      Strong interaction      Inf. strong interaction

Figure 20. Correlation Diagram for a  $d^8$  Configuration in a  $D_{3h}$  Symmetry

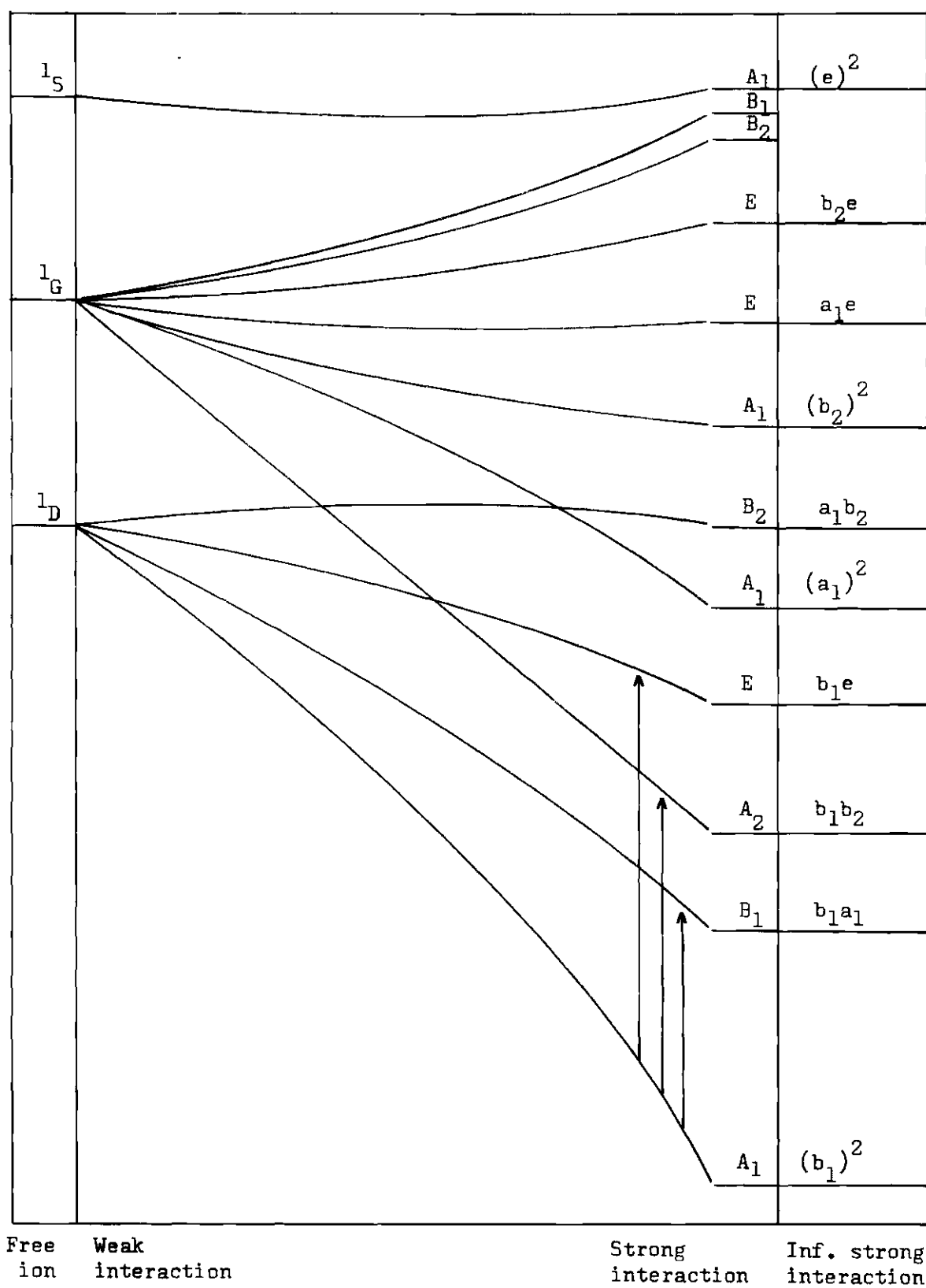
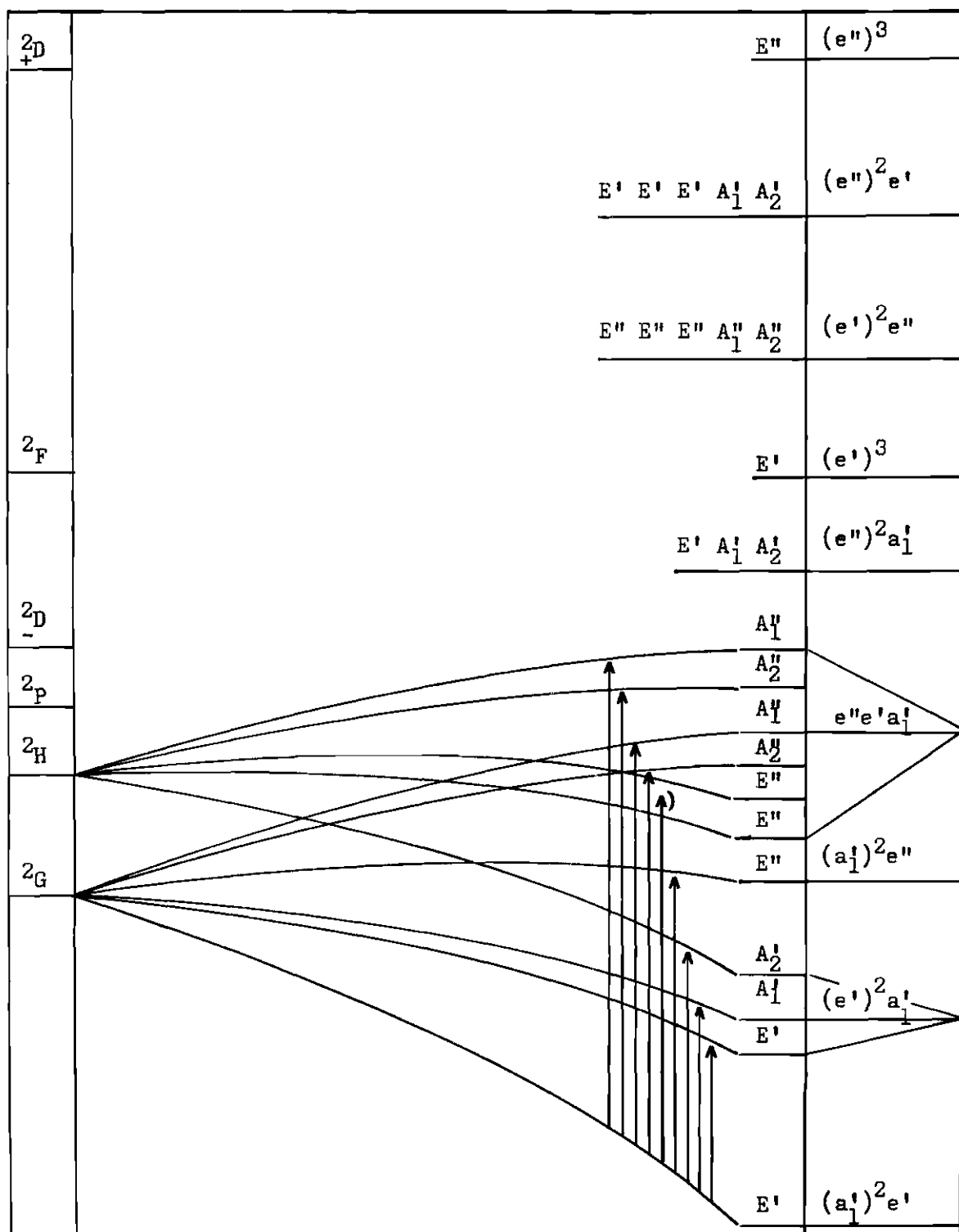
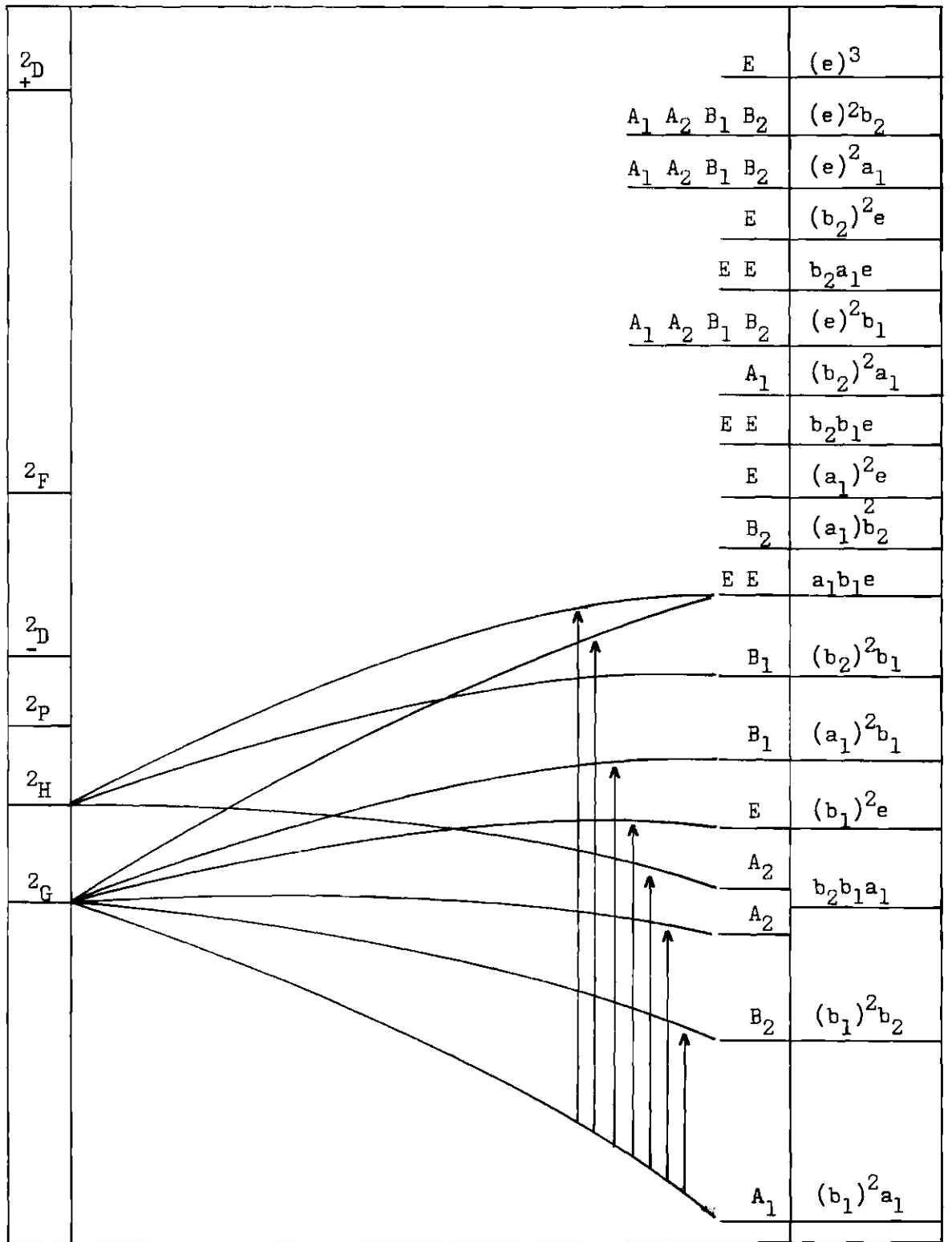


Figure 21. Correlation Diagram for a  $d^8$  Configuration in a  $C_{4v}$  Symmetry



Free ion      Weak interaction      Strong interaction      inf. strong interaction

Figure 22. Correlation Diagram for a  $d^7$  Configuration in a  $D_{3h}$  Symmetry



Free ion  
Weak interaction

Strong interaction  
Inf. strong interaction

Figure 23. Correlation Diagram for a  $d^7$  Configuration in a  $C_{4v}$  Symmetry

Table 23. Predicted Transitions for  $d^8$  and  $d^7$  Configurations in a Five-Coordinate Symmetry

Configuration	Symmetry	Multiplicity	Predicted transition	Mechanism	Polarization
$d^8$	$D_{3h}$	1	$A'_1 \longrightarrow E'$	elect.	$\perp$
			$A'_1 \longrightarrow E''$	vib.	-
	$C_{4v}$	1	$A_1 \longrightarrow B_1$	vib.	-
			$A_1 \longrightarrow A_2$	vib.	-
			$A_1 \longrightarrow E$	elect.	$\perp$
$d^7$	$D_{3h}$	2	$E' \longrightarrow E'$	vib.	-
			$E' \longrightarrow A'_2$	elect.	$\perp$
			$E' \longrightarrow A'_1$	elect.	$\perp$
			$E' \longrightarrow E''$	elect.	$\parallel, \perp$
			$E' \longrightarrow E''$	elect.	$\parallel, \perp$
			$E' \longrightarrow A''_2$	vib.	-
			$E' \longrightarrow A''_2$	vib.	-
			$E' \longrightarrow A''_1$	vib.	-
			$E' \longrightarrow A''_1$	vib.	-
	$C_{4v}$	2	$A_1 \longrightarrow B_2$	vib.	-
			$A_1 \longrightarrow A_2$	vib.	-
			$A_1 \longrightarrow A_2$	vib.	-
			$A_1 \longrightarrow E$	elect.	$\perp$
			$A_1 \longrightarrow B_1$	vib.	-
			$A_1 \longrightarrow E$	elect.	$\perp$
			$A_1 \longrightarrow E$	elect.	$\perp$

## CHAPTER VII

## RESULTS AND DISCUSSION

StructureTris(Pyridine N-Oxide)Cobalt(II) Halides

Previous reports of tris(pyridine N-oxide)cobalt(II) halides either did not attempt to assign a structure (113) or assigned a tentative structure based on very limited data (114). Quagliano and co-workers (113) indicate that the chloride complex has an infrared absorption at  $1220\text{ cm}^{-1}$  which appears to be a characteristic frequency of the N-O group in complexes containing only pyridine N-oxide in the first coordination sphere of the central ion. They also report that the complex has a low conductivity ( $30.2\text{ ohm}^{-1}\text{ cm}^2\text{ mole}^{-1}$ ) in dimethylformamide, which suggests that some chloride coordination persists even at the dilution used for the conductivity measurements. Issleib and Kreibick (114) report the bromide to have an apparent molecular weight of 247 (calculated = 504) in phenol and a conductivity of 19 to  $29\text{ ohm}^{-1}\text{ cm}^2\text{ mole}^{-1}$  depending on the concentration in acetonitrile. They have taken these data, along with the magnetic moment of 4.67 B.M. and the green color of the complex, as evidence for a tetrahedral structure. They have formulated the complex as  $[\text{Co}(\text{pyridine N-oxide})_3\text{Br}]\text{Br}$ .

The mull spectra (Figure 3) of the tris(pyridine N-oxide)cobalt(II) chloride and bromide were found to be almost identical with those of the corresponding tetrahalocobaltate(II) anions (Table 14). There are

variations in the relative intensities of the spectral bands of the bromide complex as compared with the tetrabromocobaltate(II) anion. However, the same type of variations were reported for the tetrachlorocobaltate(II) anion with different cations in crystal spectra (127).

The spectral results suggest that the solid contains the tetrachlorocobaltate(II) anion and that the compound should be formulated as the mixed complex,  $[\text{Co}(\text{pyridine N-oxide})_6][\text{CoX}_4]$ . In order to substantiate such a possibility, cadmium was substituted for the tetrahedral cobalt to give  $[\text{Co}(\text{pyridine N-oxide})_6][\text{CdX}_4]$ .

X-ray powder patterns (Table 10) for the tris(pyridine N-oxide)cobalt(II) bromide and for the hexakis(pyridine N-oxide)cobalt(II) tetrabromocadmiate (II) were found to be almost identical in both peak position and intensity, and the compounds thus appear to be isomorphous. The tris(pyridine N-oxide)cobalt(II) halide compounds, therefore, contain both tetrahedral and octahedral cobalt(II) complexes.

A similar structure was recently assigned to the cobalt(II) halide complex of the chelate ligand, bis(di-isopropoxyphosphinyl)methane, on the basis of its spectrum (128). The tris(cyclohexylphosphine)cobalt(II) halide compounds recently reported by Issleib and Roloff (85) also appear to contain both tetrahedral and octahedral cobalt(II) complexes.

Attempts were made to obtain the spectrum of  $[\text{Co}(\text{pyridine N-oxide})_6][\text{CdBr}_4]$  as a mull, but due to the low extinction coefficients of octahedral bands and the background noise encountered with the mull technique, very poor results were obtained. Attempts were also made to obtain the spectrum of this compound in dimethylformamide and in acetonitrile; in both solvents, the compound gave deep blue solutions and the spectra were



identical, with respect to absorption positions, with the spectra of  $\text{Co}(\text{pyridine N-oxide})_3\text{Br}_2$  in the same solvents; molar extinction coefficients were much lower than those of  $\text{Co}(\text{pyridine N-oxide})_3\text{Br}_2$  in solution.

The spectral results indicate that the solution measurements previously reported, such as conductivity and molecular weight, are not directly related to the species present in the solid since reaction apparently occurs on dissolving. These results also raise the question as to what species are present in solution. In an attempt to answer this, cobalt(II) bromide was dissolved in dimethylformamide and the spectrum observed as the concentration of pyridine N-oxide was increased (Figure 4). No appreciable change in any visible band was noted although the tail of an ultraviolet band did increase in intensity. The only explanations are that either there is no coordination by pyridine N-oxide in these solutions or pyridine N-oxide and dimethylformamide have identical ligand field parameters.

Studies of the  $[\text{Ni}(\text{DMF})_6](\text{ClO}_4)_2$  and the  $[\text{Ni}(\text{pyridine N-oxide})_6](\text{ClO}_4)_2$  complexes (129, 130) have been given in support of the latter explanation; however, the fact that the spectrum of the pyridine N-oxide complex was obtained in DMF does not allow one to rule out the possibility of solvent exchange.

The species present in solution are not identified; however, the spectra in DMF of  $\text{Co}(\text{pyridine N-oxide})_3\text{X}_2$  and  $[\text{Co}(\text{pyridine N-oxide})_6][\text{CdBr}_4]$  indicate that the cobalt(II) ions are probably present as various tetrahedral species.

### Diphenylphosphine Complexes

The structure of dibromotris(diphenylphosphine)cobalt(II) has been determined from three-dimensional X-ray data and the structure of diiodotris(diphenylphosphine)nickel(II) has been confirmed to be isostructural to the cobalt complex by the successful refinement of the zero level data. Bond distances and angles (131) for the heavy atoms of the two structures are given in Table 24.

A perspective drawing of one molecule of  $\text{Co}(\text{DPP})_3\text{Br}_2$  with atoms labelled, as viewed down the b-axis of the crystal, is given in Figure 24. The two bromine atoms, one phosphorus atom ( $\text{P}_3$ ), and the cobalt atom are essentially coplanar, the dihedral angle between the plane defined by  $\text{Co}-\text{Br}_1-\text{Br}_2$  and the plane defined by  $\text{Co}-\text{P}_3-\text{Br}_1$  is only  $1.9^\circ$ . The angles between the equatorial groups and each axial group are approximately  $90^\circ$ , the angles between equatorial groups and  $\text{P}_1$  are  $90.8^\circ$ ,  $86.8^\circ$  and  $89.8^\circ$ ; between equatorial groups and  $\text{P}_2$ , the angles are  $91.1^\circ$ ,  $89.2^\circ$  and  $91.3^\circ$ . Since the three atoms in the equatorial plane are not equivalent, trigonal symmetry in this plane is not possible and the structure is not a trigonal bipyramid. In addition the angles in the equatorial plane are not the required  $120^\circ$  for trigonal symmetry but range from  $98^\circ$  to  $136^\circ$ . The coordination sphere (atoms bonded to the metal) does, however, conform to a bipyramidal configuration.

A similar configuration was observed for the  $\text{Ni}(\text{DPP})_3\text{I}_2$  complex. The only differences observed in the coordination spheres of the two complexes are the metal to halide bond distances. The distances are:  $\text{Co}-\text{Br}_1 = 2.54$ ,  $\text{Co}-\text{Br}_2 = 2.33$ ,  $\text{Ni}-\text{I}_1 = 2.80$ ,  $\text{Ni}-\text{I}_2 = 2.49$ .

Table 24. Selected Intramolecular Distances and Angles for  $M(\text{DPP})_3\text{X}_2$ 

Atoms	Intramolecular Distance, Å		Atoms	Angle, Deg.	
	M=Co; X=Br	M=Ni; X=I		M=Co; X=Br	M=Ni; X=I
M - X <sub>1</sub>	2.54(1)	2.80(2)	X <sub>1</sub> - M - X <sub>2</sub>	125.6(2)	123(1)
M - X <sub>2</sub>	2.33(1)	2.49(2)	X <sub>1</sub> - M - P <sub>1</sub>	86.8(3)	87(1)
M - P <sub>1</sub>	2.23(1)	2.18(3)	X <sub>1</sub> - M - P <sub>2</sub>	89.2(3)	87(1)
M - P <sub>2</sub>	2.20(1)	2.22(3)	X <sub>1</sub> - M - P <sub>3</sub>	98.1(3)	105(1)
M - P <sub>3</sub>	2.18(1)	2.13(5)	X <sub>2</sub> - M - P <sub>1</sub>	90.9(3)	89(1)
P <sub>1</sub> - R <sub>1</sub> C <sub>1</sub>	1.85(4)		X <sub>2</sub> - M - P <sub>2</sub>	91.1(3)	93(1)
P <sub>1</sub> - R <sub>2</sub> C <sub>1</sub>	1.85(3)		X <sub>2</sub> - M - P <sub>3</sub>	136.3(3)	133(1)
P <sub>2</sub> - R <sub>3</sub> C <sub>1</sub>	1.91(3)		P <sub>1</sub> - M - P <sub>2</sub>	175.9(4)	174(2)
P <sub>2</sub> - R <sub>4</sub> C <sub>1</sub>	1.75(4)		P <sub>1</sub> - M - P <sub>3</sub>	89.9(4)	93(2)
P <sub>3</sub> - R <sub>5</sub> C <sub>1</sub>	1.78(4)		P <sub>2</sub> - M - P <sub>3</sub>	91.3(4)	91(1)
P <sub>3</sub> - R <sub>6</sub> C <sub>1</sub>	1.84(3)		Dihedral Angle, Deg.		
			X <sub>1</sub> - M - X <sub>2</sub>	1.9(3)	
			P <sub>3</sub> - M - X <sub>2</sub>		

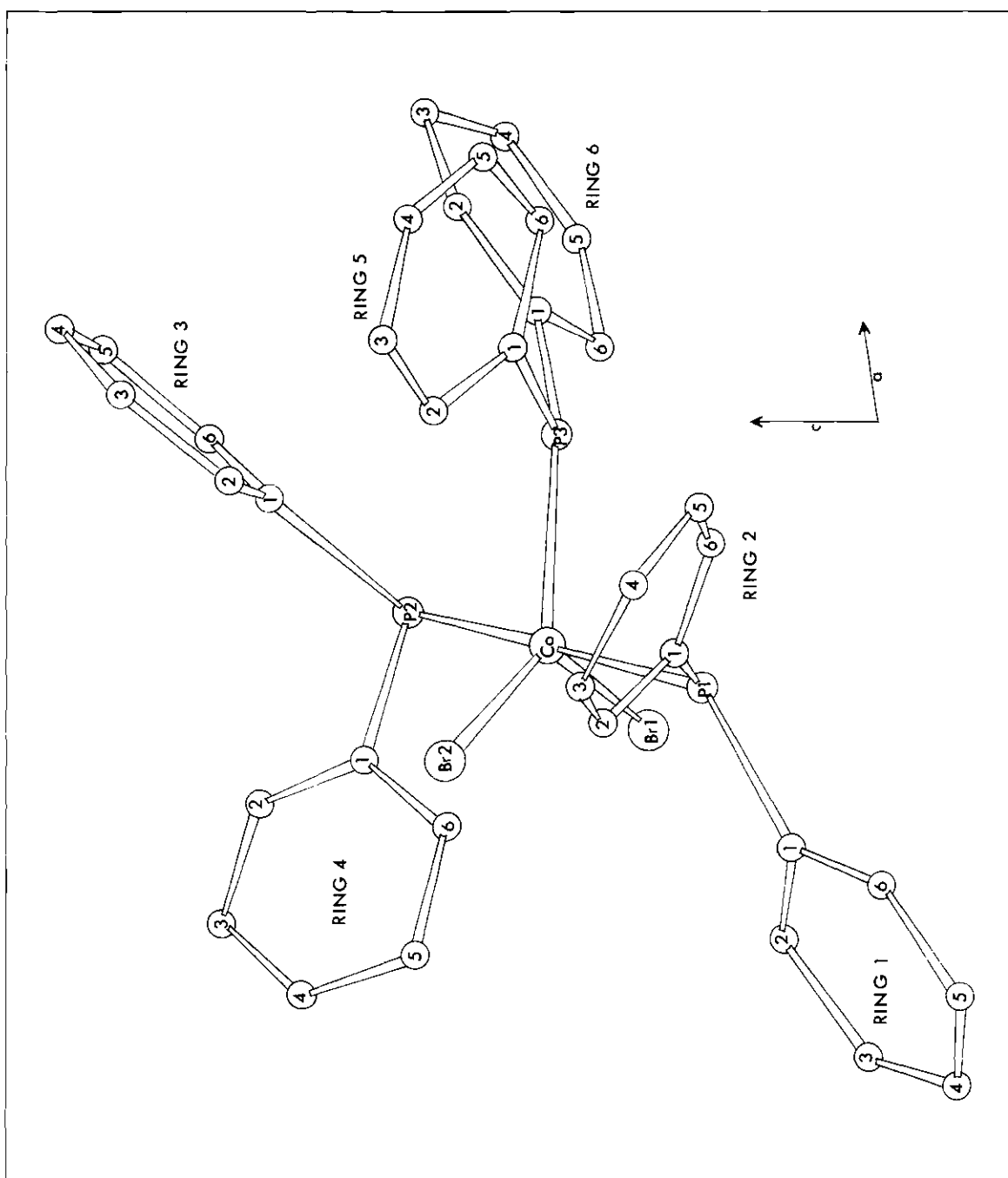


Figure 24. A Perspective Drawing of one Molecule of  $\text{Co}(\text{DPP})_3\text{Br}_2$  as Viewed Down the  $b$ -Axis of the Crystal

The structures, as predicted by Gillespie (13), are neither trigonal bipyramid nor square pyramid, but they can be thought of as intermediate between the two. The structures can be described as distorted from a trigonal bipyramid by increasing one equatorial angle to  $136^\circ$  and decreasing another to  $98^\circ$ . Also as predicted by Gillespie, there is no significant difference in the axial and equatorial metal to phosphorus distances.

The structure can also be described as distorted from a square pyramid in the same manner as  $\text{Ni}(\text{triarsine})\text{Br}_2$  (28); the basal halide atom is depressed ca.  $46^\circ$  below the plane as compared to ca.  $20^\circ$  in the triarsine complex. As in the triarsine complex, the axial metal-to-halide distance is significantly longer than the basal metal-to-halide distance.

Although it may be primarily a matter of taste, it seems more reasonable to think of the structure as a distorted trigonal bipyramid. This is particularly true when considering the polarized spectra of these complexes, since the polarized spectra can be interpreted in terms of  $C_s$  symmetry, retaining only the horizontal symmetry plane of  $D_{3h}$  symmetry. The descent from  $D_{3h}$  to  $C_s$  can be made without change in axial designations and without change in orbital designations; the same is not true in going from  $C_{4v}$  to  $C_s$  symmetry.

Furthermore, in  $D_{3h}$  symmetry, the  $d_{xy}$  and  $d_{x^2-y^2}$  orbitals are degenerate in energy as are the  $d_{xz}$  and  $d_{yz}$ ; the primary effect of the distortion, due to both angular distortion and to the difference in groups within the equatorial plane, will be in the trigonal plane and will, thus, remove the degeneracy of the  $d_{xy}$  and  $d_{x^2-y^2}$  orbitals;

a smaller effect would be experienced by the  $d_{xz}$  and  $d_{yz}$  orbitals. Considering the square pyramid structure, the highest energy orbital, the  $d_{x^2-y^2}$  would be lowered considerably and one of the lowest energy orbitals, the  $d_{xz}$  or  $d_{yz}$ , would be raised considerably, the ordering of the orbitals in the lower symmetry is not obvious because of the rather large distortion involved.

The bipyramid structure of  $\text{Co}(\text{DPP})_3\text{Br}_2$  violates the general rule (18, 19) that the more electronegative ligands are always in axial positions. There doesn't appear to be any steric factor which would prevent the more electronegative halogen atoms from occupying the axial positions.

One further fact concerning the coordination sphere should be mentioned; LaPlaca and Ibers (13) indicated that, in the square pyramidal dichlorotristriphenylphosphineruthenium(II), the sixth corner of the octahedron was occupied by a phenyl hydrogen atom. If the  $\text{Co}(\text{DPP})_3\text{Br}_2$  structure is considered, the closest carbon atom ( $\text{R}_2\text{C}_2$ ) is only 3.68 Å. away and, although the hydrogen atom would be farther from the metal atom than in the ruthenium compound, the sixth position of an octahedron would be effectively blocked.

The errors in carbon atom positions are rather large and these positions could possibly have been improved by further refinement, particularly by introducing anisotropic temperature factors for the heavy atoms and by using a different weighting of reflections in the refinement. However, the principal interest was not in the carbons and refinement was not continued. The carbon-carbon distances obtained, Table 25, range from 1.28 Å. to 1.55 Å.; the average bond distance for each ring is also given in Table 25; there is little difference in the various rings

Table 25. Carbon-Carbon Distances of the Phenyl Groups

Atoms	Ring 1	Ring 2	Ring 3	Ring 4	Ring 5	Ring 6
C <sub>1</sub> - C <sub>2</sub>	1.39(5)	1.32(4)	1.28(6)	1.39(5)	1.52(5)	1.44(5)
C <sub>2</sub> - C <sub>3</sub>	1.46(6)	1.46(5)	1.39(6)	1.39(6)	1.38(7)	1.48(5)
C <sub>3</sub> - C <sub>4</sub>	1.32(6)	1.30(6)	1.44(5)	1.34(7)	1.28(8)	1.32(6)
C <sub>4</sub> - C <sub>5</sub>	1.40(5)	1.32(6)	1.32(6)	1.49(6)	1.36(7)	1.54(6)
C <sub>5</sub> - C <sub>6</sub>	1.44(5)	1.45(6)	1.50(6)	1.54(6)	1.55(7)	1.42(5)
C <sub>6</sub> - C <sub>1</sub>	1.42(4)	1.36(5)	1.43(4)	1.41(6)	1.41(5)	1.40(5)
Avg.	1.41	1.37	1.39	1.43	1.42	1.43

and there is reasonable agreement with the expected 1.39 Å. The carbon-carbon angles for each phenyl ring along with the average angle are given in Table 26. There is reasonable agreement with the expected angle of 120°.

The orientation of the two phenyl groups of each diphenylphosphine ligand were also of interest. Although few structure are known for complexes containing phosphines with two or three phenyl groups, those that have been studied (13, 132) apparently show no preferred dihedral angle between phenyl groups. The lack of such orientation is surprising since, in the phenyl-substituted phosphines, additional back-donation from the metal d-orbitals to phosphorus d-orbitals could be stabilized if the  $\pi$ -system of each phenyl group were to interact with phosphorus d-orbitals to further delocalize this back-donation and, if this suggestion is correct, there should be a definite orientation of phenyl groups with respect to

Table 26. Carbon-Carbon Angles of the Phenyl Groups

Atoms	Ring 1 Angle, Deg.	Ring 2 Angle, Deg.	Ring 3 Angle, Deg.
$C_6 - C_1^* - C_2$	115(4)	121(4)	120(4)
$C_1 - C_2 - C_3$	120(3)	120(4)	127(4)
$C_2 - C_3 - C_4$	122(4)	115(4)	117(4)
$C_3 - C_4 - C_5$	118(4)	128(5)	118(5)
$C_4 - C_5 - C_6$	121(4)	115(5)	123(4)
$C_5 - C_6 - C_1$	<u>122(4)</u>	<u>118(3)</u>	<u>114(4)</u>
Average	120	120	120
<hr/>			
	Ring 4	Ring 5	Ring 6
$C_6 - C_1 - C_2$	125(4)	118(4)	130(3)
$C_1 - C_2 - C_3$	124(5)	111(4)	107(4)
$C_2 - C_3 - C_4$	111(5)	139(6)	126(4)
$C_3 - C_4 - C_5$	135(5)	107(7)	125(4)
$C_4 - C_5 - C_6$	109(5)	127(5)	110(4)
$C_5 - C_6 - C_1$	<u>117(4)</u>	<u>115(4)</u>	<u>121(4)</u>
Average	120	120	120
<hr/>			
* central atom			

phosphorus d-orbitals and, thus, with respect to other phenyl rings on the same phosphorus.

The absence of a definite phenyl orientation in complexes of tertiary phosphines could, of course, be due to a steric problem; the



diphenylphosphine ligands of the cobalt bromide complex should be a better measure of such effects.

For the axial phosphines, the dihedral angle between the two phenyl groups ( $82^\circ$  for  $P_1$  and  $83^\circ$  for  $P_2$ ) is close to  $90^\circ$  and may suggest that the phenyl groups are entering into d-p  $\pi$ -bonding with different phosphorus orbitals; the third phosphine does not show such orientation, the dihedral angle is only  $69^\circ$ . Steric crowding would certainly be greater in the vicinity of this phosphine and could prevent the proper orientation. It is also possible that  $\pi$ -bonding to this phosphine is less important although the equivalence of the three Co-P distances argues against this possibility.

The orientations of the three diphenylphosphine ligands with respect to each other are also worth noting. The angles between the equatorial phosphorus and the axial phosphorus are very close to  $90^\circ$  ( $89.9^\circ$  and  $91.3^\circ$  for the cobalt compound). This may very well be significant and this preferred arrangement may be the result of  $\pi$ -bonding with the metal ion.

### Spectral Properties

Only the gross features of the observed polarized spectra are interpreted. Weak absorptions were noted in the forbidden polarizations as shoulders or as small bands corresponding to the frequencies of the allowed bands in the opposite polarizations. These minor features of a spectrum could be attributed to vibronic bands which would be allowed for electronic forbidden polarizations; however, such an interpretation is not trustworthy because of the following considerations.

1. The alignment of crystal axes with the light vector is probably the source of most error. If the axes were not exactly aligned, then some absorption would be observed in the spectra of the forbidden polarization.

2. Since the polarized light is convergent, the polarized light can not be assumed pure. This would also be observed as minor features in the observed polarized spectra.

3. The polarized spectra are determined at room temperature; therefore, lattice vibration would tend to broaden the bands. Thus, a consideration of band shapes would not be valid.

4. If the molecular axes are not parallel with the crystal faces, then exact alignment is difficult; however, in such cases the crystals were aligned along the polarization axis.

Very distinct polarizations were observed for all crystals investigated (all non-centrosymmetric). However, for centrosymmetric complexes, where only weak vibronic transitions were observed, a very careful consideration of the above mentioned problems would have to be made in order to justify a reasonable interpretation.

The polarized spectra reported in this thesis represents the results obtained for several crystals of each complex. In each case the results obtained for a particular complex were essentially identical for the several crystals investigated.

#### Iodobis(dipyridyl)copper(II) Cation

Solution and Crystal Spectra. The solution and crystal spectra of this complex are shown in Figure 7. The solution spectrum shows a shift of approximately  $2000\text{ cm}^{-1}$  from the crystal spectrum and a shoulder on the crystal spectrum does not appear in the solution spectrum.

Although there is evidence that five-coordination is maintained by this complex in non-coordinating solvents (46), the solution spectrum is not consistent with any five-coordinate symmetry. Similar changes in the spectra of other five-coordinate complexes on dissolving in non-coordinating solvents seem to indicate that the non-rigidity of these complexes is an important factor in solution.

Comparison of the crystal spectrum with that expected for various symmetries suggest that  $D_{3h}$  is the effective symmetry since two transi- are observed; as expected for  $D_{3h}$  symmetry, the high-energy band is much weaker than the other band since the high-energy band is only vibronically allowed and the low-energy band is electronically allowed. However, polarized spectra show that the spectrum in this region is much more complex and, therefore, inconsistent with treatment as  $D_{3h}$  symmetry.

Effective Symmetry. In order to discuss polarized spectra, it is necessary to determine the effective point symmetry at the metal ion. However, there are several ways of considering the site symmetry of complexes in crystals.

Point ligand symmetry obtained by considering each ligand as a point has been employed in interpreting solution spectra. This approach has been particularly employed for the pseudotetrahedral complexes of the type  $ML_2X_2$ , for which the ligand field is considered to be an average of the field strengths produced by four L groups and four X groups. Recently, an attempt has been made to treat the solution spectra of five-coordinate complexes in this manner (105). Such considerations are, of course, not particularly valid in polarized spectral studies where the effective symmetry is definitely lower.

The coordination sphere symmetry is obtained by considering only the atoms bonded to the metal ion. It seems probable that, except in complexes which involve considerable delocalization of electrons through the ligand group, the bonded atoms will produce the major effects on the metal ion and, thus, such considerations should give the effective symmetry. The coordination sphere symmetry has been used to interpret polarized spectra (134).

The actual symmetry of complexes, in some cases, has been used to reach an adequate interpretation of polarized spectra (133).

Previous studies (134) have indicated that the effective symmetry is usually higher than the crystallographic symmetry. In the complex under consideration here, the crystallographic site-symmetry is  $C_1$  and the effective symmetry is certainly higher.

The  $[\text{Cu}(\text{dipyridyl})_2\text{I}]^+$  ion approaches an actual symmetry of  $C_2$ ; however, the coordination sphere symmetry shows a  $C_{2v}$  symmetry.

Polarized Spectra. In decreasing the symmetry from  $D_{3h}$  to  $C_{2v}$  or  $C_2$ , the E states are split; however, since the major factor in lowering the symmetry is the difference in field strength of the iodide as compared to the nitrogen and, since only one iodide is involved, this further splitting should be a smaller effect.

Splittings of the d-orbitals of copper in the various symmetries are indicated in Figure 25. The  $D_{3h}$  states were obtained from the correlation diagram (Figure 18); the states of the lower symmetries were obtained with the correlation tables of Wilson, Decius, and Cross (100). If the coordinate system is chosen so that the  $z$ -axis is defined by the Cu-I vector and the  $x$ -axis is defined as the line containing the copper

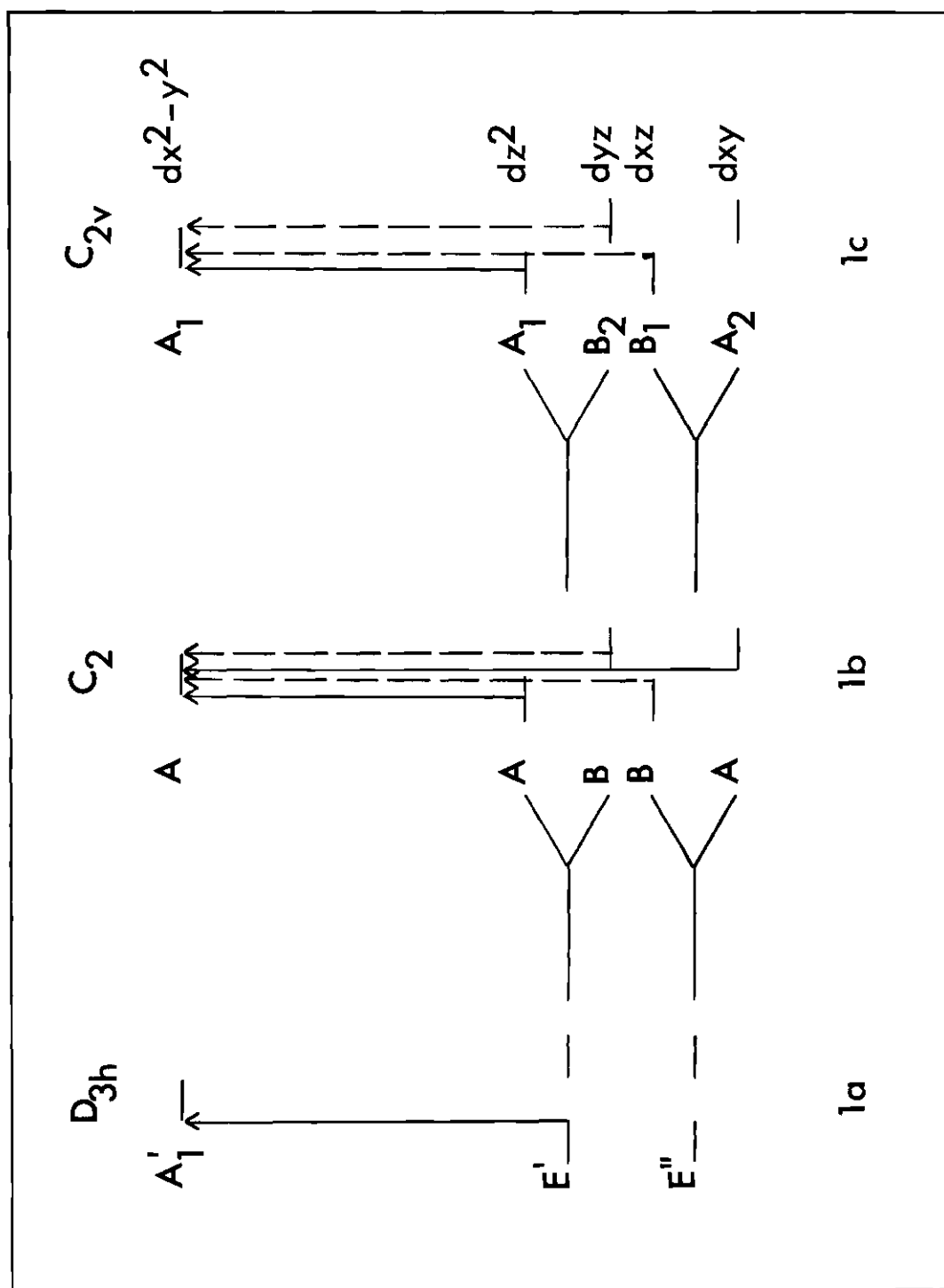


Figure 25. Splitting of the d-Orbitals of Copper in Various Possible Symmetries. Arrows indicate transitions which are allowed electronically; in C<sub>2</sub> and C<sub>2v</sub>, solid lines represent transitions allowed parallel to the principal axis, dashed lines represent transitions allowed perpendicular to the principal axis.

and two nitrogens (the axial nitrogens of the bipyramid), then the  $d_{x^2-y^2}$ , with two lobes directed toward nitrogens, would be expected to be highest in energy; the  $d_{z^2}$ , directed toward the iodide, would be somewhat lower in energy. Since the  $d_{yz}$  lobes would be directed near the remaining two nitrogens, it should be higher than the remaining two orbitals; the  $d_{xz}$  and  $d_{xy}$  would be lowest in energy and the ordering of these would be questionable.

A comparison of the polarized spectra, Figure 9, with the spectra expected for  $C_2$  and  $C_{2v}$  symmetries suggest that the effective symmetry is  $C_{2v}$ . In  $C_2$  symmetry, each polarization would be expected to show two allowed bands; in  $C_{2v}$ , the perpendicular polarization should show two allowed bands and the parallel polarization should show only one. In the observed spectra, the perpendicular polarization shows a much broader band than the parallel polarization and two distinct peaks can be resolved from the perpendicular polarization.

The three observed bands can be assigned to particular transitions according to Figure 25. This assignment is summarized in Table 27 along with the relative energies, with respect to the energy of the  $d_{x^2-y^2}$  orbital, of all d-orbitals except the  $d_{xy}$ . Since a transition from the  $d_{xy}$  is electronically forbidden in both polarizations, it is not readily observed. It is, however, vibronically allowed in both polarizations and is probably hidden near the high energy end of both envelopes; no attempt has been made to fit a weak band into the spectra.

### Diphenylphosphine Complexes

Solution and Crystal Spectra. The absorption spectra in dichloromethane of the cobalt and nickel complexes are given in Figures 6 and 7

Table 27. Assignment of Observed Transitions for the  $[\text{Cu}(\text{dipyridyl})_2\text{I}]\text{I}$  Complex

Transition assignment	Obs. freq. ( $\text{cm}^{-1}$ )
$A_1(d_{x^2-y^2}) \longrightarrow A_1(d_{z^2})$	10,500
$A_1 \longrightarrow B_2(d_{yz})$	12,000
$A_1 \longrightarrow B_1(d_{xz})$	15,000

respectively; the crystal spectra of these complexes are given in Figures 8 and 9. No similarities are observed between the solution spectra and the crystal spectra. Therefore, since there is evidence that five-coordination is maintained in this solvent, the solution spectra must represent an average over all possible conformations. Also the crystal spectra alone are not sufficient to make reliable spectral assignment.

Polarized Spectra. As indicated, the coordination spheres of these complexes have  $C_s$  symmetry retaining only the horizontal symmetry plane of  $D_{3h}$ . The descent in symmetry from  $D_{3h}$  to  $C_s$  can be made without a change in axial designation and without change in orbital designations; the same is not true in descending from  $C_{4v}$  to a  $C_s$  symmetry.

The crystallographic  $\underline{c}$ -axis of the crystal is essentially parallel to the  $P_1$ -M and  $P_2$ -M vectors of the molecule. Therefore, the  $\underline{c}$ -axis is essentially parallel to the  $\underline{z}$ -axis of the molecule ( $\underline{z}$ -axis is defined as the principal axis of the  $D_{3h}$  or  $C_s$  symmetries). Thus, correlating these facts with the previous information concerning the relationship between the polarization axis and the crystallographic  $\underline{c}$ -axis, the nickel iodide

complex shows green light perpendicular to the principal axis and appears opaque with light parallel to the principal axis. Figures 11 and 12 show the polarized spectra of  $\text{Ni(DPP)}_3\text{Br}_2$  and  $\text{Ni(DPP)}_3\text{I}_2$  respectively with light parallel and perpendicular to the  $C_s$  principal axis. The cobalt iodide complex shows red light transmitted perpendicular to the principal axis and green light parallel to the principal axis. Figures 13 and 14 illustrate the polarized spectra of the  $\text{Co(DPP)}_3\text{Br}_2$  and  $\text{Co(DPP)}_3\text{I}_2$  respectively.

Dihalotris(diphenylphosphine)nickel(II) Compounds. Figure 26 shows the spectroscopic states arising from a descent in symmetry from  $D_{3h}$  to  $C_s$  in a  $d^8$  electron shell configuration; the  $D_{3h}$  states were obtained from the correlation diagram given in Figure 20.

The E states are split on descending in symmetry from  $D_{3h}$  to  $C_s$ ; however, the splitting would represent a difference in field strengths brought about by the difference in halides and phosphines. This change in field strength would be expected to be small and the predicted spectral bands should either broaden or be slightly split; the iodide complex should show a greater splitting than the bromide complex. In a  $C_s$  environment, the theory predicts two broad transitions which are one-electron transitions, the high energy band polarized parallel to the principal axis and the low energy band polarized perpendicular to the principal axis. The observed spectra of both nickel complexes show these bands. The low energy band is polarized perpendicular and is consistent with the predicted transitions from an  $(a'_1)^2$  ground state configuration to  $(a'_1)(e')$  excited state configurations. The observed band in the iodide complex appears split into two components and does, as predicted, show greater splittings



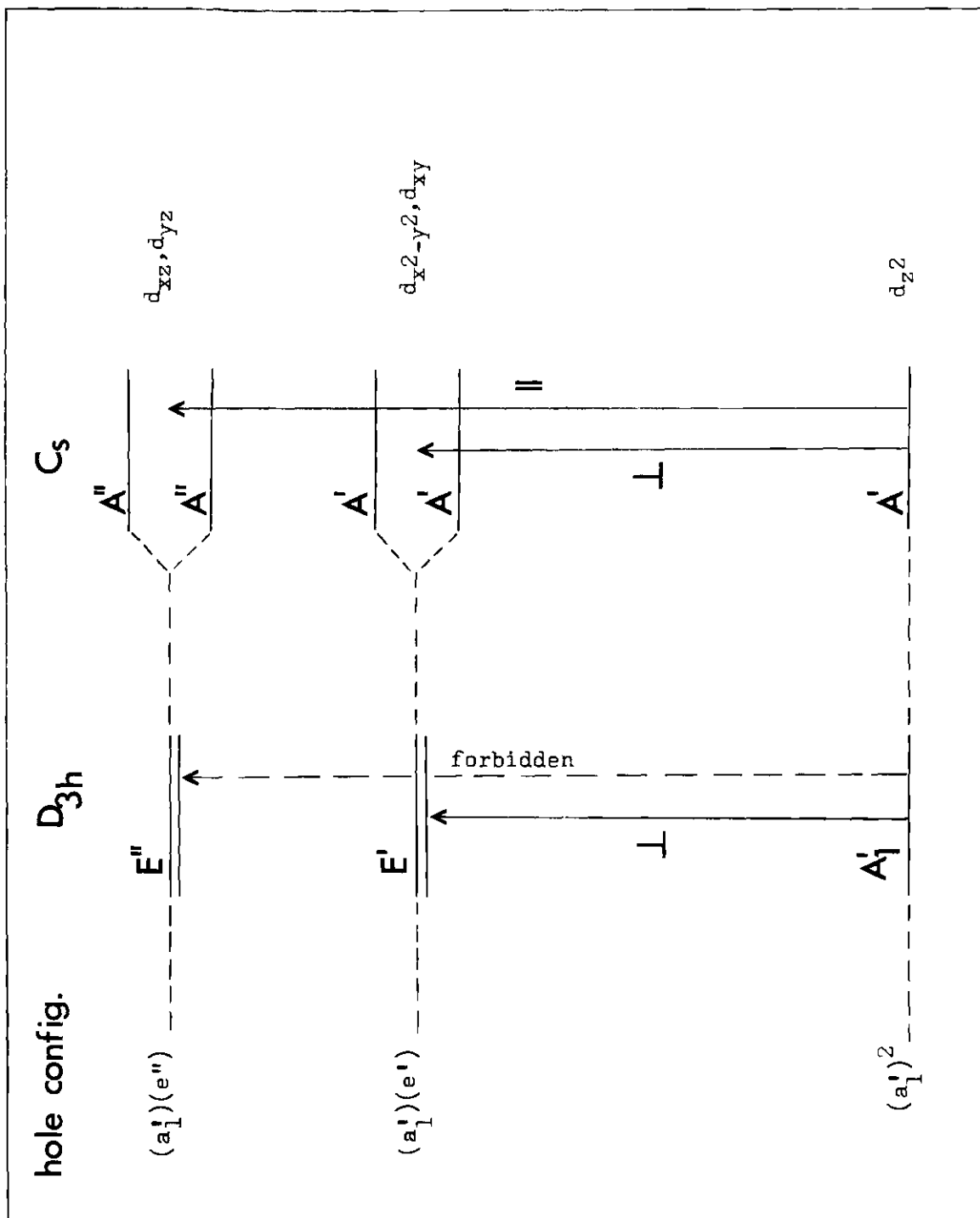


Figure 26. Spectroscopic States Arising from a Descent in Symmetry from  $D_{3h}$  to  $C_s$  in a  $d^8$  Configuration

than the bromide complex. The band of higher energy is polarized parallel and is consistent with the other one-electron transition to  $(a_1')(e'')$  excited state configurations. In both complexes this band is very broad and a frequency assignment is somewhat arbitrary. In both the perpendicular and parallel bands a shift to higher energy is observed for the bromide complex and this shift is in accordance with a field strength change from iodide to bromide. The transition assignments along with the approximate band positions are given in Table 28.

Table 28. Assignment of Observed Transitions for the  $\text{Ni}(\text{DPP})_3\text{X}_2$  Complexes

X	Transition assignment	Obs. freq. ( $\text{cm}^{-1}$ )
Br	$A' (a_1')^{2*} \rightarrow A' (a_1'e')^{**}$	14,800
	$A' \rightarrow A'' (a_1'e'')$	17,400
I	$A' \rightarrow A'$	12,600
		14,600
	$A' \rightarrow A''$	16,500

\* hole config. of the ground state  
 \*\* hole config. of the excited state

A similar assignment (79) has been made for the  $[\text{Ni}(\text{TAP})\text{X}]\text{ClO}_4$  complexes, where TAP represents the tris(3-dimethylarsinopropyl)phosphine ligand. The solution spectra (dichloromethane) have been interpreted in terms of  $C_{3v}$  symmetry. A broad peak in the visible region has been resolved into two Gaussian curves and the lower energy band

(14,170–15,400  $\text{cm}^{-1}$ ) has been assigned to the  $A_1 \rightarrow E_a$  transition; the higher energy band (16,740–17,840  $\text{cm}^{-1}$ ) has been assigned to the  $A_1 \rightarrow E_b$  transition.

Dihalotris(diphenylphosphine)cobalt(II) Compound. Figure 27 shows the spectroscopic states arising from a descent in symmetry from  $D_{3h}$  to  $C_s$  in a  $d^7$  electron configuration (derived from Figure 22).

In  $C_s$  symmetry, the theory predicts three one-electron transitions. The lowest transition from  $A'((a'_1)^2 e') \rightarrow A''((a'_1)^2 e'')$  would be expected to be of very low energy and should not occur in the spectral region under investigation. However, three distinct bands are observed in the polarized spectra. The lowest observed band, which is polarized perpendicular to the principal axis, can be assigned to a transition from  $(a'_1)^2 e'$  ground state configurations to  $a'_1(e')^2$  excited state configurations. As in the nickel iodide complex, the lowest observable band is split into two components. The medium energy band is consistent with the predicted transition which has an excited state of  $a'_1 e' e''$  configuration. This band originating from  $a'_1 e' e''$  configurations should be extremely broad because it has several (eight) components. The highest energy band may be either assigned to the lowest two-electron transition or to a charge transfer band. This band appears approximately at the same position in both the bromide and iodide complexes; however, if the band were the result of a charge transfer from halide to metal, it would be expected to occur at higher energy for the bromide than for the iodide. This band is probably, therefore, a two-electron transition. The assignment of transitions and their approximate band positions are given in Table 29.

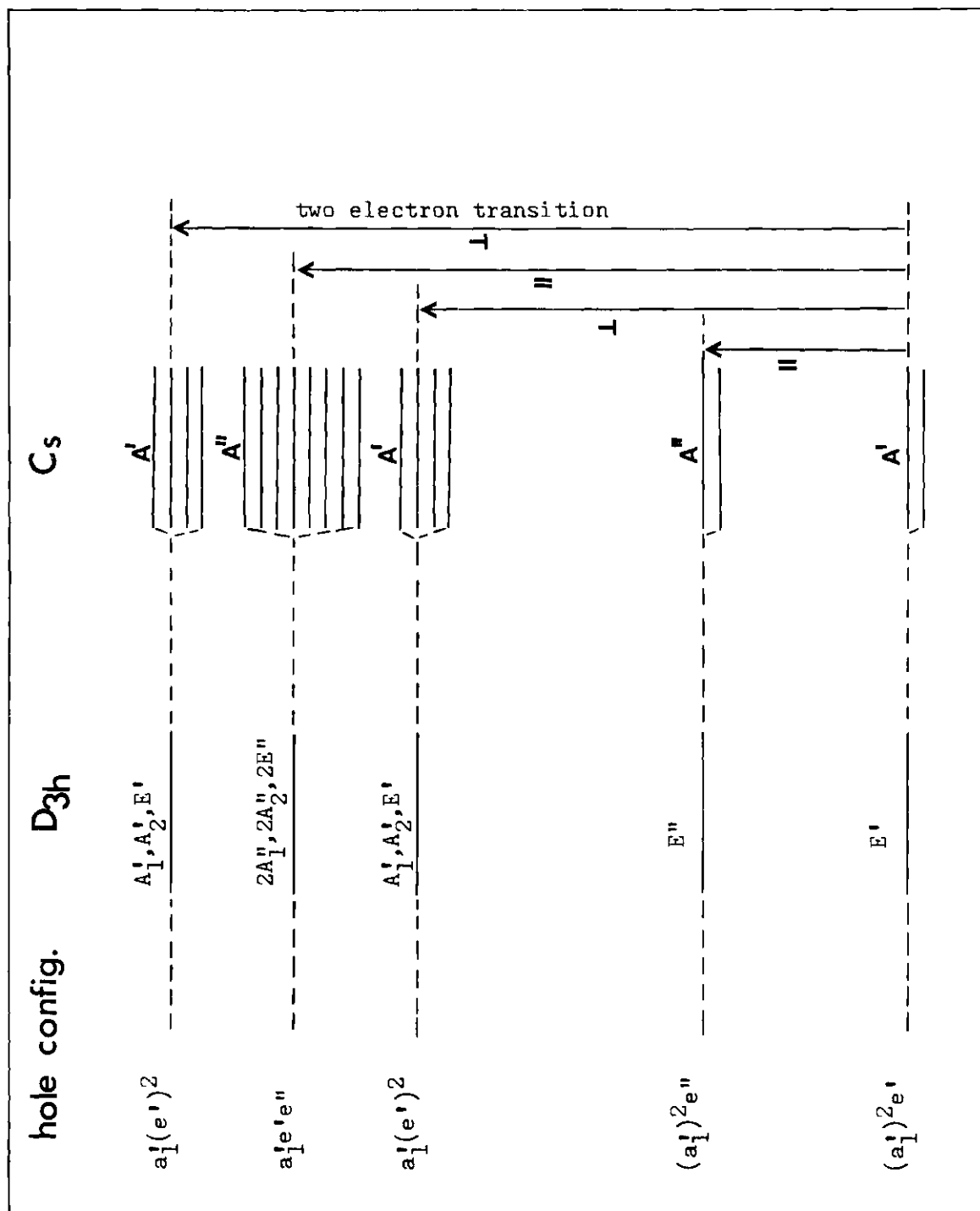


Figure 27. Spectroscopic States Arising from a Descent in Symmetry from  $D_{3h}$  to  $C_s$  in a  $d^7$  Configuration

Table 29. Assignment of Observed Transitions for the  $\text{Co}(\text{DPP})_3\text{X}_2$  Complexes

X	Transition assignments	Obs. freq. ( $\text{cm}^{-1}$ )
Br	$\text{A}' ((\text{a}_1')^2 \text{e}')^* \longrightarrow \text{A}'' ((\text{a}_1')^2 \text{e}'')^{**}$	not observed
	$\text{A}' \longrightarrow \text{A}' (\text{a}_1' (\text{e}')^2)$	13,800
	$\text{A}' \longrightarrow \text{A}'' (\text{a}_1' \text{e}' \text{e}'')$	13,800-17,000
	$\text{A}' \longrightarrow \text{A}' (\text{a}_1' (\text{e}'')^2)^{***}$	19,000
I	$\text{A}' \longrightarrow \text{A}''$	not observed
	$\text{A}' \longrightarrow \text{A}'$	13,200 14,700
	$\text{A}' \longrightarrow \text{A}''$	13,600-15,500
	$\text{A}' \longrightarrow \text{A}'$	19,000

<sup>\*</sup>hole config. of the ground state  
<sup>\*\*</sup>hole config. of the excited state  
<sup>\*\*\*</sup>two-electron or charge transfer band

### Magnetic Properties

Five-coordinate complexes of nickel which contain phosphorus or arsenic ligands are usually diamagnetic; the nickel iodide complex with diphenylphosphine is the only example of a paramagnetic complex of this type. This paramagnetism could, in the absence of structural data, be attributed to either a difference in structure or to the difference in ligand field strength for the nickel iodide and nickel bromide complexes; however, the successful refinement of the heavy atom coordinates using two zones of intensity data for the nickel iodide crystal shows that

the iodide and bromide structures are essentially identical.

The explanation of the paramagnetism of the nickel iodide complex must be related to the ligand field strength. As indicated in Figure 28a and b, nickel complexes may have a triplet ground state (spin-free complexes) or a singlet ground state (spin-paired complexes), depending upon whether the splitting,  $\Delta^8$ , is sufficient to overcome electronic repulsion and cause pairing.

The moment observed for the nickel iodide complex, 1.29 B.M., is considerably below the value for one unpaired electron (1.73 B.M.) and indicates that the ligand field strength must be slightly higher than that required to cause spin-pairing. Thus, although the ground state is a singlet state, the triplet state is only slightly higher in energy and, due to the closeness of these two levels, is thermally accessible. The resulting paramagnetism would be expected to be temperature dependent. Confirmation of a temperature dependent paramagnetism was not possible in this study since there were no provisions for temperature variation with the magnetic balance employed.

The higher field strength of the bromide complex would increase the separation between the singlet ground state and the triplet state, making the triplet state beyond reach of thermal population at room temperature.

The DPP complexes of cobalt bromide and cobalt iodide have moments (2.43 and 2.23 B.M., respectively) which are consistent with the presence of one unpaired electron. Although the values are above the spin-only value of 1.73, the difference is probably due to the orbital contribution.

Since the two cobalt complexes are essentially low-spin, this would indicate that, assuming similar crystal field splittings for the

cobalt and nickel ions, the change from a quartet to doublet state is at a lower field strength than the analogous change for nickel(II). Although the change in crystal field stabilization energy in going from a high-spin to a low-spin state would be the same for  $d^7$  and  $d^8$  complexes in  $D_{3h}$  symmetry, the further removal of d-orbital degeneracies in  $C_s$  symmetry would make the low-spin state more favorable for  $d^7$  than for  $d^8$ . This is shown in Figure 28 where the changes in crystal field stabilization energy between the high-spin and low-spin states are indicated for  $d^7$  and  $d^8$  complexes. Due to this difference between high-spin and low-spin stabilization,  $\Delta^7$  greater than  $\Delta^8$ ,  $d^7$  complexes should become spin paired at lower field strength than  $d^8$  complexes.

The polarized spectra of the nickel iodide complex might also be expected to show a partial population of the triplet state. However, the polarized spectra of the iodide and bromide complexes did not show any significant difference.

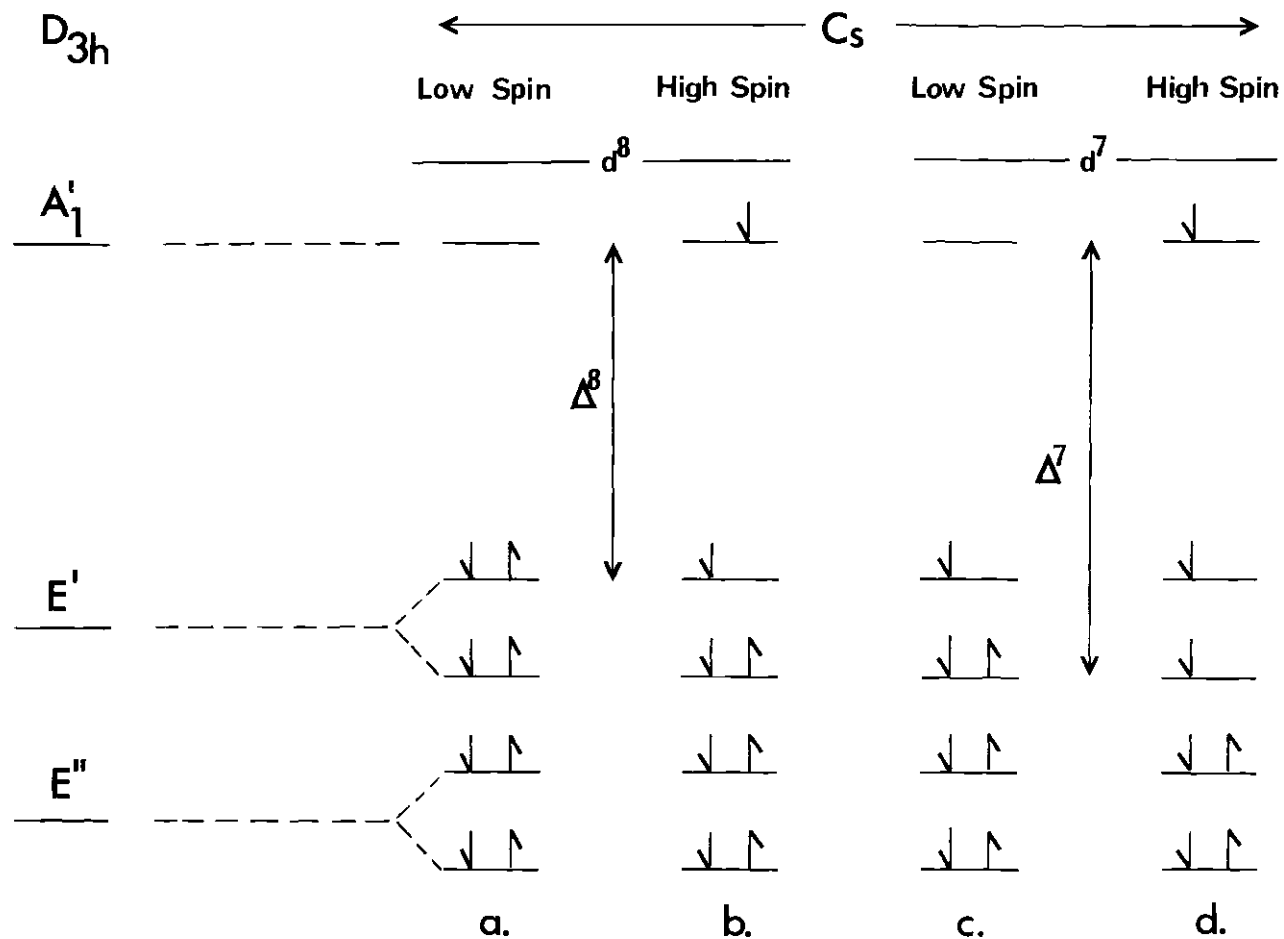


Figure 28. The Splitting of d-Orbitals in  $D_{3h}$  and  $C_s$  Symmetries



## CHAPTER VIII

## CONCLUSIONS

The five-coordinate diphenylphosphine and dipyridyl complexes discussed in this thesis appear to be non-rigid in solution and the solution spectra appear to represent an average over the possible conformations. It also seems reasonable to suggest that other five-coordinate complexes, except those restricted to a particular confirmation due to steric requirements of the ligand, may well be non-rigid in solution since the interconversion can easily occur through vibrational distortion. The crystal spectra can be interpreted in terms of a rigid molecule; the effective symmetry, at least in the cases cited, can be interpreted in terms of the coordination sphere symmetry. Further studies of additional complexes would have to be made in order to clarify whether, as a general rule, the effective symmetry is consistent with the coordination sphere symmetry or if additional considerations are necessary.

Gillespie (16) has predicted that largely covalent complexes are expected to show a trigonal bipyramid arrangement and that highly ionic complexes are expected to show a square pyramid arrangement; therefore, most five-coordinate complexes of the first transition series are expected to be intermediate between these two extremes and should show intermediate conformations. The structures of the  $M(DPP)_3X_2$  compounds can be described as bipyramidal, but they are distorted from a trigonal bipyramid arrangement and could, therefore, be described as intermediate structures.

The phenyl groups of two of the phosphines of the  $M(DPP)_3X_2$  compounds show dihedral angles close to  $90^\circ$  and this may be evidence of participation of the phenyl groups in the back-donation mechanism.

The magnetic moments of the  $M(DPP)_3X_2$  compounds, with the exception of the nickel iodide compound, show low-spin magnetic moments; the unusual paramagnetism of the nickel iodide is probably due to thermal population of a low-lying triplet state.

## APPENDIX

## COMPUTER PROGRAMS

The following unpublished programs were used by the author in the course of this research. These programs were written in a modified Algol language for the Burroughs' B-5500 computer. The magnetic susceptibility program (one) and the lattice cell program (two) were written by the author; the minimum function program (three) and the three-dimensional Fourier program (four) were written by Dr. J. A. Bertrand.

## PROGRAM ONE

## MAGNETIC SUSCEPTIBILITY PROGRAM

```

BEGIN
COMMENT MAGNETIC SUSCEPTIBILITY PROGRAM ;
REAL PASCA,MOLW,TEMP,A,C,G,V,K,AMP,B,D,X,S,E,F,BETA,XG,XM,XC,CORR,
MUF ;
INTEGER I ;
ALPHA ARRAY NA(1:12) ;
LABEL LOOP, TOP, BOTTOM ;
FILE IN F1 (2,10) ;
FILE OUT F2 (2,15) ;
FORMAT TITLE (12A6) ;
FORMAT IN FORM1 (X3,3F9.3) ;
FORMAT IN FORM2 (X5,5F9.6) ;
FORMAT IN FORM3 (X5,4F9.6) ;
FORMAT OUT FORM4 (X6,"AMP",X8,"BETA",X8 "TEMP",X9,"XG",X10
,"XC",X10,"MUF" ) ;
FORMAT OUT FORM5 (6F12.4) ;
TOP:
READ (F1,FORM1,PASCA,MOLW,TEMP) ;
IF PASCA = 0 THEN GO TO BOTTOM ;
READ (F1,FORM2,A,C,G,V,K) ;
READ (F1,TITLE, FOR I= 1 STEP 1 UNTIL 12 DO NA(I)) ;
WRITE (F2(ORL1),TITLE, FOR I= 1 STEP 1 UNTIL 12 DO NA(I)) ;
WRITE (F2(ORL1),FORM4) ;
LOOP:
READ (F1,FORM3,AMP,B,D,X) ;
IF AMP # 0 THEN BEGIN
S=B-A ;
F+(D-C-S)*1000 ;
F+(X-G-S)*1000 ;
BETA+(K*(C-A)-(0.029)*V) / F ;
XG+((0.029)*V+ BETA *F) / (G-A) ;
XM=XG*MOLW ;
XC= XM + PASCA ;
CORR= SQRT(XC*TEMP) ;
MUF +(2.84)*CORR*0.001 ;
WRITE (F2,FORM5,AMP,BETA,TEMP,XG,XC,MUF) ;
GO TO LOOP ;
END ;
GO TO TOP ;
BOTTOM :
END.

```

## PROGRAM TWO

## LATTICE CELL PROGRAM

```

BEGIN
COMMENT REAL LATTICE CONSTANTS CALCULATED FROM RECIPROCAL LATTICE ;
REAL DA,DB,DC,RA,RR,RC,A,B,C,ALPHE,BETA,GAMMA,CA,CH,CG,SA,SB,SG,SINA,
SINB,SING,V,DEN,MOLW,TA,TH,TG,ANGA,ANGB,ANGG ;
INTEGER I,N ;
LABEL TOP,LOOP,BOTTOM ;

```

```

ALPHA ARRAY NAT1:123      ;
FILE IN F1 (1,10)      ;
FILE OUT F2 1(2,15)      ;
FORMAT IN FORM1 (4F9.3)      ;
FORMAT IN FORM2 (6F9.6)      ;
FORMAT TITLE (12A6)      ;
FORMAT OUT FORM5 (Y6,"A",X9,"H",X9,"C",X7,"VOLUME")      ;
FORMAT OUT FORM6 (4F10.3)      ;
FORMAT OUT FORM7 (X10,"DENSITY["",I2,""] = ",F9.6)      ;
FORMAT OUT FORM8 (X4,"ALPHA",X5,"BETA",X5,"GAMMA")      ;
FORMAT OUT FORM9 (3F10.3)      ;
FORMAT OUT FORM3 (X2,"COSALPHA",X3,"COSBETA",X2,"COSGAMMA")      ;
FORMAT OUT FORM4 (3F10.6)      ;
TOP:
READ (F1,FORM1,DA,DB,DC,MOLW)      ;
IF DA=0 THEN GO TO BOTTOM      ;
READ (F1,TITLE, FOR I = 1 STEP 1 UNTIL 12 DD NAT(I))      ;
WRITE (F2(1RL),TITLE, FOR I = 1 STEP 1 UNTIL 12 DD NAT(I))      ;
READ (F1,FORM2,CA,CH,CG,SA,SH,SG)      ;
ALPHE = (CRX CG - CA)/(SXSG)      ;
BETA = (CA*CG - CH)/(SAXSG)      ;
GAMMA = (CA*CH - CG)/(SAXSB)      ;
SINA = 1 - (ALPHE)*(ALPHE)      ;
SINA = SQRT(SINA)      ;
SINR = 1 - (BETA*BETA)      ;
SINR = SQRT(SINR)      ;
SING = 1 - (GAMMA*GAMMA)      ;
SING = SQRT(SING)      ;
RA = DA/(42.64)      ;
RB = DB/(42.64)      ;
RC = DC/(42.64)      ;
A = 1/(RAXSRXSING)      ;
B = 1/(RBXSAXSING)      ;
C = 1/(RCXSAXSINB)      ;
V = AXHXCSINXSINHXSG      ;
WRITE (F2(1RL),FORM5)      ;
WRITE (F2(1RL),FORM6,A,B,C,V)      ;
WRITE (F2(1RL),FORM3)      ;
WRITE (F2(1RL),FORM4,ALPHE,BETA,GAMMA)      ;
COMMENT REAL ANGLE CALCULATION USING ARC FUNCTION      ;
IF ALPHE#0 THEN BEGIN
  TA = SINA/ALPHE      ;
  ANGA = ARCTAN(TA)      ;
  ANGA = 57.2958*ANGA      ;
  IF ANGA < 0 THEN
    ANGA = 180.0000 + ANGA      ;
END;
IF BETA#0 THEN BEGIN
  TB = SINR/BETA      ;
  ANGB = ARCTAN(TB)      ;
  ANGB = 57.2958*ANGB      ;
  IF ANGB < 0 THEN
    ANGB = 180.0000 + ANGB      ;
END;
IF GAMMA#0 THEN BEGIN
  TG = SING/GAMMA      ;
  ANGG = ARCTAN(TG)      ;
  ANGG = 57.2958*ANGG      ;
  IF ANGG < 0 THEN
    ANGG = 180.0000 + ANGG      ;
END;
WRITE (F2(1RL),FORM4)      ;

```

```

WRITE (F2,FURL1,FORM9,ANGA,ANGH,ANGG) ;
COMMENT UNIT CELL DENSITY CALCULATION ;
N = 0 ;
LOOP:
  N = N + 1 ;
  DEN = (N*MDLW)/(0.6023*V) ;
  WRITE (F2,FORM7,N,DEN) ;
  IF DEN < 5 THEN GO TO LOOP ;
GO TO TOP ;
BOTTOM:
END.

```

### PROGRAM THREE

#### MINIMUM FUNCTION PROGRAM

```

      BEGIN
COMMENT MINIMUM FUNCTION PROGRAM ;
ALPHA ARRAY NA(1:12) ;
INTEGER CH,CK,CL,TP ;
INTEGER V,W,VV,WW,DD,RANK,X,Y,Z,MZ,MX,MY,RX,RY,RZ,I,PR,PRNB,UZ ;
INTEGER ARRAY MMX(1:8,1:8),MMY(1:8,1:8),MMZ(1:8,1:8) ;
INTEGER ARRAY IMX(1:8,1:8),IMY(1:8,1:8),IMZ(1:8,1:8) ;
REAL T1,T2 ;
REAL ARRAY FAC(1:8,1:8) ;
REAL ARRAY HD(0:32,0:32,0:16),MD(0:32,0:32) ;
LIST L1((12-T1)/60) ;
FILE IN F1 (2,10) ;
FILE OUT F2 6(2,15) ;
SAVE FILE PATCON 2(1,256) ;
FORMAT IN FORM1 (12A6) ;
FORMAT IN INDEX (7I5) ;
FORMAT IN SHIFT (3I5,F10.4) ;
FORMAT IN TAPE1 (I8) ;
FORMAT IN TAPE2 (256F8.1) ;
FORMAT OUT FORM4 ("TIME =",F10.3) ;
FORMAT OUT FORM4 ("X DOWN",I3," TO",I3," Y ACROSS",I3," TO",I3," Z=", ;
  I2) ;
FORMAT OUT FORM5 ("Y DOWN",I3," TO",I3," X ACROSS",I3," TO",I3," Z=", ;
  I2) ;
FORMAT OUT FORM6 ("X DOWN",I3," TO",I3," Z ACROSS",I3," TO",I3," Y=", ;
  I2) ;
FORMAT OUT FORM7 ("Z DOWN",I3," TO",I3," X ACROSS",I3," TO",I3," Y=", ;
  I2) ;
FORMAT OUT FORM8 ("Y DOWN",I3," TO",I3," Z ACROSS",I3," TO",I3," X=", ;
  I2) ;
FORMAT OUT FORM9 ("Z DOWN",I3," TO",I3," Y ACROSS",I3," TO",I3," X=", ;
  I2) ;
FORMAT OUT FORM10 (16F7.1,X8) ;
FORMAT OUT FORM2 ("MINIMUM FUNCTION",X10,12A6) ;
FORMAT OUT FORM3 ("SHIFTED TO ORIGIN: X=",I5," Y=",I5," Z=",I5) ;
LABEL START,S1,S2,S3 ;
LABEL SW1,SW2,SW3,FD1,FD2,FD3,FD4,FD5,FD6,FD7,FD8,FD9,TRM ;
SWITCH CHOOSE+S3,S1,S2,S2,S2,S2,S2,S2 ;
SWITCH CALC+SW1,SW2,SW3 ;
SWITCH LP1+FD1,FD2,FD3 ;
SWITCH LP2+FD4,FD5,FD6 ;

```

```

SWITCH LP3+FD7,FD8,FD9 ;
T1←TIME(2) ;
COMMENT SECTION 2 ;
READ (F1,FIRM1,FDK I←1 STEP 1 UNTIL 12 DO NAC(I)) ;
READ (F1,INDEX,TOP,CH,CK,CL,RANK,PR,UZ) ;
FOR D←1 STEP 1 UNTIL TOP DO
  FOR DD←2 STEP 1 UNTIL RANK DO
    BEGIN
      GO TO CALC(CK) ;
      SW1:
        GO TO LP1(CK) ;
      FD1:
        GO TO TRM ;
      FD2:
        READ (F1,SHIFT,IMX(D,DD),IMY(D,DD),IMZ(D,DD),FAC(D,DD)) ;
        GO TO TRM ;
      FD3:
        READ (F1,SHIFT,IMX(D,DD),IMZ(D,DD),IMY(D,DD),FAC(D,DD)) ;
        GO TO TRM ;
      SW2:
        GO TO LP2(CK) ;
      FD4:
        READ (F1,SHIFT,IMY(D,DD),IMX(D,DD),IMZ(D,DD),FAC(D,DD)) ;
        GO TO TRM ;
      FD5:
        GO TO TRM ;
      FD6:
        READ (F1,SHIFT,IMY(D,DD),IMZ(D,DD),IMX(D,DD),FAC(D,DD)) ;
        GO TO TRM ;
      SW3:
        GO TO LP3(CK) ;
      FD7:
        READ (F1,SHIFT,IMZ(D,DD),IMX(D,DD),IMY(D,DD),FAC(D,DD)) ;
        GO TO TRM ;
      FD8:
        READ (F1,SHIFT,IMZ(D,DD),IMY(D,DD),IMX(D,DD),FAC(D,DD)) ;
        GO TO TRM ;
      FD9:
        GO TO TRM ;
      TRM:
      END;
    CLOSE (F1,RELEASE) ;
    START:
    READ (PATECN,TAPE1,PROR) ;
    IF PROR≠PR THEN BEGIN
      SPACE (PATECN,68)
      GO TO START
    END ;
    FOR Z←0 STEP 1 UNTIL 16 DO
      FOR V←0,16 DO FOR X←0,16 DO BEGIN
        VV←V+15 ;
        WW←W+15 ;
        READ (PATECN,TAPE2,FOR X←V STEP 1 UNTIL VV DO FOR Y←W STEP 1 UNTIL
          WW DO RDC(X,Y,Z)) ;
        LND ;
      LOCK (PATECN,RELEASE) ;
      COMMENT SECTION 3 ;
      FOR D←1 STEP 1 UNTIL TOP DO BEGIN
        WRITE (F2(ORL),FORM2,FDK I←1 STEP 1 UNTIL 12 DO NAC(I)) ;
        FOR DD←2 STEP 1 UNTIL RANK DO
          WRITE (F2(ORL),FDK43,IMX(D,DD),IMY(D,DD),IMZ(D,DD)) ;
        WRITE (F2(PAGE1)) ;
        FOR Z←0 STEP 1 UNTIL UZ DO BEGIN

```

```

      FOR DD=2 STEP 1 UNTIL RANK DD BEGIN
        MMZ[D,DD]=IMZ[D,DD]+Z
        IF MMZ[D,DD]>31 THEN MMZ[D,DD]=MMZ[D,DD]-32
      END ;
FOR X=0 STEP 1 UNTIL 31 DO BEGIN
  FOR DD=2 STEP 1 UNTIL RANK DD BEGIN
    MMX[D,DD]=IMX[D,DD]+X
    IF MMX[D,DD]>31 THEN MMX[D,DD]=MMX[D,DD]-32
  END ;
  FOR Y=0 STEP 1 UNTIL 31 DO BEGIN
    FOR DD=2 STEP 1 UNTIL RANK DD BEGIN
      MMY[D,DD]=IMY[D,DD]+Y
      IF MMY[D,DD]>31 THEN MMY[D,DD]=MMY[D,DD]-32
      MX=MMX[D,DD]
      MY=MMY[D,DD]
      MZ=MMZ[D,DD]
      IF MZ>16 THEN BEGIN MZ=32-MZ; MX=32-MX ; MY=32-MY ;
      IF MX=32 THEN MX=0 ; IF MY=32 THEN MY=0 ;
      END ;
      IF Z>16 THEN BEGIN RZ=32-Z ; RX=32-X ; RY=32-Y ; END
      ELSE BEGIN RZ=Z ; RX=X ; RY=Y ; END ;
      IF RX=32 THEN RX=0 ; IF RY=32 THEN RY=0 ;
      GO TO CHOOSE[DD]
S1: IF RD[MX,MY,MZ]<RD[RX,RY,RZ] THEN MD[X,Y]=RD[MX,MY,MZ]*FAC[D,DD]
      ELSE MD[X,Y]=RD[RX,RY,RZ]*FAC[D,DD] ; GO TO S3 ;
S2: RD[MX,MY,MZ]=RD[MX,MY,MZ]*FAC[D,DD]
      IF RD[MX,MY,MZ]<MD[X,Y] THEN MD[X,Y]=RD[MX,MY,MZ] ; GO TO S3
S3: END ; IF MD[X,Y] ≤ 0 THEN MD[X,Y] ← 10*6 ; END END ;
COMMENT SECTION 4
  FOR V=0,16 DO FOR W=0,16 DO BEGIN
    VV=V+15
    WW=W+15
    WRITE (F2[DRL1,FORM2,FOR I=1 STEP 1 UNTIL 12 DO NA[I])
    IF CL=3 THEN BEGIN
      IF CH=1 THEN WRITE (F2[DRL1,FORM4,V,VV,W,WW,Z)
      ELSE WRITE (F2[DRL1,FORM5,V,VV,W,WW,Z) END
      IF CK=3 THEN BEGIN
        IF CH=1 THEN WRITE (F2[DRL1,FORM6,V,VV,W,WW,Z)
        ELSE WRITE (F2[DRL1,FORM7,V,VV,W,WW,Z) END
        IF CH=3 THEN BEGIN
          IF CK=1 THEN WRITE (F2[FORM8,V,VV,W,WW,Z)
          ELSE WRITE (F2[DRL1,FORM9,V,VV,W,WW,Z) END
        FOR X=V STEP 1 UNTIL VV DO
          WRITE (F2[DRL1,FORM10,FOR Y=W STEP 1 UNTIL WW DO MD[X,Y])
          WRITE (F2[PAGE]) END
        END ;
      END ;
    T2=TIME(2)
    WRITE(F2,FORMA,(1))
    END.

```

## PROGRAM FOUR

## THREE DIMENSIONAL FOURIER PROGRAM

```

      BEGIN
      COMMENT THREE DIMENSIONAL FOURIER

```



```

      INTEGER LA ;
      INTEGER ED,CH,CK,CL,ZZ,Q,QQ,TM,LQQ,UQ,IQQ,M,N,R,S,RH,RK,RX,RY,SPA,SPB,
      SMA,SMR,X,Y,Z,HH,UK,V,UV,W,WN,T,C ;
      INTEGER LZ,SZ,XX,YY,II,CC,NN ;
      INTEGER QD,QUAD,MH,MMZ,MV,MMX,MMY,MRX,MYR,QDZ,QDN,MX,MY,MZ ;
      ALPHA ARRAY NAT(1:12) ;
      REAL A,SCF,PEF,MFO,PPA,PPB,PMA,PMH,TT,TN,TS,TR ;
      REAL T1,T2,T3,T4 ;
      REAL ARRAY FAC(0:10) ;
      REAL ARRAY H(0:1,0:1000),K(0:1,0:1000),L(0:1,0:1000),FU(0:1,0:1000),
      N(0:64,0:64),FC(0:1,0:1000) ;
      REAL ARRAY T(0:2001) ;
      LIST L1((12-T1)/60) ;
      LABEL TERM+FEED1,FEED2,FEED3,FEED4,FEED5,FEED6,FEED7,FEED8,FEED9,
      FEEDA,FEEDB,FEEDC,FEEDD,FEEDF,FEEDG,FEEDH,FEEDJ,FEEDK,DEN,PAT,SW1,
      SW2,SW3,SW4,SW5,SW6 ;
      LABEL ACEN,TRMO ;
      SWITCH START+DEN,PAT,PAT,DEN,DEN ;
      SWITCH CHOOSE+SW1,SW2,SW3 ;
      SWITCH LOUP1+FEEDB,FEED1,FEED2 ;
      SWITCH LOUP2+FEED3,FEEDD,FEED4 ;
      SWITCH LOUP3+FEED5,FEED6,FEEDF ;
      SWITCH CHOOSE+SW4,SW5,SW6 ;
      SWITCH LOUP4+FEEDF,FEED7,FEED8 ;
      SWITCH LOUP5+FEED9,FEEDG,FEEDA ;
      SWITCH LOUP6+FEEDB,FEEDC,FEEDH ;
      FILE IN F1 (2,10) ;
      FILE OUT F2 6(2,15) ;
      SAVE FILE KRYSTL 2(1,1020,6,SAVE 3) ;
      SAVE FILE PATECN 2(1,256,SAVE 60) ;
      FORMAT IN FORM1 (12A6) ;
      FORMAT IN SCALE (F10.6) ;
      FORMAT IN INDEX (9I5) ;
      FORMAT IN DATA (3I9,F9.4,X9,I9,X25,I1) ;
      FORMAT IN DATA2 (3I9,X18,I9,F9.4,X16,I1) ;
      FORMAT IN DT3 (4I7.2F9.4) ;
      FORMAT IN UNFN (4I3,I6) ;
      FORMAT IN FORM12 (8F9.6) ;
      FORMAT OUT FORM4 ("TIME IN SECONDS=",F10.3) ;
      FORMAT OUT FORM2 ("ELECTRON DENSITY",X5,12A6,X5,"AXES DIVIDED INTO",I3) ;
      FORMAT OUT FORM3 ("PATTERSON",X5,12A6,X5,"AXES DIVIDED INTO",I3) ;
      FORMAT OUT FORM44 ("X DOWN",I3," TO",I3," Y ACROSS",I3," TO",I3," Z=",
      I2) ;
      FORMAT OUT FORM45 ("Y DOWN",I3," TO",I3," X ACROSS",I3," TO",I3," Z=",
      I2) ;
      FORMAT OUT FORM46 ("X DOWN",I3," TO",I3," Z ACROSS",I3," TO",I3," Y=",
      I2) ;
      FORMAT OUT FORM47 ("Z DOWN",I3," TO",I3," X ACROSS",I3," TO",I3," Y=",
      I2) ;
      FORMAT OUT FORM48 ("Y DOWN",I3," TO",I3," Z ACROSS",I3," TO",I3," X=",
      I2) ;
      FORMAT OUT FORM49 ("Z DOWN",I3," TO",I3," Y ACROSS",I3," TO",I3," X=",
      I2) ;
      FORMAT OUT FORM10 (16F7.1,X9) ;
      FORMAT OUT LIMIT ("NUMBER OF REFLECTIONS=",I1,I3,X10,"MAX FIRST INDEX=",
      I2,X5,"MAX SECOND INDEX=",I2) ;
      FORMAT OUT FORM11 ("DIFFERENCE FOURIER",X5,12A6,X5,"AXES DIVIDED INTO",
      I3) ;
      FORMAT OUT FORM13 (I8) ;
      FORMAT OUT FORM14 (256F8.1) ;
      COMMENT SECTION 2 INPUT ;
      T1+ TIME(2) ;

```

```

T3←T1
      READ (F1,FORM1,FOR I←1 STEP 1 UNTIL 12 DO NA[I])
      READ (F1,SCALE,SCF)
      READ (F1,INDEX,ED,CH,CK,CL,I7,SZ,ZZ,XX,YY)
      READ (F1,MNEN,QQZ,QQO,MIX,MMY,MMZ)
      READ (F1,FORM12,FOR I←1 STEP 1 UNTIL MMY DO FAC[I])
      FAC[0]←1.0
      MX←XX+1 ; MY←5×XX/4
      FOR I←0 STEP 1 UNTIL XY DO BEGIN
        A←(6.2832/XX)×I
        T[I]←SIN(A) END
      FOR I←MX STEP 1 UNTIL 1Y DO BEGIN
        C←I-XX ; T[I]←T[C] END
      Q←0
      QQ←1
      GO TO START[ED]
      DEN:
        UQ←FNTIER(MMZ/1000)
        UQQ←MMZ-UQ×1000
      GO TO CHOOSE[CH]
        SW1: GO TO LOOP1[CK]
        FEED0: GO TO TERM
      FEED1:
      FOR Q←0 STEP 1 UNTIL UQ DO BEGIN IF Q<UQ THEN LQQ←1000 ELSE LQQ←UQQ
      FOR QQ←1 STEP 1 UNTIL LQQ DO BEGIN
        READ (KRYSTL,DT3,HQ,QQ),KQ,QQ),L[Q,QQ],LA,FU[Q,QQ],FC[Q,QQ]
        FQ[Q,QQ]←FH[Q,QQ]/FAC[LA]
        FC[Q,QQ]←FC[Q,QQ]/FAC[LA]
        RH←ABS(H[Q,QQ])
        IF RH>UH THEN UH←RH
        RK←ABS(K[Q,QQ])
        IF RK>UK THEN UK←RK
      END END
      GO TO ACEN
      FEED2:
      FOR Q←0 STEP 1 UNTIL UQ DO BEGIN IF Q<UQ THEN LQQ←1000 ELSE LQQ←UQQ
      FOR QQ←1 STEP 1 UNTIL LQQ DO BEGIN
        READ (KRYSTL,DT3,HQ,QQ),KQ,QQ),L[Q,QQ],LA,FU[Q,QQ],FC[Q,QQ]
        FQ[Q,QQ]←FH[Q,QQ]/FAC[LA]
        FC[Q,QQ]←FC[Q,QQ]/FAC[LA]
        RH←ABS(H[Q,QQ])
        IF RH>UH THEN UH←RH
        RK←ABS(K[Q,QQ])
        IF RK>UK THEN UK←RK
      END END
      GO TO ACEN
        SW2: GO TO LOOP2[CK]
      FEED3:
      FOR Q←0 STEP 1 UNTIL UQ DO BEGIN IF Q<UQ THEN LQQ←1000 ELSE LQQ←UQQ
      FOR QQ←1 STEP 1 UNTIL LQQ DO BEGIN
        READ (KRYSTL,DT3,KQ,QQ),HQ,QQ),L[Q,QQ],LA,FU[Q,QQ],FC[Q,QQ]
        FQ[Q,QQ]←FH[Q,QQ]/FAC[LA]
        FC[Q,QQ]←FC[Q,QQ]/FAC[LA]
        RH←ABS(H[Q,QQ])
        IF RH>UH THEN UH←RH
        RK←ABS(K[Q,QQ])
        IF RK>UK THEN UK←RK
      END END
      GO TO ACEN
        FEED4:
      FOR Q←0 STEP 1 UNTIL UQ DO BEGIN IF Q<UQ THEN LQQ←1000 ELSE LQQ←UQQ

```

```

FOR QQ=1 STEP 1 UNTIL LQQ DO BEGIN
  READ (KRYSL,DT3,LFQ,QQ),HFQ,QQ),KFQ,QQ),LA,FD(Q,QQ),FC(LQ,QQ) ;
  FQFQ,QQ)+FQFQ,QQ)/FAC(LA);
  FC(LQ,QQ)+FC(LQ,QQ)/FAC(LA);
      RH=ABS(HFQ,QQ) ;
      IF RH>UH THEN UH=RH ;
      RK=ABS(KFQ,QQ) ;
      IF RK>UK THEN UK=RK ;
END END ;
GO TO ACEN ;
SW3: GO TO LOOP3[CK] ;
FEED5:
FOR Q=0 STEP 1 UNTIL UQ DO BEGIN IF Q<UQ THEN LQQ=1000 ELSE LQQ=UQ;
FOR QQ=1 STEP 1 UNTIL LQQ DO BEGIN
  READ (KRYSL,DT3,KFQ,QQ),LFQ,QQ),HFQ,QQ),LA,FD(Q,QQ),FC(Q,QQ) ;
  FQFQ,QQ)+FQFQ,QQ)/FAC(LA);
  FC(Q,QQ)+FC(Q,QQ)/FAC(LA);
      RH=ABS(HFQ,QQ) ;
      IF RH>UH THEN UH=RH ;
      RK=ABS(KFQ,QQ) ;
      IF RK>UK THEN UK=RK ;
END END ;
GO TO ACEN ;
FEED6:
FOR Q=0 STEP 1 UNTIL UQ DO BEGIN IF Q<UQ THEN LQQ=1000 ELSE LQQ=UQ;
FOR QQ=1 STEP 1 UNTIL LQQ DO BEGIN
  READ (KRYSL,DT3,LFQ,QQ),KFQ,QQ),HFQ,QQ),LA,FD(Q,QQ),FC(Q,QQ) ;
  FQFQ,QQ)+FQFQ,QQ)/FAC(LA);
  FC(Q,QQ)+FC(Q,QQ)/FAC(LA);
      RH=ABS(HFQ,QQ) ;
      IF RH>UH THEN UH=RH ;
      RK=ABS(KFQ,QQ) ;
      IF RK>UK THEN UK=RK ;
END END ;
GO TO ACEN ;
FEED: GO TO TERM ;
PAT: GO TO CH7[CH] ;
SW4: GO TO LOOP4[CK] ;
FEED: GO TO TERM ;
FEED7:
READ (F1,DATA2,HFQ,QQ),KFQ,QQ),LFQ,QQ),LA,FD(Q,QQ),TM) ;
FQFQ,QQ)+FQFQ,QQ)/FAC(LA);
      RH=ABS(HFQ,QQ) ;
      IF RH>UH THEN UH=RH ;
      RK=ABS(KFQ,QQ) ;
      IF RK>UK THEN UK=RK ;
      IF TM=1 THEN GO TO TERM ;
      QQ=QQ+1 ;
      IF QQ=1000 THEN BEGIN
        Q=Q+1 ;
        QQ=0 ;
        GO TO FEED7 ;
      END ;
FEED8:
READ (F1,DATA,HFQ,QQ),LFQ,QQ),KFQ,QQ),FQFQ,QQ),LA,T4) ;
FQFQ,QQ)+FQFQ,QQ)/FAC(LA);
      RH=ABS(HFQ,QQ) ;
      IF RH>UH THEN UH=RH ;
      RK=ABS(KFQ,QQ) ;
      IF RK>UK THEN UK=RK ;
      IF TM=1 THEN GO TO TERM ;
      QQ=QQ+1 ;
      IF QQ=1000 THEN BEGIN

```

```

Q+Q+1
QQ+0      END
;
;
GO TO FEEDB
SW5:  GO TO LOOP5[CK]
;
FEED9:
READ (F1,DATA2,K[Q,QQ],H[Q,QQ],L[Q,QQ],LA,F0[Q,QQ],TM) ;
F0[Q,QQ]+F1[Q,QQ]/FAC[LA];
RH+ABS(H[Q,QQ])
IF RH>UH THEN UH+RH ;
RK+ABS(K[Q,QQ]) ;
IF RK>UK THEN UK+RK ;
IF TM=1 THEN GO TO TERM
QQ+QQ+1
IF QQ=1000 THEN BEGIN
Q+Q+1
QQ+0      END
;
;
GO TO FEED9
FEEDG:  GO TO TERM
;
;
FEEDA:
READ (F1,DATA2,L[Q,QQ],H[Q,QQ],K[Q,QQ],LA,F0[Q,QQ],TM) ;
F0[Q,QQ]+F1[Q,QQ]/FAC[LA];
RH+ABS(H[Q,QQ])
IF RH>UH THEN UH+RH ;
RK+ABS(K[Q,QQ]) ;
IF RK>UK THEN UK+RK ;
IF TM=1 THEN GO TO TERM
QQ+QQ+1
IF QQ=1000 THEN BEGIN
Q+Q+1
QQ+0      END
;
;
GO TO FEEDA
SW6:  GO TO LOOP6[CK]
;
FEEDR:
READ (F1,DATA2,K[Q,QQ],L[Q,QQ],H[Q,QQ],LA,F0[Q,QQ],TM) ;
F0[Q,QQ]+F1[Q,QQ]/FAC[LA];
RH+ABS(H[Q,QQ])
IF RH>UH THEN UH+RH ;
RK+ABS(K[Q,QQ]) ;
IF RK>UK THEN UK+RK ;
IF TM=1 THEN GO TO TERM
QQ+QQ+1
IF QQ=1000 THEN BEGIN
Q+Q+1
QQ+0      END
;
;
GO TO FEEDR
FEEDC:
READ (F1,DATA2,L[Q,QQ],K[Q,QQ],H[Q,QQ],LA,F0[Q,QQ],TM) ;
F0[Q,QQ]+F1[Q,QQ]/FAC[LA];
RH+ABS(H[Q,QQ])
IF RH>UH THEN UH+RH ;
RK+ABS(K[Q,QQ]) ;
IF RK>UK THEN UK+RK ;
IF TM=1 THEN GO TO TERM
QQ+QQ+1
IF QQ=1000 THEN BEGIN
Q+Q+1
QQ+0      END
;
;
GO TO FEEDC
FEEDH:  GO TO TERM
;
;
ACFN:
LOCK (KRYSTL,RELEASE)
GO TO TRMO ;

```

```

TERM:
UQ←0;UQQ←QN-1;IF UQQ<0 THEN BEGIN UQQ+999;UQ+UQ-1 END ;
IF (ED=2) AND (XX=32) THEN
BEGIN
FOR S←1 STEP 1 UNTIL (MMX-1) DO
SPACE (PATCON,69) ;
WRITE (PATCON,FORM13,MMX) ;
END;
GO TO TRM0 ;
TRM0:
CLOSE (F1,RELEASE);
BEGIN
REAL ARRAY PA,PH,MA,MBC(100,0:UK) ;
LABEL TRM2,TRM3,TRM4 ;
REAL PFC,MFC ;
INTEGER CPA,CPR,CMA,CMB ;
SWITCH CALC←TRM2,TRM3 ;
IF ED=1 OR ED=4 THEN WRITE (F2(DBL),FORM2,FOR I←1 STEP 1 UNTIL 12
DO MA(I),XX) ;
IF ED=2 OR ED=3 THEN WRITE (F2(DBL),FORM3,FOR I←1 STEP 1 UNTIL 12
DO MA(I),XX) ;
IF ED=5 THEN WRITE (F2(DBL),FORM11,FOR I←1 STEP 1 UNTIL 12 DO MA(I),
XX) ;
WRITE (F2(DBL),LIMIT,UQ,UQQ,UH,UK) ;
WRITE (F2(PAGE)) ;
COMMENT SECTION 3 ONE DIMENSION SUMMATION ;
MMY←XX/2 ;
FOR Z←LZ STEP SZ UNTIL ZZ DO BEGIN
FOR Q←0 STEP 1 UNTIL UQ DO BEGIN
IF Q<UQ THEN LQ←1000 ;
ELSE LQ←UQ ;
FOR QQ←1 STEP 1 UNTIL LQ DO BEGIN
IF Z=LZ AND LQ,QQ<0 THEN BEGIN
LQ,QQ←-LQ,QQ ;
KQ,QQ←-KQ,QQ ;
HQ,QQ←-HQ,QQ ;
END ;
MX←LQ,QQ×7 ;
MZ←ENTER(MX/XX) ;
M←MX-(MZ×XX) ;
N←M+(XX/4) ;
COMMENT SYMMETRY SECTION ;
IF LQ,QQ=0 THEN QD←QDZ ELSE QD←QD ;
FOR QUAD←1 STEP 1 UNTIL QD DO BEGIN
IF QUAD=2 THEN BEGIN
HQ,QQ←-HQ,QQ ;
IF KQ,QQ=0 THEN GO TO TRM4 ;
IF HQ,QQ=0 THEN GO TO TRM4 ;
END ;
IF QUAD=3 THEN KQ,QQ←-KQ,QQ ;
IF QUAD=4 THEN BEGIN
HQ,QQ←-HQ,QQ ;
IF HQ,QQ=0 OR KQ,QQ=0 THEN GO TO TRM4 ;
RH←ABS(HQ,QQ) ;
RK←ABS(KQ,QQ) ;
GO TO CALC(YY) ;
TRM2:
COMMENT CENTRIC MATRIX SECTION ;
IF HQ,QQ<0 AND KQ,QQ>0 THEN BEGIN SPB←1; SMA←1; SMB←-1; END
ELSE IF HQ,QQ>0 AND KQ,QQ<0 THEN BEGIN SPB←1; SMA←-1; SMB←1; END
ELSE IF HQ,QQ<0 AND KQ,QQ<0 THEN BEGIN SPB←-1; SMA←1; SMB←1; END
ELSE IF HQ,QQ>0 AND KQ,QQ=0 THEN BEGIN SPB←-1; SMA←1; SMB←1; END
ELSE BEGIN SPB←-1; SMA←-1; SMB←-1; END

```

```

PF0←F0(Q,Q0)×T(N)×SCF ;
MF0←F0(Q,Q0)×T(M)×SCF ;
      PA(RH,RK)←PA(RH,RK1)+PF0 ;
      PB(RH,RK)←PB(RH,RK1)+SPR×PF0 ;
      MA(RH,RK)←MA(RH,RK1)+SMA×MF0 ;
      MB(RH,RK)←MB(RH,RK1)+SMB×MF0 ;
GO TO TRM4 ;
TRM3:
COMMENT ACENTRIC MATRIX SECTION ;
TRM4:END ;
IF Q0=2 THEN H(Q,Q01)←H(Q,Q01) ;
IF Q0=4 THEN K(Q,Q01)←K(Q,Q01) ;
      END END ;
COMMENT SECTION 4 REMAINING DIMENSIONS SUMMATION ;
      FOR X←0 STEP 1 UNTIL MMY DO BEGIN
        RX←XX=X ;
        FOR RH←0 STEP 1 UNTIL UH DO BEGIN
          MX←RH×X ;
          MZ←ENTIER(MX/XX) ;
          M←MX-(MZ×XX) ;
          N←M+(XX/4) ;
          TN←T(N) ;
          TT←T(M) ;
          FOR Y←0 STEP 1 UNTIL MMY DO BEGIN
            RY←XX=Y ;
            IF RH=0 THEN BEGIN
              DX,Y1←0.0 ;
              DRX,Y1←0.0 ;
              DX,RY1←0.0 ;
              DRX,RY1←0.0 ;
              END ;
              FOR RK←0 STEP 1 UNTIL UK DO BEGIN
                MX←RK×Y ;
                MZ←ENTIER(MX/XX) ;
                M←MX-(MZ×XX) ;
                N←M+(XX/4) ;
                TS←T(M) ;
                TR←T(N) ;
                PPA←PA(RH,RK1)×TN×TR ;
                PPB←PB(RH,RK1)×TT×TS ;
                PMA←MA(RH,RK1)×TT×TR ;
                PMB←MB(RH,RK1)×TN×TS ;
                D(X,Y1)←D(X,Y1)+PPA+PPB+PMA+PMB ;
                IF RX≠MMY THEN
                  D(RX,Y1)←D(RX,Y1)+PPA-PPB-PMA+PMB ;
                IF RY≠MMY THEN
                  D(X,RY)←D(X,RY)+PPA-PPB+PMA-PMB ;
                IF RX≠MMY AND RY≠MMY THEN
                  D(RX,RY)←D(RX,RY)+PPA+PPB-PMA-PMB ;
                IF X=MMY AND Y=MMY THEN BEGIN
                  PA(RH,RK1)←0.0 ;
                  PB(RH,RK1)←0.0 ;
                  MA(RH,RK1)←0.0 ;
                  MB(RH,RK1)←0.0 ;
                  END ;
                END ; IF RH=UH THEN BEGIN
                  IF D(X,Y1)≤0 THEN D(X,Y1)←10*6 ; IF D(RX,Y1)≤0 THEN D(RX,Y1)←10*6 ;
                  IF D(X,RY)≤0 THEN D(X,RY)←10*6 ; IF D(RX,RY)≤0 THEN D(RX,RY)←10*6 ;
                  END END ;
                END END ;
COMMENT SECTION 5 OUTPUT ;
MMZ←XX-16 ; FOR V←0 STEP 16 UNTIL MMZ DO

```

```

      FOR W←0 STEP 16 UNTIL MMZ DO BEGIN
        VV←V+15
        WW←W+15
      IF ED=1 OR ED=4 THEN WRITE (F2[DBL],FORM2,FOR I←1 STEP 1 UNTIL 12
      DO NA[I],XX) ;
      IF ED=2 OR ED=3 THEN WRITE (F2[DBL],FORM3,FOR I←1 STEP 1 UNTIL 12
      DO NA[I],XX) ;
      IF ED=5 THEN WRITE (F2[DBL],FORM11,FOR I←1 STEP 1 UNTIL 12 DO NA[I],
      XX) ;
      IF CL=3 THEN BEGIN
        IF CH=1 THEN WRITE (F2[DBL],FORM4,V,VV,W,WW,Z)
        ELSE WRITE (F2[DBL],FORM5,V,VV,W,WW,Z) END ;
        IF CK=3 THEN BEGIN
          IF CH=1 THEN WRITE (F2[DBL],FORM6,V,VV,W,WW,Z)
          ELSE WRITE (F2[DBL],FORM7,V,VV,W,WW,Z) END ;
          IF CH=3 THEN BEGIN
            IF CK=1 THEN WRITE (F2,FORM8,V,VV,W,WW,Z)
            ELSE WRITE (F2[DBL],FORM9,V,VV,W,WW,Z) END ;
            FOR X←V STEP 1 UNTIL VV DO
              WRITE (F2[DBL],FORM10,FOR Y←W STEP 1 UNTIL WW DO D[X,Y]) ;
            IF (ED=2) AND (XX=32) THEN
              WRITE (PATFCN,FORM14,FOR X←V STEP 1 UNTIL VV DO
                FOR Y←W STEP 1 UNTIL WW DO D[X,Y]) ;
              WRITE (F2[PAGE]) END ;
            T4←TIME(2); IF (T4-T3)>36000 THEN BEGIN T3←T4; BREAK END ;
            END ;
            T2 ←TIME(2) ;
            WRITE(F2,FORMA,L1) ;
            END;
            END.

```

## LITERATURE CITED

1. C. M. Harris, R. S. Hyholm, and D. J. Phillips, Journal of the Chemical Society, 4379 (1960).
2. N. C. Stephenson, Acta Crystallographica, 17, 592 (1964).
3. N. C. Stephenson, Acta Cryst., 17, 1517 (1964).
4. W. P. Griffith and G. Wilkinson, Journal of Inorganic and Nuclear Chemistry, 7, 295 (1958).
5. W. P. Griffith and G. Wilkinson, J. Chem. Soc., 2757 (1959).
6. A. Sacco and M. Freni, Gazzetta Chimica Italiana, 89, 1800 (1959).
7. F. A. Cotton, T. G. Dunne, and J. S. Wood, Inorganic Chemistry, 3, 1495 (1964).
8. E. L. Muettertides, Inorg. Chem., 4, 769 (1965).
9. R. S. Berry, Journal of Chemical Physics, 32, 933 (1960).
10. W. Mahler and E. L. Muettertides, Inorg. Chem., 4, 1520 (1965).
11. R. S. Nyholm, Proceedings of the Chemical Society, 273 (1961).
12. N. A. Bailey, J. M. Jenkins, R. Mason, and B. L. Shaw, Chemical Communications, 237 (1965).
13. S. J. LaPlaca and J. A. Ibers, Inorg. Chem., 4, 778 (1965).
14. L. Vaska, Chemistry and Industry, 1402 (1961).
15. J. Zemann, Zeitschrift fur anorganische und allgemeine Chemie, 324, 241 (1963).
16. R. J. Gillespie, J. Chem. Soc., 4673, 4679 (1963).
17. F. Basolo and R. G. Pearson, Mechanisms of Inorganic Reactions, John Wiley and Sons, Inc., New York, N. Y., 1958.
18. E. L. Muettertides, W. Mahler, and R. Schmutzler, Inorg. Chem., 2, 613 (1963).
19. E. L. Muettertides, W. Mahler, K. J. Packer, and R. Schmutzler, Inorg. Chem., 3, 1298 (1964).



20. C. J. Ballhausen and H. B. Gray, Inorg. Chem., 2, 426 (1963).
21. R. P. Dodge, D. H. Templeton, and A. Zalkin, Journal of Physical Chemistry, 35, 55 (1961).
22. J. A. Ibers, Annual Review of Physical Chemistry, 16, 375 (1965).
23. M. DiVaria and P. L. Orioli, Chem. Commun., 590 (1965).
24. P. R. H. Alderman and P. G. Owston, Nature, 178, 1071 (1956).
25. P. R. H. Alderman, P. G. Owston, and J. M. Rowe, J. Chem. Soc., 668 (1962).
26. A. Earnshaw, P. D. Hewlett, and L. F. Larkworthy, Nature, 199, 483 (1963).
27. P. Pauling, G. B. Robertson, and G. A. Rodley, Nature, 207, 73 (1965).
28. J. Lewis, R. S. Nyholm, and G. A. Rodley, Nature, 207, 72 (1965).
29. F. A. Cotton, T. G. Dunne, and J. S. Wood, Inorg. Chem., 4, 318 (1965).
30. A. Sacco and M. Freni, Gazz. Chim. Ital., 89, 1800 (1959).
31. G. A. Mair, H. M. Powell, and D. E. Henn, Proc. Chem. Soc., 415 (1960).
32. G. A. Barclay and R. S. Nyholm, Chem. and Ind., 378 (1953).
33. G. A. Barclay, R. S. Nyholm, and R. V. Parish, J. Chem. Soc., 4433 (1961).
34. L. Sacconi, P. L. Orioli, and M. DiVaria, Journal of the American Chemical Society, 87, 2059 (1965).
35. L. Sacconi, P. Nannelli, N. Nardi, and V. Campigli, Inorg. Chem., 4, 943 (1965).
36. J. W. Collier, F. G. Mann, D. G. Watson, and H. R. Watson, J. Chem. Soc., 1803 (1964).
37. F. G. Mann, Chem. and Ind., 944 (1965).
38. J. W. Collier and F. G. Mann, J. Chem. Soc., 1815 (1964).
39. G. A. Mair, H. M. Powell, and L. M. Venanzi, Proc. Chem. Soc., 170 (1961).
40. J. G. Hartley, L. M. Venanzi, and D. C. Goodall, J. Chem. Soc., 3930 (1963).

41. T. E. N. Howell, S. A. J. Pratt, and L. M. Venanzi, J. Chem. Soc., 3167 (1961).
42. L. M. Venanzi, Angewandte Chemie International Edition in English, 3, 453 (1964).
43. G. Dyer, J. G. Hartley, and L. M. Venanzi, J. Chem. Soc., 1293 (1965).
44. G. Dyer and L. M. Venanzi, J. Chem. Soc., 2771 (1965).
45. R. D. Cramer, R. V. Lindsey, Jr., C. T. Prewitt, and U. G. Stolberg, J. Am. Chem. Soc., 87, 658 (1965).
46. R. D. Cramer, E. L. Jenner, R. V. Lindsey, Jr., and U. G. Stolberg, J. Am. Chem. Soc., 85, 1691 (1963).
47. G. A. Barclay, B. F. Hoskins, and C. H. L. Kennard, J. Chem. Soc., 5691 (1963).
48. C. M. Harris, T. N. Lockyer, and H. Waterman, Nature, 192, 424 (1961).
49. M. Mori, Y. Saito, and T. Watanabe, Bulletin of the Chemical Society of Japan, 34, 295 (1961).
50. M. Mori, Bull. Chem. Soc. Japan, 33, 985 (1960).
51. F. J. Llewellyn and T. N. Waters, J. Chem. Soc., 2639 (1960).
52. T. N. Waters and D. Hall, J. Chem. Soc., 1200 (1959).
53. T. N. Waters and D. Hall, J. Chem. Soc., 1203 (1959).
54. E. Frasson, R. Bardi, and S. Beggi, Acta Cryst., 12, 201 (1959).
55. J. A. Berron, D. P. Graddon, and J. F. McConnell, Nature, 199, 373 (1963).
56. G. A. Barclay and L. H. L. Kennard, J. Chem. Soc., 3289 (1961).
57. D. Hall and T. N. Waters, J. Chem. Soc., 2644 (1960).
58. A. Pignedoli and G. Peyronel, Gazz. Chim. Ital., 92, 745 (1962).
59. G. A. Barclay, C. M. Harris, B. F. Hoskins, and E. Kokot, Proc. Chem. Soc., 264 (1961).
60. E. L. Lippert and M. R. Truter, J. Chem. Soc., 4996 (1960).
61. H. Montgomery and E. C. Lingafelter, Acta Cryst., 16, 748 (1963).
62. D. E. C. Corbridge and E. G. Cox, J. Chem. Soc., 594 (1956).

63. G. Morgan and F. H. Burstall, J. Chem. Soc., 1649 (1937).
64. D. Hall and F. H. Moore, Proc. Chem. Soc., 256 (1960).
65. J. Chatt and A. E. Underhill, J. Chem. Soc., 2089 (1963).
66. P. L. Orioli, M. Divaria, and L. Sacconi, Chem. Commun., 103 (1965).
67. L. Sacconi, M. Ciampolini, and G. P. Speroni, J. Am. Chem. Soc., (1965).
68. D. F. Koenig, Acta Cryst., 18, (1965).
69. M. J. Hamor, T. A. Hamor, J. L. Hoard, and W. S. Caughey, Abstr. K-12, Am. Cryst. Assoc. Meeting, Bozeman, Montana, 26-31 July 1964.
70. J. A. Bertrand and D. L. Plymale, Inorg. Chem., 5, May (1966).
71. V. K. Issleib and E. Wenschuh, Z. anorg. allg. Chem., 305, 15 (1960).
72. R. G. Hayter, Inorg. Chem., 2, 932 (1963).
73. K. A. Jensen and B. Nygaard, Acta Chemica Scandinavica, 3, 474 (1949).
74. K. A. Jensen, P. H. Nielsen, and C. T. Pedersen, Acta Chem. Scand., 17, 1115 (1963).
75. K. A. Jensen, B. Nygaard, and C. T. Pedersen, Acta Chem. Scand., 17, 1126 (1963).
76. K. A. Jensen and C. K. Jorgensen, Acta Chem. Scand., 19, 451 (1965).
77. G. Dyer and D. W. Meek, Inorg. Chem., 4, 1398 (1965).
78. G. Dyer and D. W. Meek, Chemical and Engineering News, 43(38), 50 (1965).
79. G. S. Benner, W. E. Hatfield, and D. W. Meek, Inorg. Chem., 3, 1544 (1964).
80. R. G. Hayter, J. Am. Chem. Soc., 84, 3046 (1962).
81. M. Ciampolini and N. Nardi, Inorg. Chem., 5, 41 (1966).
82. M. Ciampolini and G. P. Speroni, Inorg. Chem., 5, 45 (1966).
83. I. Bernal, Inorg. Chem., 3, 1465 (1964).

84. C. H. Langford, E. Billig, S. I. Shupack, and H. B. Gray, J. Am. Chem. Soc., 86, 2958 (1964).
85. V. K. Issleib and H. P. Roloff, Z. anorg. allg. Chem., 324, 250 (1963).
86. N. S. Gill, Chem. and Ind., 989 (1961).
87. V. K. Issleib and G. Boln, Z. anorg. allg. Chem., 301, 188 (1959).
88. G. W. Fowles and C. M. Pleass, Chem. and Ind., 1743 (1955).
89. M. Antler and A. W. Laubergayer, J. Am. Chem. Soc., 77, 5250 (1955).
90. J. Becquerel, Zeitschrift fur Physik, 58, 205 (1929).
91. H. Bethe, Annalen der Physik, 3, 133 (1929).
92. J. H. Van Vleck, J. Chem. Phys., 3, 803 (1935).
93. J. H. Van Vleck, J. Chem. Phys., 3, 807 (1935).
94. R. S. Mulliken, The Physical Review, 40, 55 (1932).
95. H. N. Russell and F. A. Saunders, The Astrophysical Journal, 61, 38 (1925).
96. F. A. Cotton, Chemical Applications of Group Theory, Interscience Publishers, a division of John Wiley and Sons, New York, N. Y., 1963.
97. C. E. Moore, Atomic Energy Levels, National Bureau of Standards Circular 467, vol. 1, 1949; vol. 2, 1952; vol. 3, 1958.
98. L. E. Orgel, J. Chem. Phys., 23, 1004 (1955).
99. L. J. Ballhausen, Introduction to Ligand Field Theory, McGraw-Hill, New York, N. Y., 1962.
100. E. B. Wilson, J. C. Decius, and P. C. Cross, Molecular Vibrations, McGraw-Hill, New York, N. Y., 1955.
101. D. S. McClure, Solid State Physics, 9, 399 (1959).
102. Y. Tanabe and S. Sugano, Journal of the Physical Society of Japan, 9, 753, 766 (1954).
103. A. Davydov, Zhurnal Eksperimentalnoi i Theoreticheskoi Fiziki, 18, 210 (1948).
104. H. Winston and R. S. Halford, J. Chem. Phys., 17, 607 (1949).

105. M. Ciampolini, Inorg. Chem., 5, 35 (1966).
106. W. E. Hatfield, H. D. Bedon, and S. H. Horner, Inorg. Chem., 4, 1181 (1965).
107. P. Day, Proc. Chem. Soc., 18 (1964).
108. J. Lewis and R. G. Wilkins, Modern Coordination Chemistry, Principles Methods, Interscience Publishers, Inc., New York, N. Y., 1960.
109. B. N. Figgis and R. S. Nyholm, J. Chem. Soc., 4190 (1958).
110. K. Issleib and H. D. Frohlich, Naturforsch., 14b, 349 (1959).
111. D. Wittenberg and H. Gilman, Journal of Organic Chemistry, 23, 1063 (1958).
112. K. Starke, J. Inorg. Nucl. Chem., 11, 77 (1959).
113. J. V. Quagliano, Jr. Fujita, G. Franz, D. J. Phillips, J. A. Walmsley, and S. Y. Tyree, J. Am. Chem. Soc., 83, 3770 (1961).
114. K. Issleib and A. Kreibich, Z. anorg. allgem. Chem., 313, 339 (1962).
115. J. A. Bertrand and D. L. Plymale, Inorg. Chem., 3, 775 (1964).
116. F. A. Cotton, D. M. L. Goodgame, and M. Goodgame, J. Am. Chem. Soc., 83, 4690 (1961).
117. M. J. Buerger, The Precession Method, John Wiley and Sons, New York, N. Y., 1964.
118. M. J. Buerger, X-Ray Crystallography, John Wiley and Sons, New York, N. Y., 1942.
119. J. Waser, The Review of Scientific Instruments, 22, 567 (1951).
120. H. J. Grenville-Wells and S. C. Abrahams, Rev. Sci. Inst., 23, 328 (1952).
121. E. R. Howells, D. C. Phillips, and D. Rogers, Acta Cryst., 3, 210 (1950).
122. E. Jahnke and F. Emde, Funktionen Tafeln mit Formeln und Kurven, Teubner, Leipzig, Germany, 1933.
123. H. Lipson and W. Cochran, The Determination of Crystal Structure, Volume 3, G. Bell and Sons, London, England, 1953.

124. M. J. Buerger, Vector Space, John Wiley and Sons, New York, N. Y., 1959.
125. M. J. Buerger, Crystal-Structure Analysis, John Wiley and Sons, New York, N. Y., 1960.
126. L. J. Gallaher and M. I. Kay, A Translation of a Fortran Crystallographic Least Squares Program by W. R. Busing, K. O. Martin and H. A. Levy to Extended Algol, Georgia Institute of Technology, Technical Report No. 1, Project B-270, May 27, 1964.
127. J. Ferguson, J. Chem. Phys., 39, 116 (1963).
128. J. A. Walmsley and S. Y. Tyree, Inorg. Chem., 2, 312 (1963).
129. D. W. Meek, R. S. Drago, and T. S. Piper, Inorg. Chem., 1, 285 (1962).
130. R. S. Drago, D. W. Meek, M. D. Joesten, and L. LaRoche, Inorg. Chem., 2, 124 (1963).
131. L. J. Gallaher and F. C. Taylor, Jr., A Translation of a Fortran Crystallographic Function and Error Program by W. R. Busing, K. O. Martin and A. A. Levy to Extended Algol, Georgia Institute of Technology, Technical Report No. 2, Project B-270, October 1, 1964.
132. R. Eisenberg and J. A. Ibers, Inorg. Chem., 4, 773 (1965).
133. T. S. Piper and R. L. Carlin, J. Chem. Phys., 35, 1809 (1961).
134. J. Ferguson, J. Chem. Phys., 32, 528 (1960).

## VITA

Donald Lee Plymale was born on June 12, 1934 in Huntington, West Virginia, the son of Leo and Vivian Harvey Plymale. He attended public schools in Huntington and received his Bachelor of Science degree cum laude from Marshall University in 1957.

He received his Master of Science in Chemistry from Marshall University in May 1962. From June 1959 to September 1962, he was employed as a spectroscopist at The International Nickel Company in Huntington, West Virginia. He entered Georgia Institute of Technology in September of 1962 in order to attain his Doctor of Philosophy in chemistry.

On June 19, 1959, he married Carole Lynn Wallace of Barboursville, West Virginia. He is the father of two children, Carole Anne and Robert Andrew.

He is a member of Chi Beta Phi, Sigma Xi, and the American Chemical Society.

His research was done under the direction of Dr. J. Aaron Bertrand. During his course of study, he was supported by a part-time instructorship at Georgia Institute of Technology and the National Science Foundation Research Grants GP1999 and GP3826.